TRANSAT

Research and Innovation Action (RIA)

This project has received funding from the European Union's Horizon 2020 research and innovation programme under grant agreement No 754586.

Start date : 2017-09-01 Duration : 48 Months

Report on review of gas treatment technologies

Authors : Mrs. Silvano TOSTI (ENEA), Alessia Santucci, Ion Cristescu, Serena Bassini, Dario Diamanti, Marco Utili

TRANSAT - Contract Number: 754586
TRANSversal Actions for Tritium Project Officer: Angelgiorgio IORIZZO

Document title	Report on review of gas treatment technologies
Author(s)	Mrs. Silvano TOSTI, Alessia Santucci, Ion Cristescu, Serena Bassini, Dario Diamanti, Marco Utili
Number of pages	66
Document type	Deliverable
Work Package	WP01
Document number	D1.3
Issued by	ENEA
Date of completion	2019-02-21 09:35:15
Dissemination level	Public

Summary

TRANSAT (TRANSversal Actions for Tritium) is a 4 years multidisciplinary project built to contribute to Research and Innovation on "cross-cutting activities" needed to "improve knowledge on tritium management in fission and fusion facilities". It proposes actions answering the main following challenges: i) tritium release mitigation strategies; ii) waste management improvement; iii) refinement of the knowledge in the field of radiotoxicity, radiobiology, and dosimetry. Among the activities included in this project, it is foreseen the assessment of the processes for the treatment of the operational tritiated gases and the analysis of their applicability to fusion and fission purposes. The present work is a part of the activities foreseen in the ambit of the Work Package 1 - Assessment and proposal for developments of barriers against tritium permeation and the treatment of the operational tritiated gases. In particular it refers to the Task 1.2 - Treatment of the operational tritiated gases generated in the fission (plenum gas purification, He purification in gas reactors) and fusion (He purification system in TBM) activities. Assessment of a viable route for the separation of lithium isotopes. The scope of this report is to carry out a review of the tritiated gas treatment technologies used in both fission (cover gas purification, helium purification in gas cooled reactors) and fusion (helium coolant purification), to compare the processes and to perform their validations. The review will include the study of the transferability of the main technologies selected for the International Thermonuclear Experimental Reactor (ITER) and for the gas cooled fission reactors, to the tritium extraction and purification systems to be used in the Coolant Purification System (CPS) of the DEMOnstrating fusion power reactor (DEMO) and in the cover gas purification system of the Advanced Sodium Technological Reactor for Industrial Demonstration (ASTRID).

Approval

Date	By
2019-02-21 09:44:38	Dr. Ion CRISTESCU (KIT)
2019-03-22 09:49:39	Mr. Christian GRISOLIA (CEA)

Table of contents

Index of Tables

This project has received funding from the Euratom research and training programme 2014-2018 under the grant agreement n°754586. The content in this report reflects only the views of the authors. The European Commission is not responsible for any use that may be made of the information it contains.

Index of Figures

Abbreviations

AGR	Advanced Gas-cooled Reactors
ALFRED	Advanced Lead cooled Fast Reactor European Demonstrator
ASTRID	Advanced Sodium Technological Reactor for Industrial Demonstration
BB	Breeding Blanket
CCS	Chemical Cleanup System
CPS	Coolant Purification System
DEMO	DEMOnstrating fusion power reactor
EFPD	Effective Full Power Day
FPTS	Fission Product Trapping System
FSV	Fort St. Vrain
GCR	Gas Cooled Reactor
GHSV	Gas Hourly Space Velocity
GIF	Generation IV International Forum
GFR	Gas Cooled Fast Reactor
GT-MHR	Gas-Turbine Modular Helium Reactor
HCCB	Helium Cooled Ceramic Breeder
HCPB	Helium Cooled Pebble Bed
HCLL	Helium Cooled Lithium Lead
HCS	Helium Cooling System
HTGR	High Temperature Gas Reactor
HTR	High Temperature Reactor
HTTR	High Temperature engineering Test Reactor
ITER	International Thermonuclear Experimental Reactor
LMFR	Liquid Metal Fast Reactor
LFR	Lead cooled Fast Reactor
MHTGR	Modular High-Temperature Gas-Cooled Reactor
MTZ	Mass Transfer Zone
NA	Not Available
PBMR	Pebble Bed Modular Reactor
PCRV	Prestressed Concrete Reactor Vessel
PFD	Process Flow Diagram
PRF	Permeation Reduction Factor
PSA	Pressure Swing Adsorption
PTSA	Pressure Temperature Swing Adsorption
SG	Steam Generator
SFR	Sodium Fast Reactors
TBM	Test Blanket Module
TBR	Tritium Breeding Ratio
TES	Tritium Extraction System
TEP	Tokamak Exhaust Processing
THTR	Thorium High Temperature Reactor
TSA	Temperature Swing Adsorption
WP	Work Package
ZMS	Zeolite Molecular Sieve

Summary

TRANSAT (TRANSversal Actions for Tritium) is a 4 years multidisciplinary project built to contribute to Research and Innovation on "cross-cutting activities" needed to "improve knowledge on tritium management in fission and fusion facilities". It proposes actions answering the main following challenges:

i) tritium release mitigation strategies;
ii) waste management improvement;
iii) refinement of the knowledge in the field of radiotoxicity, radiobiology, and dosimetry.

Among the activities included in this project, it is foreseen the assessment of the processes for the treatment of the operational tritiated gases and the analysis of their applicability to fusion and fission purposes.

The present work is a part of the activities foreseen in the ambit of the Work Package 1 (WP1) – Assessment and proposal for developments of barriers against tritium permeation and the treatment of the operational tritiated gases. – In particular it refers to the Task 1.2 – Treatment of the operational tritiated gases generated in the fission (plenum gas purification, He purification in gas reactors) and fusion (He purification system in TBM) activities. Assessment of a viable route for the separation of lithium isotopes.

The scope of this report is to carry out a review of the tritiated gas treatment technologies used in both fission (cover gas purification, helium purification in gas cooled reactors) and fusion (helium coolant purification), to compare the processes and to perform their validations. The review will include the study of the transferability of the main technologies selected for the International Thermonuclear Experimental Reactor (ITER) and for the gas cooled fission reactors, to the tritium extraction and purification systems to be used in the Coolant Purification System (CPS) of the DEMOnstrating fusion power reactor (DEMO) and in the cover gas purification system of the Advanced Sodium Technological Reactor for Industrial Demonstration (ASTRID).

The corresponding deliverable is D1.3 – Report on review of gas treatment technologies.

1 Introduction

Tritium ${}^{3}_{1}H$ (or T) is a radioactive isotope of hydrogen, having a half-life of 12.32 years. It is a beta emitter having a maximum electron energy of approx. 19 keV and a mean energy of 5.7 keV [1]; it decays according to:

$$ {}^{3}_{1}H \rightarrow {}^{3}_{2}He + e^{-} + \bar{\nu}_e \quad (1.1) $$

The other two naturally occurring isotopes of hydrogen are the ordinary hydrogen, or protium, ${}^{1}_{1}H$ and the deuterium ${}^{2}_{1}H$ (or D), that are stable isotopes. The natural abundance of the ordinary hydrogen is greater than 99.9 %, while that of the deuterium is about 0.02 %. The tritium is present only in traces (10^{-16} %) [1].

Tritium is a very mobile isotope and it can be released in the environment from different anthropogenic sources. The developments of the deuterium-tritium fusion reactors and the studies on the future fission reactors (GEN IV) suggest that the release of tritium in the environment is expected to increase. This increase leads to the need of new strategies to limit the release of tritium in the environment.

1.1 Natural and anthropogenic sources of tritium

The tritium present in the atmosphere, having a natural origin, is mainly produced by reactions between cosmic ray neutrons and nitrogen atoms, according to the following reactions [2]:

$$ {}^{14}_{7}N + {}^{1}_{0}n \rightarrow {}^{12}_{6}C + {}^{3}_{1}H - 4.3\ MeV \quad (1.2) $$

$$ {}^{14}_{7}N + {}^{1}_{0}n \rightarrow 3\ {}^{4}_{2}He + {}^{3}_{1}H - 11.5\ MeV \quad (1.3) $$

Since the tritium atoms have initially a high energy, they can react with molecular hydrogen to produce HT. In the atmosphere, the HT molecules are oxidized into HTO and it is mainly in this form that tritium is present on the earth surface and, in particular, in the oceans.

The most important anthropogenic source of tritium in the environment has been weapon testing. Other sources include release from nuclear reactors, facilities for the reprocessing of nuclear fuel, commercial facilities for tritium production, commercial facilities for hydrogen isotope separation, research installations using relevant amount of tritium.

The main sources of tritium in a fission reactor are:

- fuel rods, via ternary fission of fissile nuclides;
- reactions with boron in control and shielding rods;
- reactions with coolant in water reactors;
- reactions with impurities (mainly lithium).

Ternary fission is a rare type of nuclear fission in which three charged nuclides are produced instead of two. The specific amount (atom/fission) of tritium produced by ternary fission depends on the fissile nuclides and neutron flux spectrum [1].

The tritium inside the control and shielding rods can be produced directly from boron capture, according to [1] [2]:

$$ {}^{10}_{5}B + {}^{1}_{0}n \rightarrow 2\ {}^{4}_{2}He + {}^{3}_{1}H \quad (1.4) $$

$$ {}^{11}_{5}B + {}^{1}_{0}n \rightarrow 2\ {}^{4}_{2}He + {}^{1}_{0}n + {}^{3}_{1}H \quad (1.5) $$

or indirectly, producing firstly ${}^{7}_{3}Li$ atoms, and then by means of neutron capture of lithium:

$$ {}^{10}_{5}B + {}^{1}_{0}n \rightarrow {}^{4}_{2}He + {}^{7}_{3}Li \quad (1.6) $$

$$ {}^{7}_{3}Li + {}^{1}_{0}n \rightarrow {}^{4}_{2}He + {}^{1}_{0}n + {}^{3}_{1}H \quad (1.7) $$

The production of tritium in the water coolant is due to neutron capture reactions involving hydrogen and deuterium atoms [2]:

$$ D_2O + n \rightarrow DTO + \gamma \quad (1.8) $$

$$H_2O + n \rightarrow DHO + \gamma \quad (1.9)$$

$$DHO + n \rightarrow THO + \gamma \quad (1.10)$$

The main impurities responsible for the tritium production are the lithium atoms; these atoms react with neutrons according to (1.7) and:

$$^{6}_{3}Li + ^{1}_{0}n \rightarrow ^{4}_{2}He + ^{3}_{1}H \quad (1.11)$$

1.2 Tritium in fusion

In the ambit of thermonuclear fusion, different reactions can be considered as source of energy. A fundamental parameter, useful to evaluate the most indicated fusion reaction, is the cross-section, which is a measure of the probability that a certain reaction occurs [3]. In the following Figure, the cross sections of some reactions having an interest for the production of energy by fusion have been reproduced [4].

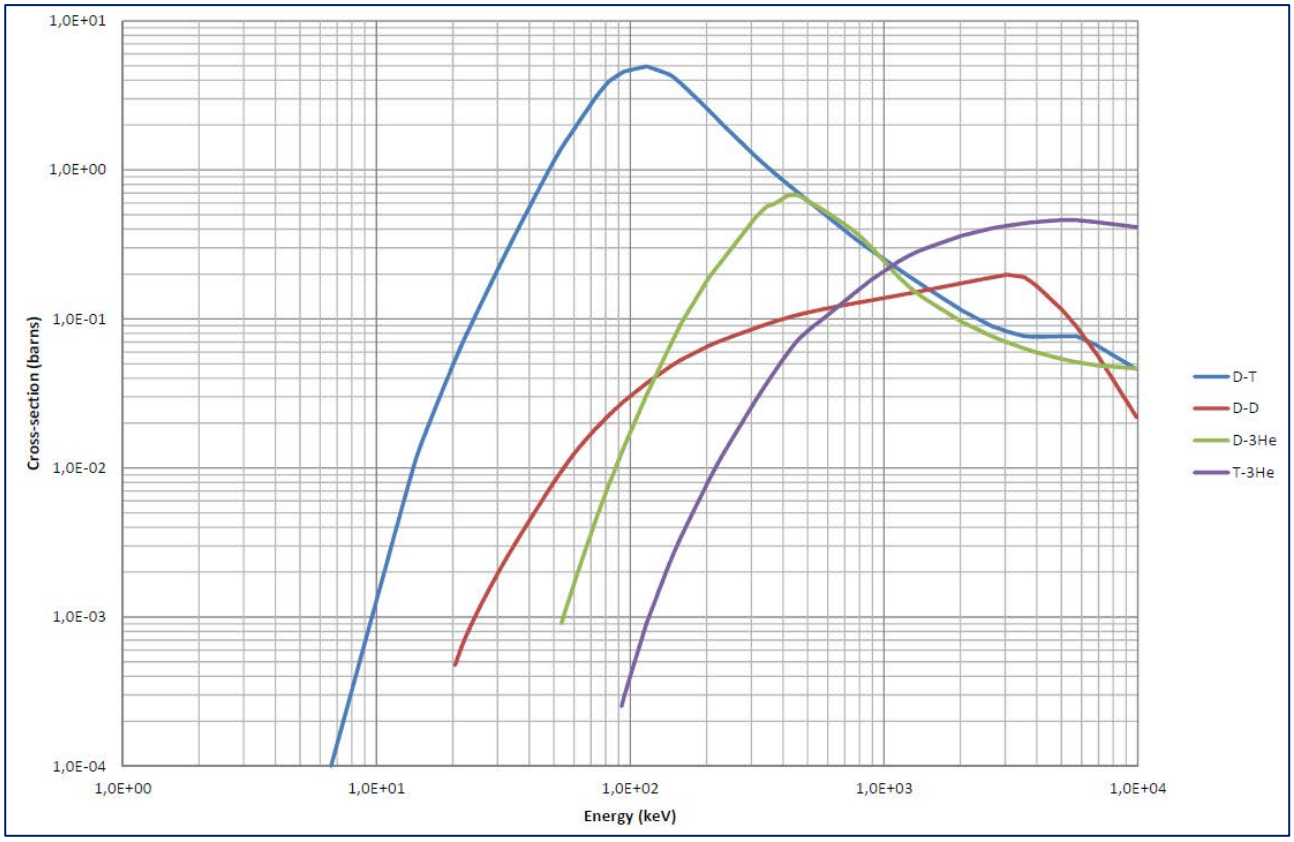

Figure 1: Fusion reaction cross sections

From the above Figure it is possible to note that the reaction:

$$D + T \rightarrow ^{4}_{2}He + ^{1}_{0}n + 17.59\ MeV \quad (1.12)$$

shows the largest cross-section at the lowest energy [3]. For this reason the reaction D-T has been considered for ITER and DEMO reactors. The main drawback of this reaction is that the tritium is a radioactive isotope, present only in traces in nature, and it is necessary to produce it.

There are two main reactions considered to produce tritium in the blanket of the fusion reactor:

$$^{6}_{3}Li + ^{1}_{0}n \rightarrow ^{4}_{2}He + ^{3}_{1}H + 4.8\ MeV \quad (1.13)$$

$$^{7}_{3}Li + ^{1}_{0}n \rightarrow ^{4}_{2}He + ^{1}_{0}n + ^{3}_{1}H - 2.5\ MeV \quad (1.14)$$

Observing the Figure reproducing the cross-sections relevant to the two reactions [4], it is possible to note that (1.13) has a higher probability, in particular with slowing down neutrons. Since the

natural abundance of ^{6}Li and ^{7}Li is 7.4% and 92.6%, respectively, an enrichment of ^{6}Li will be necessary [3].

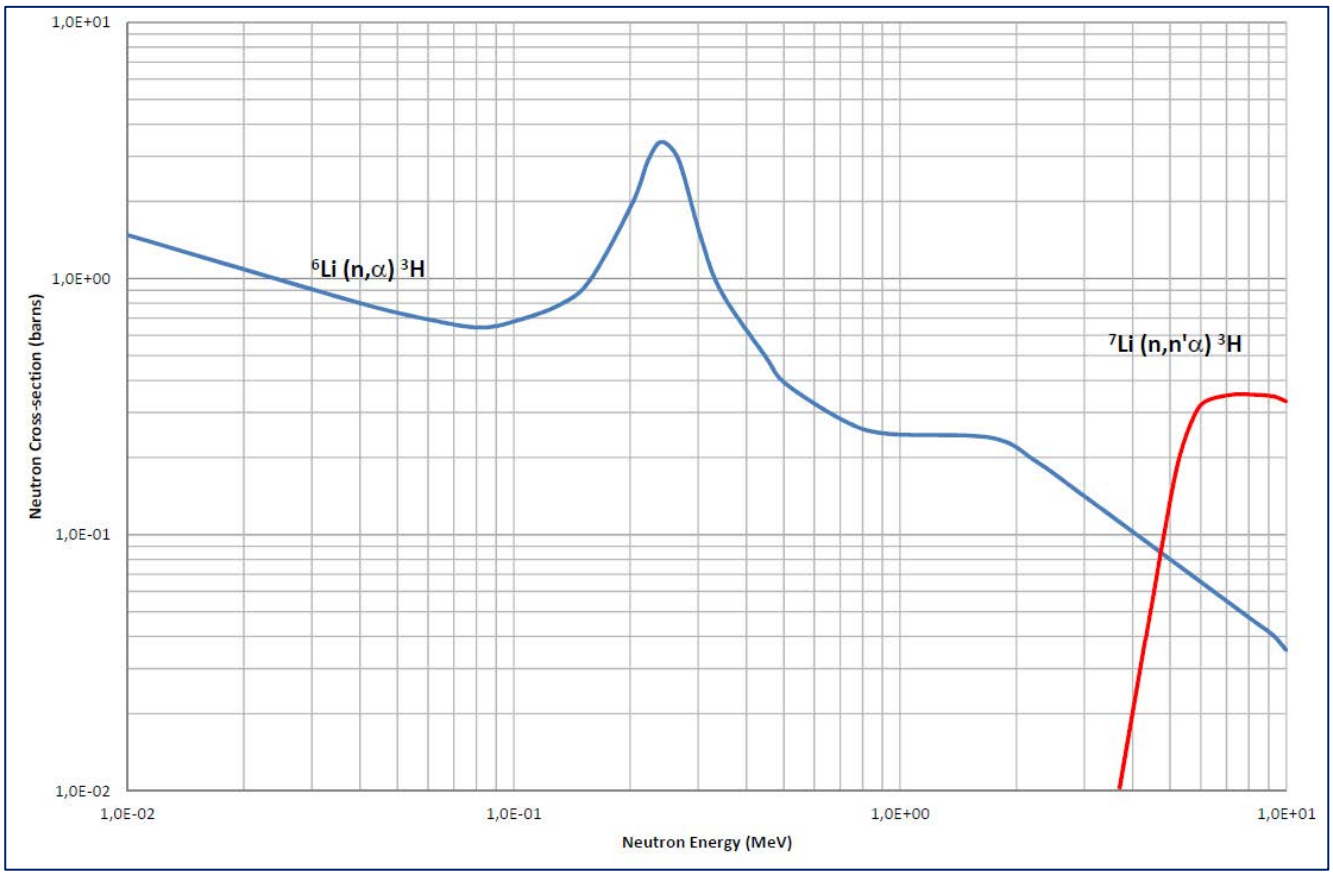

Figure 2: Neutron cross sections of ^{6}Li and ^{7}Li

2 Purification systems for gas treatment in fission

In the present chapter, the existing knowledge relevant to the systems for the treatment of tritiated gases used in fission reactors will be illustrated. Particular attention will be given to the parts of the systems having the scope to treat the hydrogen isotopes.

2.1 Evolution of helium cooled fission reactors

Coolant Purification Systems (CPS) have been used in the past for helium cooled fission reactors, mainly to eliminate impurities causing the oxidation of the graphite moderator and the corrosion of the materials operating at high temperature. The most significant purification systems used in helium cooled reactors will be described in the following paragraphs. The purification systems are linked to the designs of the Gas Cooled Reactors (GCRs) and their evolution. A short description of the evolution of the GCRs design will be shown in the following [6].

The first commercial GCRs were manufactured in U.K. with the scope to combine the plutonium production with electric power generation. These first reactors used graphite as moderator, metallic natural uranium as fuel and CO_2 as cooling gas. These technologies were in the following applied in the U.K.'s reactors type MAGNOX and Advanced Cooled Reactors (AGRs).

In 1951 a research reactor having a power of 2 MW became operating in France (Saclay); this reactor used initially nitrogen as coolant and later CO_2, similarly to UK's reactors.

In Japan, the first reactor became operative in 1966; it was a 166 MWe reactor, CO_2 cooled.

In the 1950s, High Temperature Gas Cooled Reactor (HTGR) studies started, to improve the performances of GCRs. The studies foresaw the use of prismatic blocks of graphite as moderator

or spherical fuel elements. The use of helium instead of CO_2 permitted to increase the operating temperature.

In the 1960s, the first HTGR prototypes became operative, including the Dragon Reactor Experiment (U.K.), the AVR (Germany) and the Peach Bottom (U.S.A.). The Dragon Reactor Experiment was a 20 MWth reactor using graphite fuel elements with high-enriched uranium-thorium carbide coated fuel particles and helium as coolant. During the periods of operation at full power, it was possible to demonstrate the correct functioning of different components, and in particular, of the purification system. The AVR reactor, having a power of 15 MWe (46 MWth) and using spherical fuel particles, was able to reach an outlet coolant temperature of 1223 K. The Peach Bottom Unit 1 was a 40 MWe plant built in the U.S.A. All these prototypes of reactors provided an important demonstration of the HTGR concept, confirming methodologies of analysis/calculation and producing experimental data for further design activities.

The following step in the HTGR evolution consisted of the construction of demonstration plants. Two basic core designs were taken into account: the German concept, which used spherical fuel elements and the U.S. concept, which considered rods with inside ceramic coated fuel elements, inserted in hexagonal shaped graphite elements. The demonstration plants that followed the first HTGR prototypes were the reactors Fort St. Vrain (FSV) and Thorium High Temperature Reactor THTR-300. The FSV plant generated a power of 330 MWe (842 MWth); it included advanced characteristics such as a Prestressed Concrete Reactor Vessel (PCRV), containing the primary coolant system, and a core having hexagonal fuel elements made of graphite, with ceramic coated particles as fuel. The FSV was characterized by a low availability due to problems with helium circulators; despite the problems, the reactor was able to demonstrate the good performances of several systems, such as the purification system. The THTR-300 plant generated a power of 296 MWe; the short life of the reactor was sufficient to validate the safety characteristics of the plant, the thermodynamics of the primary system and the good retention of the fission products inside the fuel elements.

In the 1970s and early 1980s the work of the HTGR designers was focused to the study of large steam cycle HTGR plants. These studies included the German HTR-500, the Russian VG-400 and the U.S. HTGR-Steam Cycle plants. In addition to the above studies, in the 1970s U.S., Germany, U.K. and France started to study the possibility to use the high temperature capability of the primary helium coolant to drive a gas turbine in a direct closed cycle.

In the 1980s the modular concept of the HTGR started to be developed, because able to improve further the safety, thanks to the capability to cool down the reactor by means of passive heat transfer mechanisms, avoiding damaging of the fuel particles. The 80 MWe HTR-MODULE was the first modular HTGR proposed by Germany. The design of this reactor foresaw that, even in case of complete failure of all active cooling systems, no release of fission products from fuel elements it would have occurred. Other modular HTGRs have been studied in Russia (VGM modular HTGR) and U.S. (Modular High-Temperature Gas-Cooled Reactor (MHTGR)).

In the 1980s and early 1990s, the interest of the international HTGR community focused on the capability of the modular HTGR to supply high temperature process heat for industrial applications. In this context JAERI (Japan) and INET (China) decided to construct the High Temperature Engineering Test Reactor (HTTR) and the High Temperature Gas Cooled Reactor Test Module (HTR-10), respectively. The 30 MWth HTTR is a reactor using graphite as moderator and helium as coolant; it includes hexagonal fuel elements with TRISO coated fuel particles. The 10 MWth HTR-10 is a pebble bed reactor using helium as cooling gas.

In the same period, the interest of the designers moved from the Rankine steam cycle to the Brayton cycle, for the electricity production. Direct coupling of HTGRs to a gas turbine allows to have higher efficiency and lower costs, due to the plant simplification. This interest materialized in some new designs such as the Gas Turbine-Modular Helium Reactor (GT-MHR) and the Pebble Bed Modular Reactor (PBMR).

The interest on HTGRs never decreased over the years; in the ambit of the international cooperation in research on the advanced nuclear systems, called Generation IV, two of the six systems included in the Generation IV list are gas cooled reactors, and in particular a Very High Temperature Reactor and a Gas cooled Fast Reactor (GFR).

2.2 Impurity issue in HTGRs

Impurities present in the main cooling system of a HTGR can originate various types of issues to be taken into account for the design of the CPS. The main impurities expected in the helium coolant of a HTGR are H_2, CO, CO_2, O_2, N_2, CH_4, H_2O, Ar, Ne and the fission products Xe and Kr [8]. These impurities can have different origins, as shown in the following Table.

Table 1: Sources of impurities in HTGRs

Graphite outgassing	H_2, CO, CO_2, N_2, CH_4, H_2O
Air entrance	CO, CO_2, O_2, N_2, Ar,
Steam entrance	H_2, CO, CO_2, H_2O, CH_4
Oil entrance	H_2, CH_4
Charging tank contamination	Ne, Ar, H_2O, air
Proton diffusion through steam pipe	H_2

The purification system must reduce the impurity concentration to the level required to avoid the following phenomena [7]:

- hydrogen embrittlement;
- core graphite oxidation;
- carbon deposition;
- decarburization of the high-temperature materials.

The most important reactions among impurities and core graphite are [7]:

$$C + H_2O \leftrightarrow CO + H_2 \quad (2.1)$$

$$C + CO_2 \leftrightarrow 2CO \quad (2.2)$$

$$CO + H_2O \leftrightarrow CO_2 + H_2 \quad (2.3)$$

$$CH_4 \leftrightarrow C + 2H_2 \quad (2.4)$$

$$C + xO_2 \leftrightarrow yCO + zCO_2 \quad (2.5)$$

$$2CO + O_2 \leftrightarrow 2CO_2 \quad (2.6)$$

The carbon deposition reactions are the reverse reactions of (2.1) and (2.2). They generally occur at a temperature between 573 and 873 K, with a maximum reaction velocity between 723 and 773 K. Water and carbon dioxide react with graphite at temperature above 973 K.

Other important reactions concern the oxidation of the steels [8]:

$$Fe + H_2O \leftrightarrow FeO + H_2 \quad (2.7)$$

$$3Fe + 4H_2O \leftrightarrow Fe_3\,O_4 + 4H_2 \quad (2.8)$$

2.3 Coolant purification systems in HTGRs

In the context of the fusion program F4E-2008-Grant09, a review of the purification systems used in helium cooled reactors has been carried out in order to study their applicability to the CPS of the ITER Test Blanket Modules (TBMs), type Helium Cooled Pebble Bed (HCPB) and Helium Cooled Lithium Lead (HCLL) [5]. Purification systems have been used in the past for helium cooled fission reactors, mainly to eliminate impurities causing the oxidation of the graphite moderator and the corrosion of the materials exposed to high temperature. Three examples were considered particularly interesting: the Fort St. Vrain HTGR and the experimental gas reactors HTR-10 and HTTR. In the following paragraphs will be described the main characteristics of the purification systems used in the most interesting helium cooled reactors, starting from the first prototype reactors, until the last designs.

2.3.1 Dragon Reactor Experiment

The 20 MWth Dragon Reactor Experiment, a prototype of HTGR using helium as coolant, was built in U.K. and operated from 1964 to 1975. The helium coolant was characterized by a pressure of 2.0 MPa, a temperature, at the inlet/outlet of the core, of 623/1023 K and a flow rate of approx. 9.6 kg/s [9]. A simplified Process Flow Diagram (PFD) of the system is shown in Figure 3.

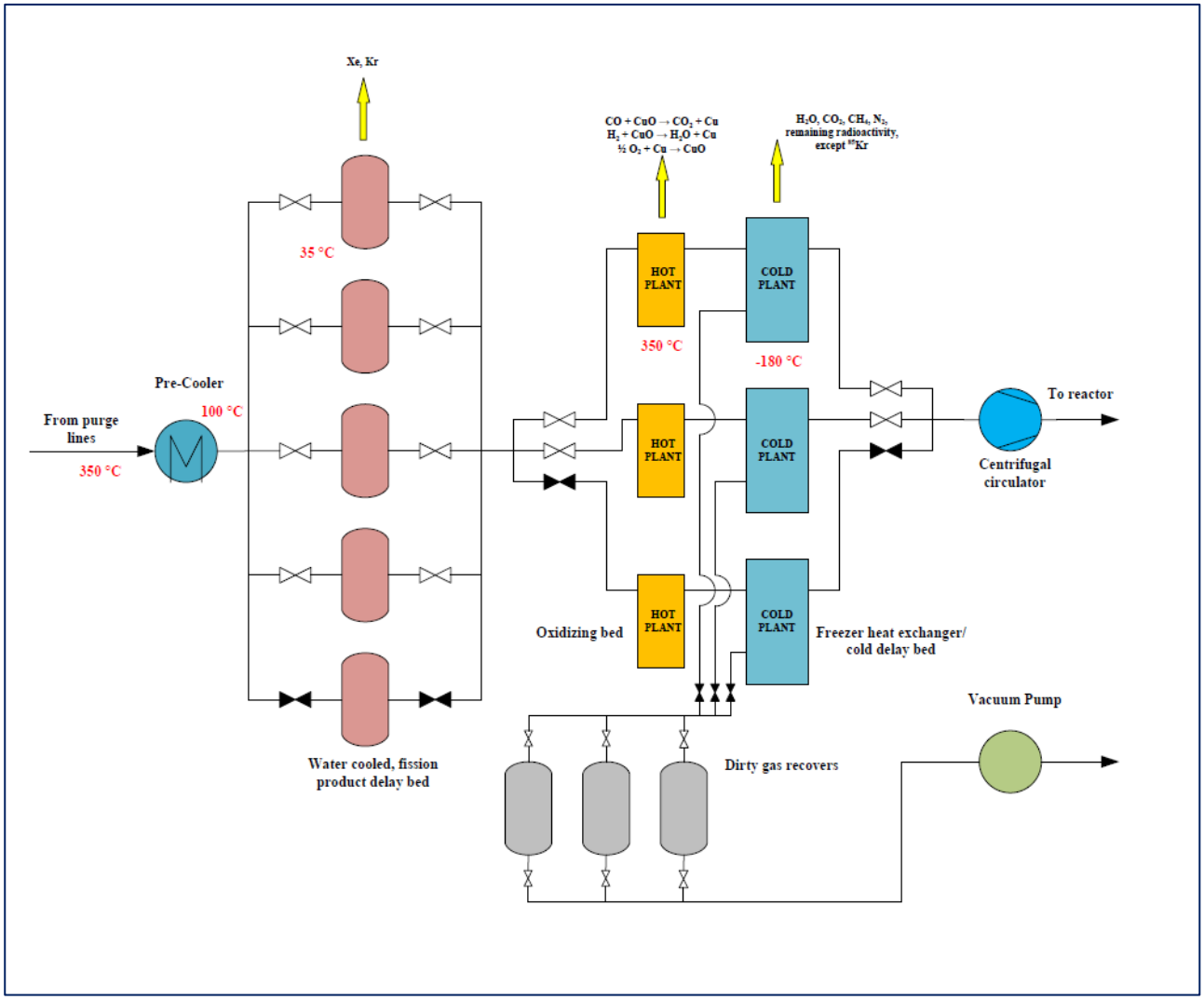

Figure 3: PFD of Dragon Reactor Experiment CPS

The purification system of the reactor foresaw purge lines, located at the bottom of each fuel element, from which purge streams were collected in a manifold and the main flow (0.0078 kg/s) sent to a pre-cooler, which reduced the helium temperature from 623 to 373 K. Then the purification flow was directed to five water-cooled, fission product delay beds, which were filled with charcoal. The decay heat of the fission products having short life was removed by delay beds, reducing the temperature of helium at approx. 308 K. Usually, only four out of five delay beds were used in parallel (the fifth is a spare). In HTGRs, some gaseous fission products are condensable or have short life, producing condensable long life daughters. With the scope to avoid the deposition of long life isotopes in different parts of the plant, these beds delayed the transport of short life fission products, allowing them to decay inside the adsorption material in which the long life daughters remain trapped. After the delay beds, the gas was sent to the chemical purification plant, consisting of three identical purification systems, two of them working in purification phase and one in regeneration phase. The scope of the chemical purification plant was to clean the helium from both chemical (H_2, H_2O, CO, CO_2, CH_4, N_2) and radioactive impurities. Each purification system consisted of a high temperature part, followed by a low temperature part. In the hot part, an oxidizing bed of CuO, working at approx. 623 K, transformed carbon monoxide and hydrogen into

carbon dioxide and water, respectively; oxygen was removed by pure Cu, located at the end of the bed. In the low temperature part, the gas was cooled at approx. 93 K in a freezer heat exchanger, and CO_2 and H_2O removed as solid deposits. Then, a small cold delay bed, in which charcoal was cooled by boiling liquid nitrogen, removed all remaining radioactivity (except $^{85}_{36}Kr$). The purified gas, before being routed to the reactor by means of a centrifugal circulator, was cooled, passing through a pipe immersed in the liquid nitrogen of the delay bed, and used to cool down the gas entering in the freezer heat exchanger; in this manner the temperature of the purified gas increased up to room temperature.

The following Table summarizes the operating conditions of the primary cooling system and impurity levels in normal operating operation [9].

Table 2: Conditions and impurity levels in primary cooling system of Dragon Reactor Experiment

Primary coolant conditions and impurities	Values
Pressure (MPa)	2.0
Core inlet/outlet temperature (K)	623/1023
Coolant flow rate (kg/s)	9.6
H_2O (ppmv)	0.1
H_2 (ppmv)	0.1
CO (ppmv)	0.05
CO_2 (ppmv)	0.02
CH_4 (ppmv)	0.1
N_2 (ppmv)	0.05
O_2 (ppmv)	0.1

2.3.2 Peach Bottom

The Peach Bottom was a nuclear plant of 40 MWe (115 MWth) using helium as coolant. The reactor operated in U.S.A from 1967 to 1974. The helium coolant was characterized by a pressure of 2.4 MPa, a temperature, at the inlet/outlet of the core, of 600/1000 K and a flow rate of 58.3 kg/s [8], [10], [11]. Two independent purification loops were foreseen to clean fission products and chemical impurities. A simplified PFD of the system is shown in Figure 4 [12].

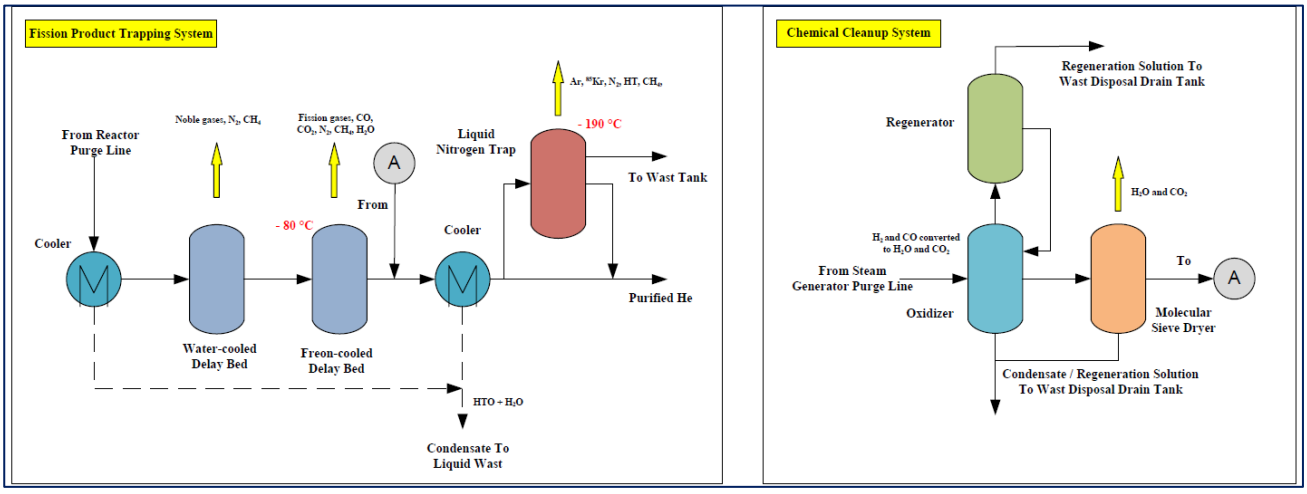

Figure 4: PFD of Peach Bottom CPS

Inside the reactor, a helium flow rate of approx. 0.094 kg/s was withdrawn from the primary coolant system and sent to Fission Product Trapping System (FPTS). In addition, a flow rate of 0.022 kg/s of helium was withdrawn from the Steam Generator (SG) and sent to a Chemical Cleanup System (CCS) to remove impurities as H_2O, H_2, CO and CO_2 [8]. The FPTS was composed by a series of water cooled activated carbon beds, followed by Freon cooled delay beds, having the scope to

remove fission gases by delay and subsequent decay of radioactive elements. Because the beds worked at low temperature (193 K), they were also able to remove CO_2 and H_2O. In addition, the beds adsorbed a quite large amount of N_2, CO, CH_4. The beds were not very effective for hydrogen and tritium. After the delay beds, a liquid nitrogen cooled carbon bed was present, in which a small bypass stream (22.7 to 45.4 kg/h), withdrawn from the purified helium, was directed. This trap, working at 83 K, removed by adsorption all gaseous impurities not previously removed (except H_2 and Ne), and in particular ^{85}Kr, Ar, N_2 and CH_4. This trap was very effective to remove tritium [11].

The bypass stream of the CCS, having a flow rate of 79.4 kg/h, was sent to a copper oxide bed, to oxidize CO and H_2 into CO_2 and H_2O, respectively. Then the bypass stream entered one of the two molecular sieve beds, for CO_2 and H_2O removal. This purification loop effectively removed tritium, in the form of tritiated water, as well as CO, H_2, CO_2 and H_2O [8], [11].

The technical specification foresaw the following impurity upper limits: 10 ppmv of CO, 2 ppmv of CO_2, 2 ppmv of CH_4. The following Table summarizes the operating conditions of the primary cooling system and impurity levels at steady-state operation (the impurities are referred to a condition with the reactor at 100% of nominal power) [10]:

Table 3: Operating conditions and impurity levels in primary cooling system of Peach Bottom

Primary coolant conditions and impurities	**Values**
Pressure (MPa)	2.4
Core inlet/outlet temperature (K)	600/1000
Coolant flow rate (kg/s)	58.3
H_2O (ppmv)	0.5
H_2 (ppmv)	10
CO (ppmv)	0.5
CO_2 (ppmv)	< 0.05
CH_4 (ppmv)	1
N_2 (ppmv)	0.5
O_2 (ppmv)	NA

2.3.3 Fort St. Vrain HTGR

The Fort St. Vrain HTGR was a nuclear plant of 330 MWe (842 MWth) using helium as coolant. The reactor operated in U.S.A from 1979 to 1989. The helium coolant was characterized by a pressure of 4.8 MPa, a flow rate of 428 kg/s and a temperature, at the inlet/outlet of the core, of 680/1050 K [10], [13], [14]. The fission products and the chemical impurities were controlled by a bypass purification stream having a flow rate corresponding to 12%/h of the primary coolant (51.4 kg/s) [11]. The CPS was composed of two identical loops; during normal operation of the reactor, one was in operation, while the other one was in regeneration phase or on standby.

Each of the two loops was composed by the following components [15]:

- a filter-adsorber for high temperature;
- a purification cooler, including a water-cooled heat exchanger and a separator for the removal of the condensed water;
- a molecular sieve bed (dryer);
- a gas to gas exchanger operating at low temperature;
- a charcoal adsorber operating at liquid nitrogen temperature;
- a filter to protect the compressors from the dust of the adsorber bed;
- a helium compressor (with another in standby).

The main loop was completed by two subsystems, the first one for regeneration of the adsorbing beds and the second one to remove H_2 and tritium. The regeneration loop included a cooler, a knockout drum (vapor-liquid separator), a molecular sieve dryer, a compressor and a heater. The

loop for the H_2 and tritium removal included an economizer, two getter beds, using titanium sponge material, a filter and a cooler. A simplified PFD of the system is shown in the following Figure [15].

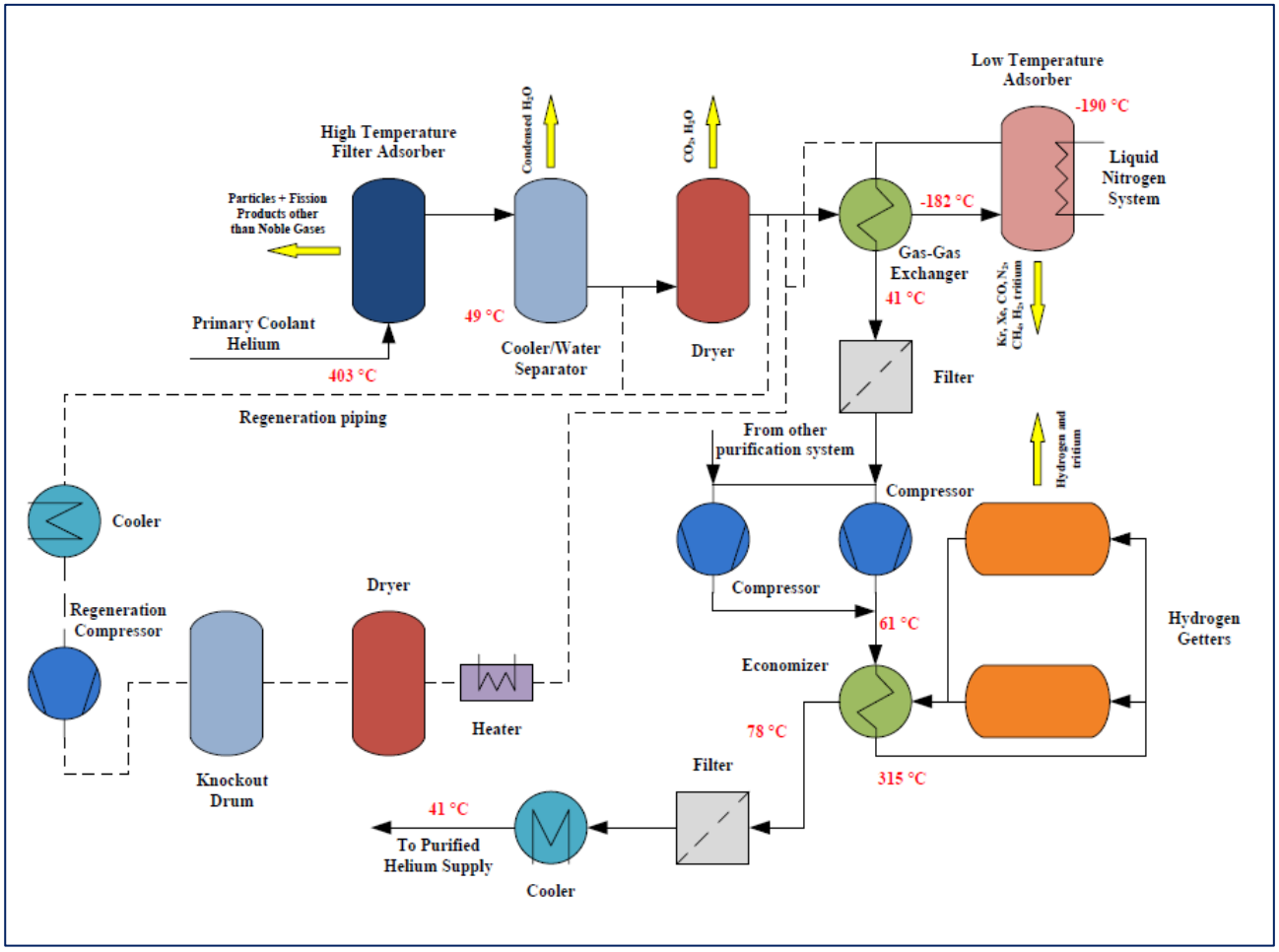

Figure 5: PFD of Fort St. Vrain CPS

In normal operating conditions, helium entered at approx. 676 K in the high temperature filter-adsorber, where dust particles, metallic fission products and some volatile electronegative fission products were eliminated by a centrifugal dust separator and a potassium-impregnated charcoal adsorber. At the exit of the adsorber, a filter eliminated the charcoal dust. After the filter, the helium gas entered in a water-cooler, in which the temperature was reduced at approx. 322 K; a water separator included in the component had the scope to remove the condensed water. Then, the cooled helium flowed through a molecular sieve dryer, which removed water vapor and CO_2 by adsorption. The helium, cooled to 91 K by a gas-gas heat exchanger, entered in a low temperature adsorber, using liquid nitrogen to have a gas temperature of 83 K. The charcoal adsorber removed the impurities Kr, Xe, CO, O_2, N_2, CH_4 and some H_2 and tritium. The helium was re-heated to about 314 K, passing through the gas-gas exchanger, and then filtered, to remove solid particles released by the low temperature adsorber. After the compressor, the gas, at a temperature of approx. 334 K, entered in the subsystem dedicated to the removal of the hydrogen isotopes. In this system the helium was heated at approx. 588 K, by an economizer heat exchanger. Two getters, one in operation and the other one in standby, used hot titanium sponge material to remove hydrogen isotopes by adsorption. Finally the purified helium passed again through the economizer, reducing the temperature to approx. 351 K, a filter and a cooler, to be available to the users at a temperature of approx. 314 K.

Initially the loop had to operate in purification phase for six months without regeneration. Before starting with the regeneration, a waiting time of two months was considered necessary, to allow the decay of the entrapped radionuclides (in particular for the low temperature adsorber). In reality the loop required to be regenerated after 1-3 months and the regeneration didn't need to wait two months, due to a presence of radionuclides lower than expected. The loop was depressurized to

approx. 0.7 MPa(a) before regeneration. Liquid and gaseous impurities were removed by hot helium and discharged in the waste systems. The hydrogen and tritium subsystem operated approx. twice a year. At the beginning the hydrogen isotopes had to be released to the gaseous waste systems by heating the titanium sponge. Later it was decided to replace the titanium sponge material, in general after significant shutdown of the plant [15].

The purification system had good performances, with the exception of the titanium getter beds. Occasional contaminations of the helium with nitrogen reduced the H_2 removal efficiency of the beds (the nitrogen came from the liquid-nitrogen-cooled carbon beds). Despite the hydrogen getters worked only sporadically, an increase of the H_2 concentration in the helium coolant was not noted; it was deduced that the excess of H_2 was trapped by the graphite components.

Tritium can be produced by ternary fission, neutron reactions with impurities in the graphite and with boron in control rods. Tritium can be also generated by a reaction involving the helium isotope ${}^{3}_{2}He$, present in very small quantity in the helium coolant:

$$ {}^{3}_{2}He + {}^{1}_{0}n \rightarrow {}^{1}_{1}H + {}^{3}_{1}H \qquad (2.9) $$

Since ^{3}He is included in the primary coolant helium, the generated tritium was supposed to be removed in the purification system. The circulating tritium can produce tritiated compounds (mainly water and methane); during an initial period of 101 Effective Full Power Days (EFPDs), a total of 307 Ci of tritium, in HTO form, was removed by the purification system. The amount removed by titanium getters was not measured. In this period, the main part of tritium was in HTO form and the 307 Ci correspond approx. to the amount produced by the activation of ${}^{3}_{2}He$[10].

The oxidation of the graphite was minimal, due to the low impurity concentration allowed for high coolant temperatures. For example, for temperature higher than 922 K, the sum of all the oxidant impurities (CO, CO_2, H_2O) had to be lower than 10 ppmv. The limits of the impurities were set considerably higher for helium temperature lower than 922 K, because for these temperatures the corrosion of the graphite by the impurities is expected to be low.

The following Table summarizes the operating conditions of the primary cooling system and impurity levels at steady-state operation (with the reactor at 63% of nominal power) [10], [11].

Table 4: Operating conditions and impurity levels in primary cooling system of FSV

Primary coolant conditions and impurities	**Values**
Pressure (MPa)	4.8
Core inlet/outlet temperature (K)	680/1050
Coolant flow rate (kg/s)	428
H_2O (ppmv)	< 1
H_2 (ppmv)	7
CO (ppmv)	3
CO_2 (ppmv)	1
CH_4 (ppmv)	0.1
N_2 (ppmv)	NA
O_2 (ppmv)	NA

2.3.4 HTR-10

The Chinese High Temperature Reactor HTR-10 is a 10 MWth prototype pebble-bed reactor, cooled with helium having a flow rate of 4.3 kg/s, a pressure of 3.0 MPa and a temperature, at reactor inlet/output, of approx. 523/923 K [16]. The construction began in 1995, the first criticality was reached in 2000 and the operation in full power condition started in 2003. The purification system is designed to purify a bypass stream corresponding to 5% of the helium inventory in the

primary coolant every hour (10.5 kg/h of helium) [17]. The CPS is mainly composed by the following components [17]:

- a cartridge filter;
- a heater;
- a copper oxide bed;
- a dust filter;
- a gas-gas heat exchanger;
- a water cooler;
- a helium cooler;
- a moisture separator;
- a molecular sieve adsorber;
- a low temperature gas-gas heat exchanger;
- a low temperature adsorber;
- two diaphragm compressors.

A simplified PFD of the system is shown in the following Figure 6 [17].

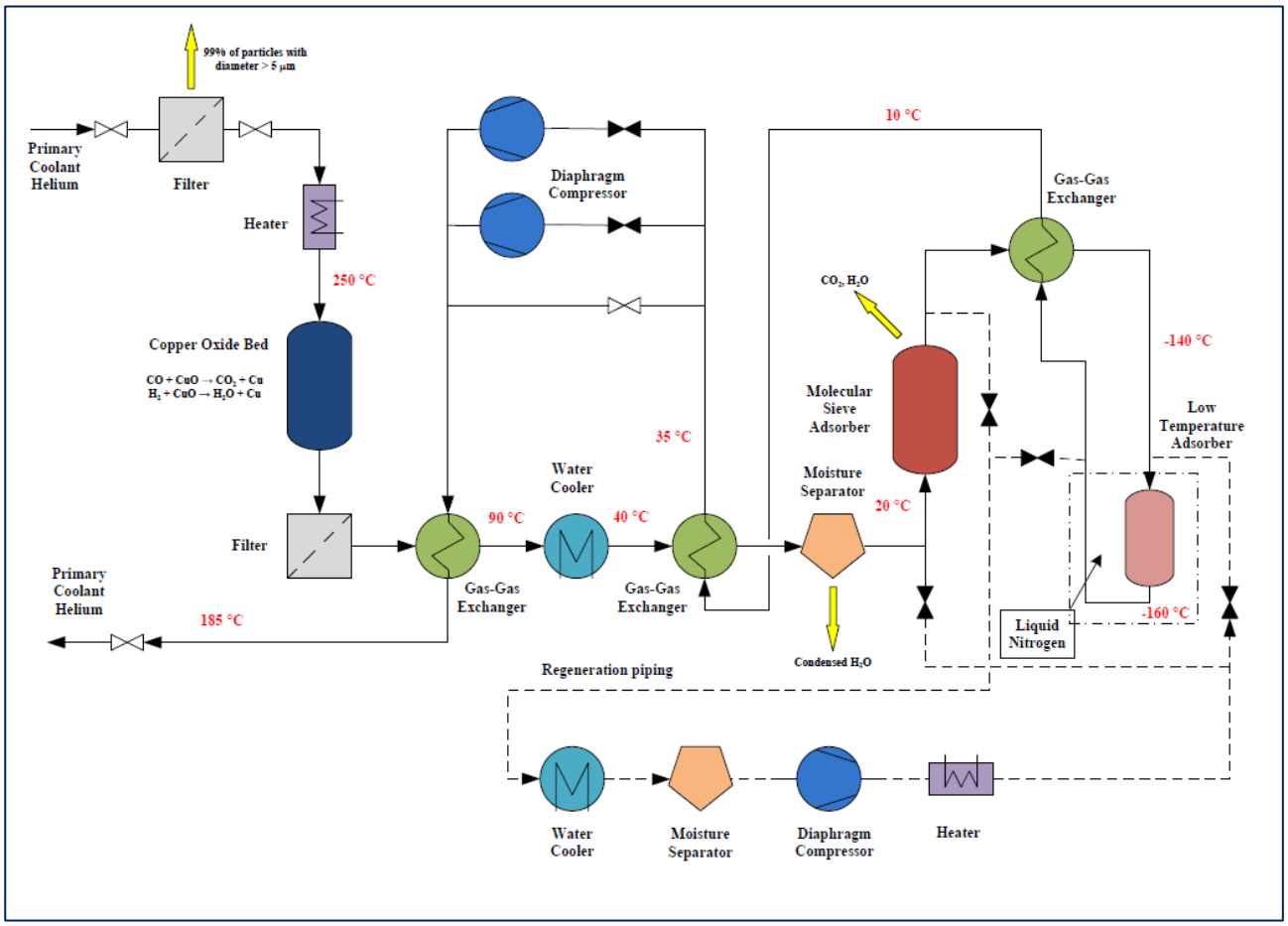

Figure 6: PFD of HTR-10 CPS

In normal operating conditions, from the outlet of the primary helium circulator, a bypass stream (10.5 kg/h) at 523 K and 3.0 MPa is driven at the inlet of the CPS by the pressure head of the circulator. At the exit of the purification system, the helium is sent back at approx. 458 K to the inlet of the primary helium circulator. Two diaphragm circulators (one in stand-by) provide the necessary pressure head to drive the helium stream when the primary helium circulator is shutdown. At the inlet of the CPS, the cartridge filter has the scope to remove dust impurities with an efficiency of approx. 99%, for particles having a diameter greater than 5 μm. The helium flows through a heater, where it is heated at 523 K, and enters in a copper oxide bed in which hydrogen/tritium and carbon monoxide are oxidized into tritiated water vapor and carbon dioxide, respectively. At high temperature, the copper present in the bed removes also the oxygen, by adsorption. After a dust

filter, the helium passes through gas-gas heat exchanger where its temperature decreases from approx. 523 K to 363 K. The helium temperature is further decreased from 363 K to 313 K, passing through a water cooler, and from 313 K to approx. 293 K in a cold helium cooler. The moisture separator operates only in case of accidental entry of water because, in normal conditions, the relative humidity of the primary coolant helium is very low. The water and carbon dioxide included in the helium are then adsorbed in a molecular sieve bed. Then helium is cooled at approx. 133 K, passing through a low temperature He-He heat exchanger, in which energy is exchanged with the cooled helium coming back from the low temperature adsorber. Methane, oxygen, nitrogen, krypton and xenon are removed in a low temperature adsorber, using charcoal at a temperature of approx. 113 K, obtained by liquid nitrogen. The purified helium is re-heated up to 283 K, in the low temperature He-He heat exchanger, then heated up to 308 K, in the second He-He heat exchanger, and finally up to 458 K, after the last heat exchanger. The preliminary purification tests have shown that the efficiency of the system is higher than 99% [17].

The regeneration system includes a cooler, a moisture separator, a diaphragm compressor and a heater. For the regeneration of the adsorbers, the loop is depressurized to 0.6 MPa. The molecular sieve adsorber is insulated from the purification loop and connected to the regeneration system. Then, the molecular sieve adsorber is crossed by the regeneration gas, heated up to 553 K by a heater and driven by the diaphragm compressor; the value of the regeneration flow rate is 10.5 kg/h. The helium circulates inside the adsorber until its temperature reaches 523 K. At this temperature CO_2 and water are desorbed from the bed and enter in the helium flow. In the water cooler the helium temperature decreases at approx. 293 K. The main part of water is condensed and removed in the moisture separator. Then, the cooler, diaphragm compressor and the moisture separator are disconnected and the regeneration gas in the molecular sieve is released in the waste system until the pressure of 0.1 MPa is reached. By further evacuation, the pressure reaches values less than 100 Pa; at this pressure, only very small residual amount of CO_2 and water remain in the adsorber. The procedure for the regeneration of the low temperature adsorber is very similar, with the exception of the regeneration temperature, which is 423 K instead of 523 K, and the thawing of the bed that must precede the heating [17].

The regeneration of the cooper oxide bed is performed at 353 K, fluxing continuously oxygen with a flow rate of 0.52 kg/h, at the inlet of the bed; at the end of the operation, the system is depressurized at approx. 100 Pa [17].

In normal operating conditions, the impurities are originated by desorption of reactor components, residual air and leakage from the external environment, leakage of fission products from fuel, water leakage from steam generator, contaminants from new helium supply. The following Table summarizes the operating conditions of the primary cooling system and the expected impurity levels at steady-state operation [17].

Table 5: Operating conditions and expected impurity levels in primary cooling system of HTR-10

Primary coolant conditions and impurities	**Values**
Pressure (MPa)	3.0
Core inlet/outlet temperature (K)	523/973
Coolant flow rate (kg/s)	4.3
H_2O (ppmv)	≤ 0.2
H_2 (ppmv)	≤ 3
CO (ppmv)	≤ 3
CO_2 (ppmv)	NA
CH_4 (ppmv)	≤ 1
N_2 (ppmv)	≤ 1
O_2 (ppmv)	NA

2.3.5 HTTR

The Japanese High Temperature Engineering Test Reactor HTTR is a 30 MWth test reactor, which reached its full design power in 1999. The reactor is moderated by graphite and cooled by helium, having a flow rate of 10.2 kg/s and a pressure of 4.0 MPa. The reactor maximum output temperature is 1223 K, while the input temperature is 668 K [18].

The loop of the CPS is mainly composed by the following components [19]:

- an inlet filter;
- a pre-charcoal trap;
- a heater;
- two copper oxide fixed beds;
- a cooler;
- two molecular sieve traps;
- two cold charcoal traps;
- a circulator filter;
- two gas circulators;
- a re-heater.

A simplified PFD of the system is shown in the following Figure.

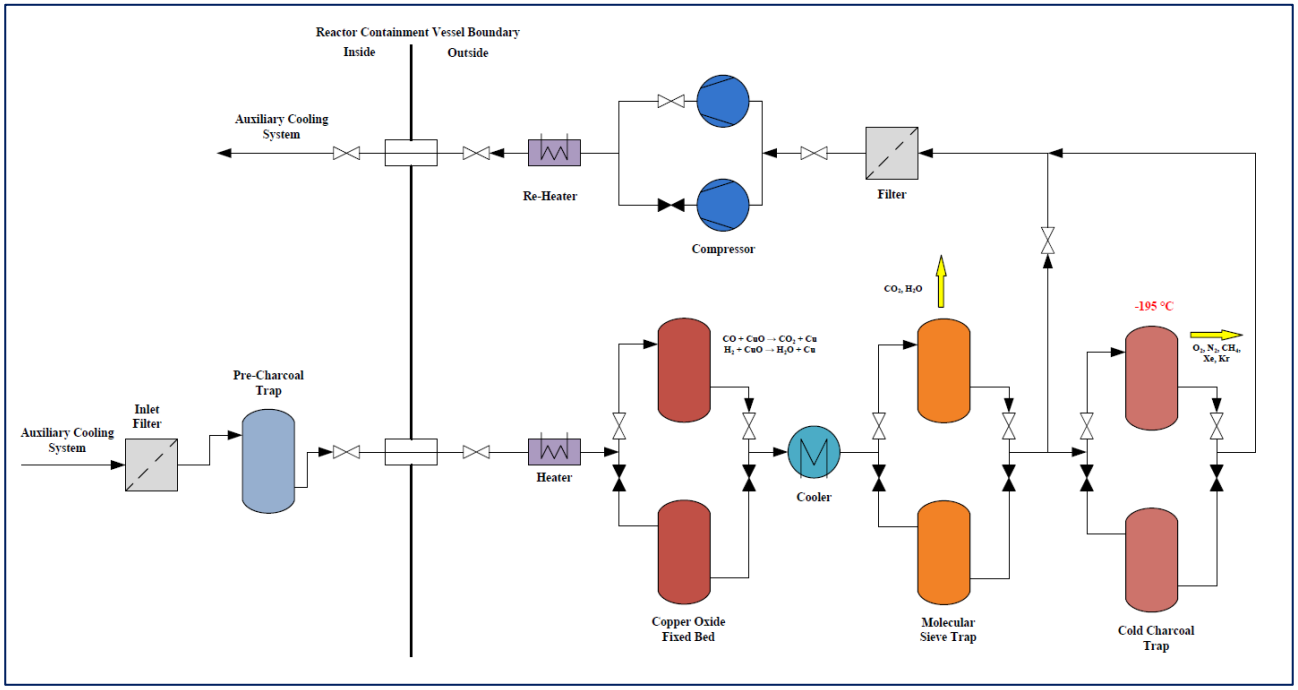

Figure 7: PFD of HTTR CPS

The CPS foresees three different types of traps for the removal of chemical impurities. With the exception of the pre-charcoal trap, for reliability reasons of the plant operation, each trap consists of two identical components. After the pre-charcoal trap, a heater increases the temperature of helium to 553 K. Then the helium enters in a copper oxide fixed bed in which hydrogen and CO are oxidized into water and CO_2, respectively. A cooler reduces the temperature of the gas before entering in a molecular sieve bed, in which water and CO_2 are adsorbed. The third trap has the scope to remove O_2, N_2, CH_4, Xe and Kr. The trap operates at 78 K. The main flow rate of the CPS is 0.055 kg/s. The flow rate passing through the cold charcoal trap is 0.014 kg/s; the remaining flow passes through a by-pass line [19].

The following Table summarizes the operating conditions of the primary cooling system and limit levels of the impurities [19].

Table 6: Operating conditions and limit levels of impurities in primary cooling system of HTTR

Primary coolant conditions and impurities	Values
Pressure (MPa)	4.0
Core inlet/outlet temperature (K)	668/1223
Coolant flow rate (kg/s)	10.2
H_2O (ppmv)	≤ 0.2
H_2 (ppmv)	≤ 3
CO (ppmv)	≤ 3
CO_2 (ppmv)	≤ 0.6
CH_4 (ppmv)	≤ 0.5
N_2 (ppmv)	≤ 0.2
O_2 (ppmv)	≤ 0.04

2.3.6 MHTR/GT-MHR

The purification systems relevant to the MHTTR and GT-MHR are very similar [11] and, for this reason, only the GT-MHR will be considered.

The reference concept consists of four identical modules, each of them includes a 600 MWth reactor, coupled with a gas turbine. The reactor is moderated by graphite and cooled by helium at approx. 7.1 MPa. The reactor inlet/output temperature is 764/1123 K and the total coolant flow rate is approx. 320 kg/s [20].

For a typical four module plant, the purification system consists of four purification sections and two regeneration sections (one for two reactor modules). Each section can purify a maximum flow rate of 0.567 kg/s. In normal operating conditions, helium is withdrawn at the outlet of the cooling system compressor and returns, after purification, to the cooling system. The system includes filters, dryers, packed beds, heat exchangers and compressors. The simplified PFD of the system is shown in the following Figure in which it is possible to observe that, for some components, it is foreseen a redundancy.

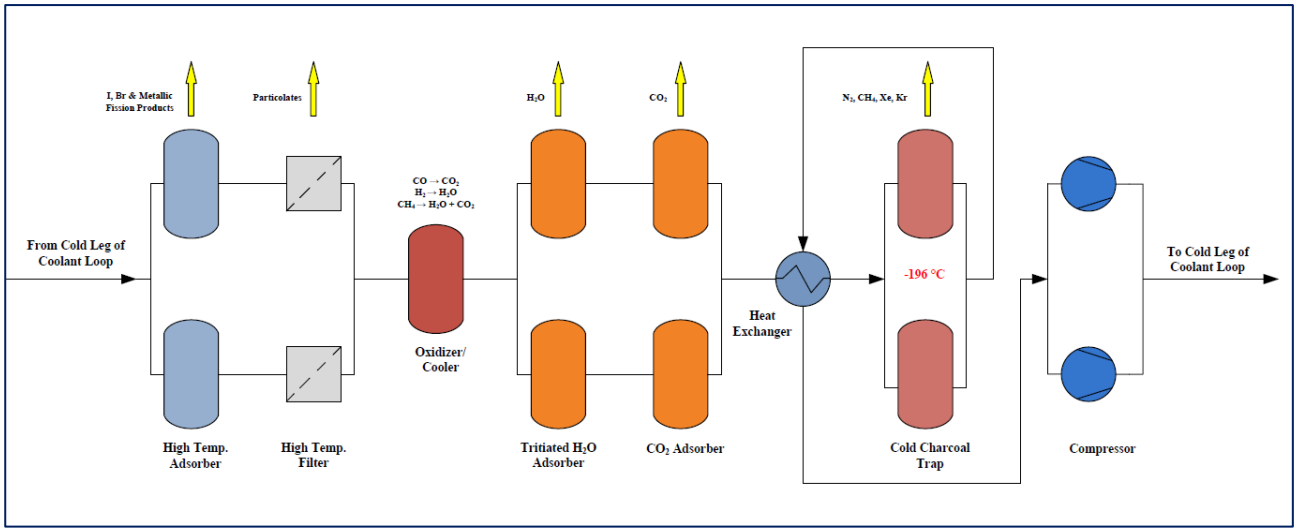

Figure 8: PFD of GT-MHR CPS

The purification system foresees, at the inlet, a high temperature adsorber, to remove iodine, bromine and metallic fission products and a high temperature filter, to remove particulate materials. The helium goes through an oxidizer, in which the hydrogen and the carbon monoxide are oxidized

into water and carbon dioxide, and then it is cooled by a water cooler at approx. 311 K. The cooled helium passes through an adsorber cartridge, to remove the water, and then through a carbon dioxide adsorber. Finally the helium goes through a low temperature adsorber, operating at liquid nitrogen temperature, in which charcoal remove noble gases and other fission products [11], [20].

The following Table summarizes the operating conditions of the primary cooling system and limit levels of the impurities. Since the GT-MHR has been designed but not built, the impurity levels, referred to normal operating conditions, has to be considered an estimate [11].

Table 7: Operating conditions and limit levels of impurities in primary cooling system of GT-MHR

Primary coolant conditions and impurities	Values
Pressure (MPa)	7.1
Core inlet/outlet temperature (K)	764/1123
Coolant flow rate (kg/s)	320
H_2O (ppmv)	≤ 2
H_2 (ppmv)	NA
CO + CO_2 (ppmv)	≤ 6
CH_4 (ppmv)	NA
N_2 (ppmv)	NA
O_2 (ppmv)	NA

2.3.7 Comparison of the purification systems in HTGRs

In the following Table, the components used in the purification systems of the different HTGRs and their operating conditions are compared [11].

Table 8: CPS components and their operating conditions

Reactor Type	Component	Removed Impurity	Type of Reaction	Operating Temperature (K)	Flow Rate (kg/s)
Dragon Reactor Experiment	Water-cooled charcoal delay beds	Fission product noble gases	Adsorption	308	0.0078
	Copper-oxide oxidizing bed	H_2 and CO are transformed into H_2O and CO_2; O_2 removed by pure Cu	Oxidation	623	0.0078
	Freezer heat exchanger	H_2O and CO_2	Deposition	93	0.0078
	Liquid-nitrogen charcoal delay beds	N_2, CH_4 and remaining radioactive impurities, excluding Kr	Adsorption	93	0.0078
Peach Bottom	Water-cooled activated carbon beds	Fission product noble gases, N_2, CH_4	Adsorption	-	0.094
	Freon-cooled delay beds	Fission gases, N_2, CO, CO_2, CH_4, H_2O	Adsorption	193	0.094
	Liquid-nitrogen cooled carbon bed	Ar, N_2, CH_4, ^{85}Kr, HT (excluded H_2 and Ne),	Adsorption	83	0.0063 – 0.0126

	Copper oxide bed	H_2 and CO are transformed into H_2O and CO_2	Oxidation	-	0.022
	Molecular sieve bed	H_2O and CO_2	Adsorption	-	0.022
Fort St. Vrain	High temperature, potassium impregnated charcoal, filter adsorber	Dust particles, metallic and volatile fission products	Filter and deposition	676	51.4
	Cooler/water separator	Condensed H_2O	Condensation	322	51.4
	Molecular sieve dryer	H_2O and CO_2	Adsorption	322	51.4
	Liquid-nitrogen cooled charcoal bed	Xe, N_2,CO, O_2, Kr, CH_4 and some H_2 and HT	Adsorption	83	51.4
	Filter	Particles and dust	Filter	314	51.4
	Titanium sponge getter	Hydrogen isotopes	Adsorption	588	51.4
	Filter	Removes particles and dust	Filter	351	51.4
HTR-10	Cartridge Filter	Particles and dust	Filter	523	0.0029
	Copper oxide bed	H_2 and CO transformed into H_2O and CO_2. O_2 removed by pure Cu	Oxidation	523	0.0029
	Molecular sieve adsorber	H_2O and CO_2	Adsorption	293	0.0029
	Low temperature adsorber	Xe, Kr, O_2, N_2, CH_4	Adsorption	113	0.0029
HTTR	Filter	Particles and dust	Filter	< 553	0.055
	Pre-charcoal trap	Gaseous fission products	Adsorption	553	0.055
	Copper oxide fixed bed	H_2 and CO transformed into H_2O and CO_2	Oxidation	553	0.055
	Molecular sieve trap	H_2O and CO_2	Adsorption	-	0.055
	Cold charcoal trap	Xe, Kr, N_2, O_2, CH_4	Adsorption	78	0.014
GT-MHR	High Temperature adsorber	I, Br, metallic fission products	Filter and deposition	-	0.567
	High temperature filter	Particulates	Filter	-	0.567
	Oxidizer	H_2 and CO are transformed into H_2O and CO_2	Oxidation	-	0.567
	Adsorber cartridge	H_2O	Adsorption	-	0.567
	Carbon dioxide adsorber	CO_2	Adsorption	-	0.567
	Cold charcoal trap	Xe, Kr, N_2, CH_4	Adsorption	77	0.567

Comparing the components used in the different purification systems it is possible to note that they are very similar. In particular, five different components are used for the separation of the impurities from the helium coolant [11]:

- filter/adsorber;
- oxidizing bed;
- molecular sieve bed;
- cooled charcoal bed;
- getter bed.

The filter/adsorber operates at temperatures lower than the outlet temperatures of the reactors, allowing the removal of particulate matter and the deposition of long-lived fission products. In the oxidizing beds some impurities, such as hydrogen and carbon monoxide, are oxidized; the resulting chemical species are more easily removable from the coolant gas. The molecular sieve beds are able to adsorbe different impurities until their saturation is reached and then regeneration is required. The charcoal beds are able to remove impurities by trapping them in the charcoal; lower is the operating temperature, higher is the effectiveness of the component. The metallic getters are able to react with specific gas species, such as hydrogen. Metallic getter was used only in FSV to remove hydrogen and tritium, but it resulted highly ineffective due to the contamination of the helium coolant from nitrogen and water vapor.

With the exception of FSV, all the purification systems foresee the presence of an oxidizing bed to transform H_2 and HT into H_2O and HTO, respectively. Apart from Dragon Reactor Experiment, in which H_2O/HTO were removed in a freezer heat exchanger, in the remaining purification systems the water is adsorbed by molecular sieve beds. At very low temperature (83 K), also the cooled charcoal beds are effective to remove tritium from helium coolant; at higher temperature (193 K) the beds were not very effective for hydrogen and tritium.

Concluding, the most widely used way for tritium removal foresees the transformation of HT into HTO, in high temperature copper oxide beds, and the following adsorption of the tritiated water in molecular sieve beds, at room temperature.

3 Tritium purification systems for cover gas of Liquid Metal Fast Reactors (LMFRs)

As already mentioned, two main sources of tritium exist: a natural source, due to the interaction of cosmic rays with some atoms present in the atmosphere (in particular nitrogen atoms), and an anthropogenic source, mainly due to activities connected to fission reactor operation, reprocessing of nuclear fuel, facilities for tritium production, research installations using relevant amount of tritium.

The tritium release in the environment is foreseen to increase, not only due to the utilization in fusion reactors, but also for new fuel management and conceptual choices considered for the future fission reactors (GEN IV reactors) [21].

Also for the future fission reactors, it is important to study strategies to limit tritium release. A way to limit the tritium release is the treatment of the cover gas of the GEN IV fast reactors, with the scope to extract the generated tritium. In the present chapter the transferability of the CPS technologies used in HTGRs, and taken into account also for ITER (see next chapter), to the purification of the cover gas of fast fission reactors will be analyzed.

Among the technologies selected by the Generation IV International Forum (GIF) as the most interesting for the development of the future fission reactors, two are Liquid Metal Fast Reactors [22]:

- Sodium Fast Reactors (SFR);
- Lead cooled Fast Reactors (LFR).

SFR is a fast reactor using liquid sodium as coolant. Using a fast neutron spectrum it is possible to convert fertile nuclides in fissile, improving the exploitation of the nuclear fuel. Sodium is considered a good coolant because it is characterized by a high specific heat without

pressurization and a low melting point (371 K); in addition, it is less corrosive than other liquid metals. On the other hand, sodium reacts with water and air; this fact causes to adopt engineering solutions to avoid accidental interactions between sodium and air/water. The boiling point (1156 K) limits the maximum temperature of the reactor. Two different options are considered for the reactor layout: pool and loop. The pool option, which foresees that all radioactive sodium is contained in the reactor pressure vessel, seems to have the greatest consents [22].

LFR is a fast reactor using lead or lead-bismuth eutectic alloy as coolant. The main advantages of lead are the excellent neutron and thermo-fluid-dynamic properties, the absence of interaction with air and water, the high boiling point. The main drawbacks are the corrosive behaviour towards the structural materials, which forces a careful introduction of oxygen to form protective layers of oxide on steel surfaces, and the production of the radioactive nuclide ^{210}Po. In addition, devices operating with the lead are, in general, more demanding [22].

In Europe, two different demonstrators of the above mentioned technologies are actually under study: ASTRID (Advanced Sodium Test Reactor for Industrial Demonstration) and ALFRED (Advanced Lead cooled Fast Reactor European Demonstrator).

ASTRID is a pool type reactor of 600 MWe proposed by CEA (Commissariat à l'énergie atomique et aux énergies alternatives). This reactor uses sodium as coolant and follows the three previous fast reactors manufactured in France: Rapsodie, Phénix and Superphénix.

ALFRED is a pool type reactor of 300 MWth, proposed by FALCON consortium, using lead as coolant.

3.1 Past experiences in cover gas purification

During the specialists' meeting on fast reactor cover gas purification, held in Richland (Washington, USA) in 1986, the presence of tritium in the gas processing systems was discussed [23]. France, UK and Germany considered the tritium concentration in the primary cover gas very low in the reactors using steam generator, due to the efficiency of the cold traps for the tritium removal. For this reason, no dedicated device for tritium removal was considered for the cover gas purification systems. In general, the devices present in the cover gas purification systems had the target to remove aerosols and xenon.

The control of tritium released in the primary sodium coolant is important to reduce its concentration in the cover gas and in the secondary loop, via permeation through the intermediate heat exchanger. The use of the above mentioned cold traps is an effective method to remove hydrogen and tritium from the primary coolant. The effectiveness of the cold traps in the reduction of the tritium level in cover gas has been confirmed in [23].

However, to reduce the release of tritium in the environment at a level as low as reasonably achievable, it is necessary to consider also the treatment of the cover gas.

As an example of the cover gas purification systems used in the past, the French experience concerning the SFRs Rapsodie, Phénix and Superphénix will be reported in the following [24].

Rapsodie was a loop-type fast reactor, cooled with sodium, having a thermal power of 40 MWth; it reached the first criticality in 1967 [25]. A continuous injection of helium (250 Nl/h) in a gas plenum of 2 Nm^3 was performed through the annular space of the rotating plug, in order to avoid leakages [24]. A purification unit was installed only in 1977, due to an increased number of experiments consisting in fuel irradiation up to failure. Two cold traps were installed, the first one in operation and the second one in regeneration. The cold traps consisted of two adsorption columns using charcoal cooled by liquid nitrogen at 78 K (– 195 °C).

Phénix was a pool-type fast reactor, cooled with sodium, having a thermal power of 563 MWth (250 MWe); it reached the first criticality in 1973 [25]. The cover gas purification flow rate was 7 Nm^3/h (max. 20 Nm^3/h in case of fuel failure) [24]. The purification of the cover gas was carried out in three steps. In the first step, the argon flowed through a condenser-separator, where its temperature was decreased to 403 K, and then through a sintered stainless steel filter. Then, the argon flowed in six tanks of 100 m^3, to allow the decay of fission products. Finally, the gas flowed in a charcoal adsorber, cooled by liquid nitrogen; the efficiency was 99% for Xe, but only 1% for Kr.

Since the efficiency for the Kr removal was very low, a cryogenic distillation unit was installed; this unit did not work in normal operation.

Superphénix was a pool-type fast reactor, cooled with sodium, having an electrical output of 1200 MWe; it reached the first criticality in 1985 [25]. The cover gas purification flow rate was between 10 and 25 Nm^3/h (max. 130 Nm^3/h in case of start-up) [24]. At the exit of the cover gas, argon entered in a condenser-separator having the scope to remove aerosols. It consisted in a cold trap cooled by air and filled with pall rings: the sodium dropped down in a cold tank (343 K), containing frozen Na, and the Argon leaved the condenser-separator filtered by the pall rings. Then sodium passed through three tanks having the scope to empty the primary sodium and two parallel filters. Two parallel cold traps (charcoal cooled by liquid nitrogen) were used to adsorb xenon, whose contribution to the total activity of the gas is 99%. Finally the gas went through a tank filled with knitted stainless steel doughnuts and NaK, to remove oxygen before entering in the reactor cover gas. In the following Table, the main characteristics of the three fast reactors are summarized.

Table 9: French LMFR characteristics

	Rapsodie	Phénix	Superphénix
Power	40 MWth	250 MWe	1200 MWe
Type	Loop-Type	Pool-Type	Pool-Type
Coolant	Sodium	Sodium	Sodium
Cover Gas	Helium	Argon	Argon
Gas Plenum Volume	2 Nm^3	40 Nm^3	500 Nm^3
Cover Gas Flow Rate	250 Nl/h	7 – 20 Nm^3/h	10 – 25 Nm^3/h

In the following Figure a PFD of the cover gas purification system of Superphénix reactor is shown.

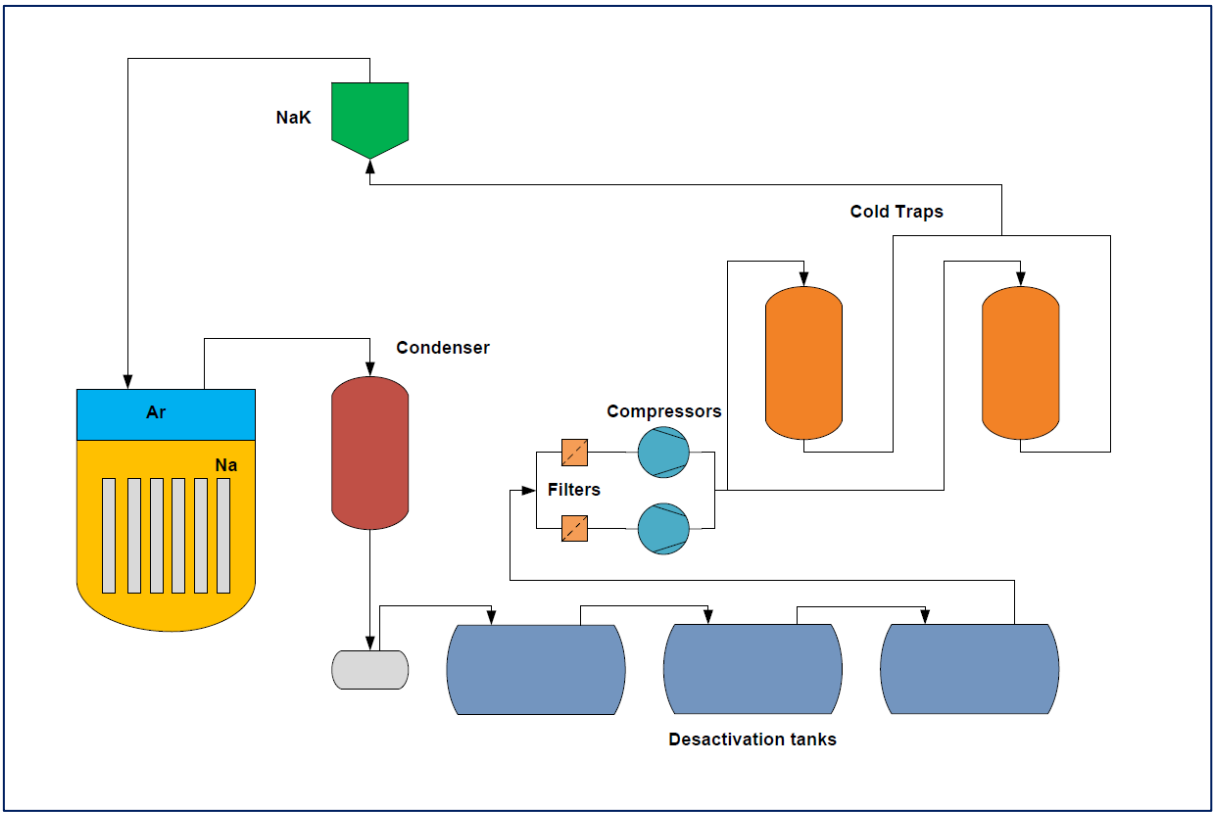

Figure 9: PFD of Superphénix cover gas purification system

3.2 Tritium purification for the cover gas of a LMFR

In chapter 2, the purification systems of the helium coolant used in GCRs have been described. In these purification systems, the most widely used process for tritium removal foresees the transformation of HT into HTO, in high temperature oxidizing beds, and the following adsorption of the tritiated water in molecular sieve beds, at room temperature. In the next chapter, it will be shown that this is also the reference process considered for ITER CPS.

In the present paragraph, a study of the applicability of the same process will be performed for the tritium purification of the cover gas of a pool-type SFR, such as ASTRID reactor.

3.2.1 Purification system input data

For the sizing of the components of the purification system it is necessary to know the type, the temperature and the pressure of the cover gas, the purification flow rate and the concentrations of the hydrogen isotopes.

3.2.1.1 Cover gas characteristics

The cover gas considered for this application is argon, the most widely used gas in SFRs. Pressure and temperature of the Superphénix reactor will be considered as reference for the calculations [24]:

- $T_{cover\ gas}$ = 723 K;
- $p_{cover\ gas}$ = 1.1 x 10^5 Pa.

3.2.1.2 Purification flow rate

The electrical output of ASTRID is 600 MWe, intermediate value between the powers of Phénix and Superphénix. As shown in the above Table, the operating range of the cover gas purification flow rate is very similar for the two reactors. A flow rate of 25 Nm^3/h will be considered for the cover gas purification system.

3.2.1.3 Hydrogen isotope concentrations

The sources of tritium in a fission reactor are described chapter 1. For a preliminary estimation of the tritium level in the cover gas, the tritium specific activity measured in the primary sodium of some SFRs will be considered. In the following Table, these specific activities are shown [1].

Table 10: Tritium specific activity in SFRs

Reactor	Primary circuit type	Tritium specific activity in primary sodium (Bq / kg Na)
EBR-II	pool	1.8 x 10^6
Phénix	pool	1.0 x 10^6
FFTF	loop	1.2 x 10^7
BN-350	loop	1.0 x 10^7
PFR	pool	3.7 x 10^7
Superphénix	pool	(5 – 20) x 10^6

The tritium concentration is lower in the pool-type reactors because the sodium volumes are quite larger than in the loop-type reactors. The only exception is the PFR, probably due to a limited use of the cold traps [1].

For the Superphénix reactor, a maximum activity of 2.0 x 10^7 Bq/(kg Na) has been measured. This activity corresponds to a concentration of 1.12 x 10^{16} (atoms T)/(kg Na), having considered a decay constant of 1.78 x 10^{-9} s^{-1}. Conservatively, this value of tritium concentration will be considered as reference.

The tritium concentration (C_T) inside the sodium is correlated to the partial pressure of tritium in gas phase (p_{T2}) by means of the Sieverts' law:

$$C_T = K_{ST}(T)\sqrt{p_{T_2}} \quad (3.1)$$

The Sieverts' constant K_{ST} is a function of the temperature; in [26], the following formula for the Sieverts' constant K_{ST} is reported:

$$K_{ST}(T) = 1.2616 \times 10^{22} exp\left(-\frac{280.92}{T} + 1.9802\right)\left[\frac{atoms\ T}{kg\ Na - atm^{1/2}}\right] \quad (3.2)$$

Considering a temperature of 723 K, the calculated value of the Sieverts' constant is:

$$K_{ST}(723\ K) = 6.1968 \times 10^{22}\left[\frac{atoms\ T}{kg\ Na - atm^{1/2}}\right] \quad (3.3)$$

Using (3.1), the tritium partial pressure in the cover gas results:

$$p_{T_2} = \left(\frac{C_T}{K_{ST}}\right)^2 = 3.2666 \times 10^{-14} atm = 3.3099 \times 10^{-9} Pa \quad (3.4)$$

Due to the high value of the equilibrium constant of the reaction $H_2 + T_2 \leftrightarrow 2HT$, in correspondence of this temperature, it is possible to consider:

$$p_{HT} = 2p_{T_2} = 6.6198 \cdot 10^{-9} Pa \quad (3.5)$$

The main hydrogen sources in the primary sodium are [27]:

- protons generated by fission;
- protons generated by neutron activation of core materials;
- cover gas moisture;
- hydrogen and water adsorbed on surface of new items to be installed.

To estimate the hydrogen concentration in the cover gas, the simulation results reported in [26] will be considered. In this work, a tritium and hydrogen transport model was used to estimate the distribution of their concentrations in EBR-II, CRBR and FFTF fast reactors.

The hydrogen concentration in the primary sodium, evaluated for the three reactors, is approximately in the range 3 ÷ 4 x 10^{19} (atoms H)/(kg Na) [26]. Also in this case, the hydrogen partial pressure in gas phase (p_{H2}) will be calculated by means of the Sieverts' law:

$$C_H = K_{SH}(T)\sqrt{p_{H_2}} \quad (3.6)$$

The Sieverts' constant considered for hydrogen in sodium is [26]:

$$K_{SH}(T) = 1.6604 \times 10^{22} exp\left(-\frac{280.92}{T} + 1.9802\right)\left[\frac{atoms\ H}{kg\ Na - atm^{1/2}}\right] \quad (3.7)$$

The calculated value at 723 K is:

$$K_{SH}(723\ K) = 8.1556 \times 10^{22}\left[\frac{atoms\ H}{kg\ Na - atm^{1/2}}\right] \quad (3.8)$$

Using the (3.6), the hydrogen partial pressure in the cover gas results:

$$p_{H_2} = \left(\frac{C_H}{K_{SH}}\right)^2 = 1.1787 \times 10^{-7} atm = 1.1943 \cdot 10^{-2} Pa \quad (3.9)$$

having considered a hydrogen concentration of 2.8 x 10^{19} (atoms H)/(kg Na), corresponding to the value calculated for the pool type EBR-II reactor.

Comparing (3.5) with (3.9) it is possible to note that, from point of view of the purification system sizing, the tritium presence in cover gas can be neglected compared to hydrogen.

As above mentioned, additional hydrogen and water could be introduced in the cover gas during reactor operation, increasing their levels; because it is difficult to predict these accidental entries, in absence of data, the sizing of the purification system components will be carried out considering different hydrogen and water concentrations deduced from impurity levels detected in the coolant of HTGRs. In particular, the following three cases will be considered:

Table 11: Impurity concentrations

	Case#1	Case#2	Case#3
H_2 molar fraction (ppmv)	0.109	1	10
H_2 partial pressure (Pa)	0.012	0.11	1.1
H_2O molar fraction (ppmv)	0	1	1
H_2O partial pressure (Pa)	0	0.11	0.11

In case#2 and case#3, the impurity concentrations are included in the range of values measured in the cooling gas of HTGRs.

3.3 Sizing of the purification system fixed beds

In the following paragraphs a preliminary sizing of the oxidizing beds and of the water adsorption beds to be included in the cover gas purification system of a pool-type LMFR will be carried out.

Fixed beds are common components used in the process industry as catalytic chemical reactors and adsorption/desorption beds; in these components, a transfer of heat and mass takes place between a gas phase and a solid phase. The solid phase can be in different forms, for example granular material randomly charged. Usually, the fixed bed geometry is cylindrical, with the gas flow having a direction parallel to the cylinder axis.

3.3.1 Sizing of an oxidizing bed

The oxidizing material considered is a commercial copper catalyst, used for the oxidation of hydrogen and CO in gases. The main characteristics of this material are summarized in the following Table [28]:

Table 12: Catalyst characteristics

Data	**Unit**	**Value**
Type	-	CuO
Composition	-	45 wt% CuO
Shape	-	Tablet
Size	mm	5 x 3
Bulk density	kg/m^3	830
Operating temperature	K	Max 548

The input data used for the oxidizing bed sizing are shown in the following Table:

Table 13: Operating conditions at the inlet of the Oxidizing Bed

Data	**Unit**	**Value**
Mass Flow Rate	kg/s	0.0124
Flow Rate	Nm^3/h	25
Pressure	MPa	0.11
Inlet Temperature	K	523
H_2 molar fraction	ppmv	0.109 ÷ 10

The operating temperature has been selected in order to have the maximum efficiency for the transformation of hydrogen into water; as shown in [29], in correspondence of 523 K, the efficiency is approx. 100% for CuO.

The evaluation of the oxidizing bed dimensions, the amount of catalyst, the required regeneration time and the regeneration flow rate will be performed considering the following steps:

a. evaluation of the internal bed diameter;
b. evaluation of the bed height;
c. evaluation of the catalyst amount;
d. evaluation of the maximum pressure;
e. evaluation of the Gas Hourly Space Velocity (GHSV);
f. evaluation of the maximum oxidable amount of hydrogen;
g. evaluation of the operating time before regeneration;
h. evaluation of regeneration flow rate.

a. Evaluation of the internal bed diameter

The internal bed diameter is an important parameter to be evaluated because the superficial velocity of the gas depends on this and the pressure drop through the bed depends on the superficial velocity. The value of the pressure drop defines the operating limits of the bed. In case of too low pressure drop, uneven distribution and channeling of the flow will result. To the opposite, in case of too high pressure drop, a bed compaction or a bed lifting (in case of up-flow direction) will result. Pressure drop guidelines to be considered for the design of fixed beds can be found in the technical literature [30].

The value of the pressure drop can be evaluated using the Ergun's equation [31]:

$$\frac{\Delta P}{L} = \frac{G\,(1\,-\,\varepsilon)}{\rho\,D_p\,\varepsilon^3}\left[\frac{150\,(1\,-\,\varepsilon)\mu}{D_p} + 1{,}75\,G\right] \qquad (3.10)$$

or the equivalent:

$$\frac{\Delta P}{L} = \frac{150\,(1-\varepsilon)^2}{D_p^2\,\varepsilon^3}\mu u + \frac{1{,}75(1-\varepsilon)}{D_p\,\varepsilon^3}\rho u^2 = \mathrm{B}\mu u\,+\,\mathrm{C}\rho u^2 \qquad (3.11)$$

where:

ΔP = pressure drop (Pa);
L = bed length (m);
μ = dynamic viscosity of fluid (Pa s);
G = ρ u = superficial mass velocity of the fluid (kg/m^2 s);
u = superficial velocity (ratio between volumetric gas flow rate and cross-sectional area of the bed) (m/s);
ρ = actual density of the fluid (kg/m^3);
D_p = equivalent diameter of the particle (m);
ε = void fraction of the bed.

Fixing a maximum allowable value for the pressure drop, it is possible to evaluate the corresponding maximum value for the superficial velocity. Considering the above mentioned pressure drop guidelines, it is possible to assume a maximum value of $\Delta P/L$ equals to 2.5 kPa/m; in correspondence of this value, up-flow and down-flow operations are allowed. With this value of pressure drop it is possible to solve the equation (3.11) to find the corresponding value of the superficial velocity. For the calculation, the value ε = 0.37 will be used; according to [32], this value is considered a good approximation for most particle shape. For extruded particles the equivalent spherical diameter D_p can be evaluated considering the Sauter mean diameter: this is defined as the diameter of a sphere having the same ratio Volume/Surface of the particle of interest. In particular:

$$D_p = \frac{6\,V_p}{S_p} = 4.091\ mm \qquad (3.12)$$

where:

- V_p = volume of the particle (mm^3);
- S_p = surface of the particle (mm^2).

For the evaluation of the viscosity μ and density ρ of the argon cover gas, the data of NIST Chemistry WebBook, SRD 69 will be used [33]:

- ρ = 1.010 kg/m^3;
- μ = 3.518 x 10^{-5} Pa s.

Including the above values and solving the equation (3.11) it is possible to find the maximum value of the superficial velocity: u_{max} = 0.490 m/s.

The corresponding value of the minimum internal diameter of the bed is:

$$D_{min} = \left(\frac{4\,q}{\pi\,u}\right)^{0.5} = 0.177\ m \tag{3.13}$$

where q is the actual flow rate of the gas:

$$q = \left(\frac{\dot{m}}{\rho}\right) = 0.012\ m^3/s \tag{3.14}$$

and ṁ = 0.0124 kg/s is the mass flow rate.

The selected internal diameter has to be greater than D_{min}. For the present application a near standard diameter will be considered, in particular an 8" pipe, sch. 5. For this pipe, the value of outside diameter is 219.1 mm and the thickness is 2.77 mm.

The selected internal diameter is $D_{selected}$ = 0.214 m and the corresponding superficial velocity is:

$$u_{adjusted} = u_{max}\left(\frac{D_{min}}{D_{selected}}\right)^2 = 0.335\ m/s \tag{3.15}$$

The value of ΔP/L, corresponding to the selected internal diameter, can be evaluated replacing the value of $u_{adjusted}$ in equation (3.11); the calculated value results:

$$\left(\frac{\Delta P}{L}\right) = 1.431\ kPa/m \tag{3.16}$$

The minimum pressure drop required to avoid uneven distribution and channeling is: ΔP/L = 0.23 kPa/m [34]; this condition is satisfied.

b. Evaluation of the bed height

In general, in case of gas operation, commercial vessels with a value of L/D in the range of 1 ÷ 3 are frequently used. In this case, a value of L/D = 1 will be considered: the bed height results 0.214 m.

The corresponding total pressure drop is:

$$\Delta P = 0.306\ kPa \tag{3.17}$$

c. Evaluation of the catalyst amount

For the catalyst bulk density, the following value will be considered:

$$\rho_{catalyst} = 830\ kg/m^3 \tag{3.18}$$

The volume of the bed is:

$$V_{bed} = 0.008\ m^3 \tag{3.19}$$

The corresponding amount of catalyst is:

$$M_{catalyst} = 6.64\ kg \tag{3.20}$$

d. Evaluation of the maximum pressure

The particles located at the bottom of the bed have to withstand the sum of the pressure drop through the bed and the pressure due to the weight of the catalyst material. The total pressure should not be greater than 55 kPa, to avoid damaging of the catalyst. The limit of 55 kPa is used for the sizing of the molecular sieve beds [34], but can also be used for the copper oxide catalyst since the values of the crush strength are similar. Because the pressure can increase during the operation time, a reference value to be considered for the design could be approx. 35 kPa.

The mass of the catalyst column produce a force of 65.14 N, corresponding to a pressure of 1.809 kPa.

Adding the above value to (3.17), the resulting pressure is 2.115 kPa < 35 kPa.

e. Evaluation of the GHSV

Other important parameter for the oxidizing bed sizing is the rate of interaction. The reaction kinetics criteria are usually defined by means of operating parameters such as the GHSV. GHSV is defined as:

$$GHSV = \frac{Flow\ Rate\ of\ Gas\ in\ Normal\ Condition}{Catalyst\ Volume}\ [h^{-1}] \qquad (3.21)$$

The calculated value of GHSV results 3125 h^{-1}: this value can be considered acceptable.

f. Evaluation of the maximum oxidable amount of hydrogen

For a preliminary evaluation, a maximum reduction of 70% at the end of operation can be considered. With this assumption, the amount of catalyst available for the hydrogen oxidation is:

$$M_{cat,available} = 0.70 \times M_{catalyst} = 4.65\ kg \qquad (3.22)$$

Considering that the amount of CuO in the catalyst is approx. 45 wt%, the mass of CuO contained in the bed results M_{CuO} = 2.093 kg, corresponding to a number of moles:

$$n_{CuO} = 26.312\ mol\ of\ CuO, \qquad (3.23)$$

assuming for CuO a molar mass of 79.545 g/mol.

According to the reaction:

$$CuO + H_2 \rightarrow H_2O + Cu$$

the above value is also the maximum number of H_2 moles that it is possible to transform into H_2O:

$$N_{H2} = 26.312\ mol\ of\ H_2 \qquad (3.24)$$

g. Evaluation of the operating time before regeneration

To evaluate the operating time before regeneration, it is necessary to calculate the molar flow rate of H_2:

$$\dot{n}_{H2} = x_{H2}\ \dot{n}_{tot}\ (mol/s) \qquad (3.25)$$

where x_{H2} is the molar fraction of H_2 and $\dot{n}_{tot} = \frac{p_n \dot{V}_{tot}}{R\ T_n} = 0.310\ mol/s$

Considering the data included in Table 11, the operating times before regeneration for the three cases considered are the following:

Table 14: Operating times before regeneration

	Case#1	Case#2	Case#3
H_2 molar fraction (ppmv)	0.109	1	10
H_2 molar flow rate (mol/s)	3.379×10^{-8}	3.100×10^{-7}	3.100×10^{-6}
Time before regeneration (d)	9010	982	98.2

In case#1 and case#2 the regeneration is not necessary. In case#3, it is necessary to proceed with the regeneration. In case#3, increasing the bed height to have L/D = 4, the regeneration is necessary after approx. one year; in this case it is possible to decide to replace the oxidizing bed, if the reactor can be stopped (for example in concurrence with the replacement of the fuel), or to regenerate it.

h. Evaluation of the regeneration flow rate

The regeneration can be carried out considering two vessels, the first one working in purification phase and the second in regeneration phase. When the first one is exhausted, it is placed in regeneration and the second one put in service. For the regeneration of the exhausted catalyst, a flow of argon, with a very low concentration of oxygen can be used. To avoid any problem related to the direct interaction between oxygen and hydrogen, the operation can be preceded by flushing pure argon or by creating vacuum inside the vessel. Since the oxidation of copper is an exothermic reaction, the regeneration needs to be carried out under controlled conditions to avoid too much heat generation, leading to the damage of the catalyst. For this purpose, the oxygen concentration in argon must to be increased very slowly. For the same reason, the argon temperature, at the inlet of the vessels, has not to be too high. In the present case, the argon flow rate will be evaluated considering that its function is only to convey oxygen for the regeneration of the catalyst.

For the evaluation of the regeneration flow rate, the following data, relevant to the regeneration gas, will be considered:

Table 15: Operating conditions of the regeneration gas Ar + O_2

Data	**Unit**	**Value**
Pressure	MPa	0.11
Temperature	K	473
Density	kg/m^3	1.117
Viscosity	Pa s	3.261×10^{-5}

The regeneration flow rate has to guarantee a pressure drop greater than 0.23 kPa/m, to avoid uneven distribution and channeling. Considering the equation (3.11) and replacing the above values of pressure drop, density and viscosity, it is possible to calculate the minimum value of the superficial velocity. This value is u_{min} = 0.083 m/s, corresponding to the flow rate q_{min} = 0.003 m^3/s.

3.3.2 Sizing of the Molecular Sieve beds

In the present analysis, the materials considered for the adsorption of the tritiated water are the Zeolite Molecular Sieves (ZMSs). ZMSs are highly porous materials synthetically produced, belonging to the class of alumino-silicates. They are characterized by a structure having a system of identical pores with precisely defined diameter. This characteristic allows the zeolites to have a sieve-like behavior: molecules of different dimensions and polarity can be readily adsorbed, slowly adsorbed or completely excluded [35].

ZMSs are formed by tetrahedral fundamental blocks of AlO_4 and SiO_4, having four oxygen anions surrounding a silicon or aluminum cation. Due to the presence of AlO_4, the zeolites have a deficit in positive charge, which is balanced by positive cations (sodium or other cations). The crystal has a honeycomb structure, with large cavities connected together through pores. In general, only

molecules up to 0.5 Å larger than the pores are allowed to enter; this is due to the elasticity and the kinetic energy of the molecules.

In addition to the selection based on the size, ZMSs can preferentially adsorb molecules on the basis of their polarity. Indeed, the presence of cations is particularly important for the adsorption capacity of the ZMSs. The positive charge of the cations attracts the negative side of the polar molecules. In addition, the cations can induce polarity in the molecules and the polarized molecules can be strongly adsorbed due to the electrostatic attraction of the cations.

The ZMS capacity to retain adsorbates is mainly due to physical forces rather than chemisorption; for this reason, their adsorption behavior is characterized by an isotherm having the form of a Langmuir curve; for this type of isotherm the amount of the adsorbed molecules increases very quickly to a saturation value, increasing their concentration in the external bulk phase. The saturation is reached when a complete filling of the internal void volume is obtained. In the following Figure the isotherms of some adsorbing materials, at a temperature of 25 °C, are shown [35]; it is possible to see that the adsorption performed by ZMSs generates a Langmuir-type isotherm. The isotherms shown in the Figure describe how the adsorption capacity of the materials depends on the water content in the gas phase. It is also possible to notice that ZMSs are characterized by a high capacity even at low water concentration. In general, ZMS adsorption capacity decreases lowering the water partial pressure and increasing the temperature.

ZMSs have a strong adsorption capacity for water. Due to this strong affinity, water can displace any other material already adsorbed. However, in the case in which the water has to displace other materials, the rate of adsorption could be reduced.

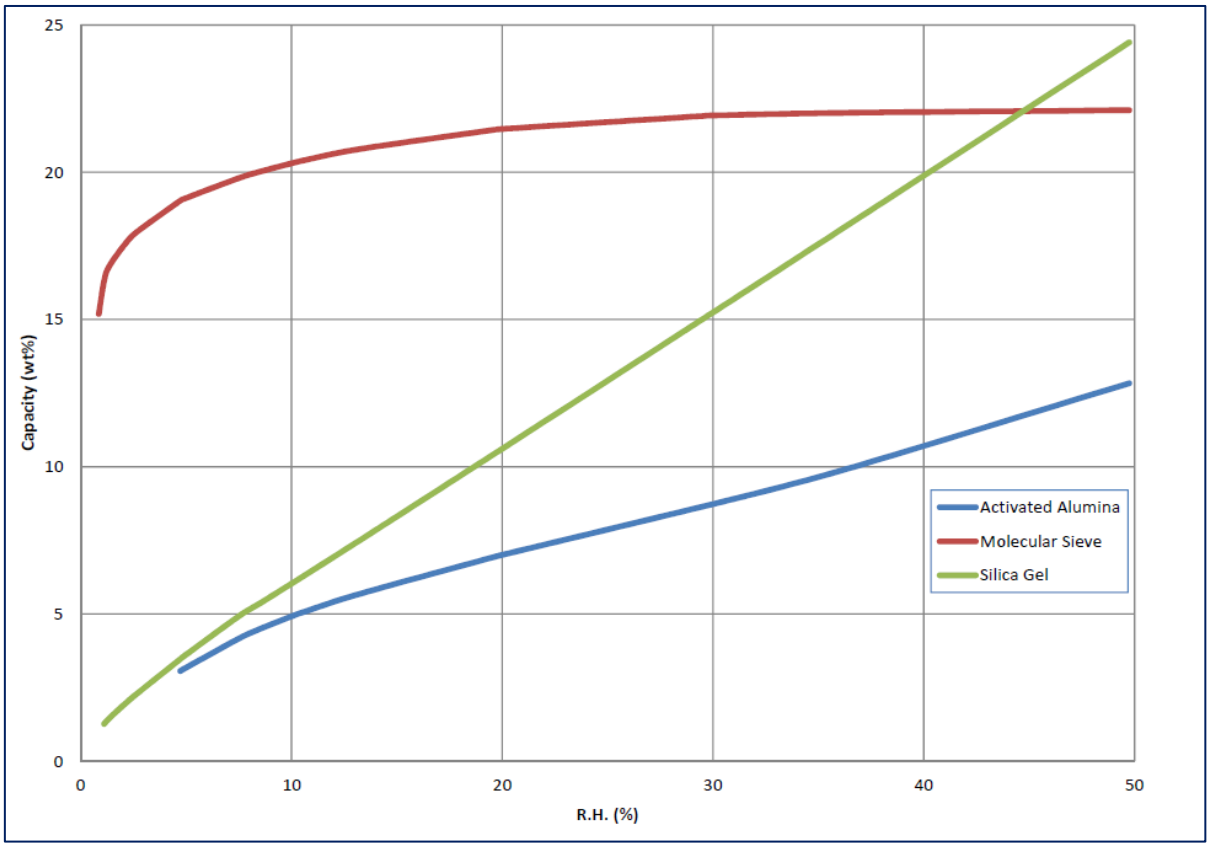

Figure 10: Water adsorption isotherms at 25 °C

The ZMSs are commercially available in shape of pellets or beads in which the crystals are mixed with special clay binders. For the present analysis, a ZMS type 4A will be considered. This type of zeolite is able to adsorbe molecules having an effective diameter less than 4 angstroms (for the water, the value is 2.6 Å) [36]. The main characteristics of a commercial zeolite type 4A are shown in the following Table [37]:

Table 16: Zeolite Molecular Sieve type 4A characteristics

Data	Unit	Value
Type	-	4A
Shape	-	Bead
Size	mm	1.6 – 2.5
Bulk density	kg/m^3	720

According to [32], the equivalent diameter for a granular media can be evaluated multiplying the mean diameter by 0.8: the coefficient 0.8 is used to take into account the increased packing density characterizing the granular media. In this case, the value of the calculated equivalent diameter is 1.64 mm.

The gas conditions at the inlet of the molecular sieve bed, operating in adsorption phase, are shown in the following table:

Table 17: Operating conditions at the inlet of the Molecular Sieve Bed

Data	Unit	Value
Mass Flow Rate	kg/s	0.0124
Flow Rate	Nm^3/h	25
Pressure	MPa	0.110
Inlet Temperature	K	298
H_2O Partial Pressure from H_2 oxidation	Pa	0.012 ÷ 1.1 (0.109 ÷ 10 ppmv)
H_2O Partial Pressure from impurities	Pa	0 ÷ 0.110 (0 ÷ 1 ppmv)

The evaluation of the amount of molecular sieves and the regeneration flow rate will be performed considering the following steps:

a. evaluation of the internal bed diameter;
b. evaluation of the bed height and molecular sieve amount;
c. evaluation of the removed amount of water and saturation time;
d. evaluation of the maximum pressure;
e. evaluation of the heat required for the regeneration;
f. evaluation of the regeneration flow rate.

The adsorption mechanism operated by ZMSs on H_2O is mainly physisorption. Since most physical adsorption interactions occur very quickly, the design of the ZMS beds can be based only on the adsorbent capacities and pressure drop, neglecting the reaction kinetics [30].

a. Evaluation of the internal bed diameter

For the evaluation of the internal bed diameter, the same considerations already shown in the previous paragraph can be applied. In particular, the equations (3.10) and (3.11) can be applied for the pressure drop evaluation.

Typically, the gas direction during adsorption is downflow; an allowable pressure drop $\Delta P/L$ = 7.5 kPa/m will be considered [34]. Using this value of pressure drop it is possible to solve the (3.11) to find the corresponding value of the superficial velocity. Also in this case, for the calculation the value ε = 0.37 will be used.

For the evaluation of the dynamic viscosity μ and density ρ the data reported in [33] will be used. In this case:

- ρ = 1.774 kg/m^3
- $\mu = 2.256 \times 10^{-5}$ Pa s

Including the above values in (3.11), the maximum value of the superficial velocity results:

- u_{max} = 0.393 m/s.

The corresponding minimum value of the internal bed diameter is:

$$D_{min} = \left(\frac{4\,q}{\pi\,u_{max}}\right)^{0.5} = 0.151\,m \tag{3.26}$$

where q is the actual flow rate of the gas:

$$q = \left(\frac{\dot{m}}{\rho}\right) = 0.007\,m^3/s \tag{3.27}$$

and ṁ = 0.0124 kg/s is the mass flow rate.

For the present analysis, a near standard diameter will be considered; in particular a 6" pipe, sch. 5, having an external diameter of 168.3 mm and a thickness of 2.77 mm.

Considering this pipe, $D_{selected}$ = 0.163 m and the corresponding superficial velocity is:

$$u_{adjusted} = u_{max}\left(\frac{D_{min}}{D_{selected}}\right)^2 = 0.337\,m/s \tag{3.28}$$

The ΔP/L value corresponding to the selected diameter can be evaluate replacing the above value of $u_{adjusted}$ in (3.11), obtaining ΔP/L = 5.996 kPa/m; this value is greater than the minimum pressure drop ΔP/L = 0.23 kPa/m required to avoid uneven distribution of the flow and channeling.

b. Evaluation of the bed height and molecular sieve amount

In adsorption phase, the bed can be considered divided in three zones. The inlet zone is called saturation or equilibrium zone. In this zone equilibrium between molecular sieve and wet gas is present. In the middle zone, called Mass Transfer Zone (MTZ), the water content in the gas decreases from its inlet value to the required value. The outlet zone contains the unused material and is called active zone.

In the following Figure, the displacement of the MTZ through the bed, during the adsorption operation, is shown. At the start of operation, the MTZ is in correspondence of gas inlet. Then, the MTZ begins to move downward. When the adsorbing material reaches the saturation, the MTZ is at the bottom end of the bed: this is known as the breakthrough point.

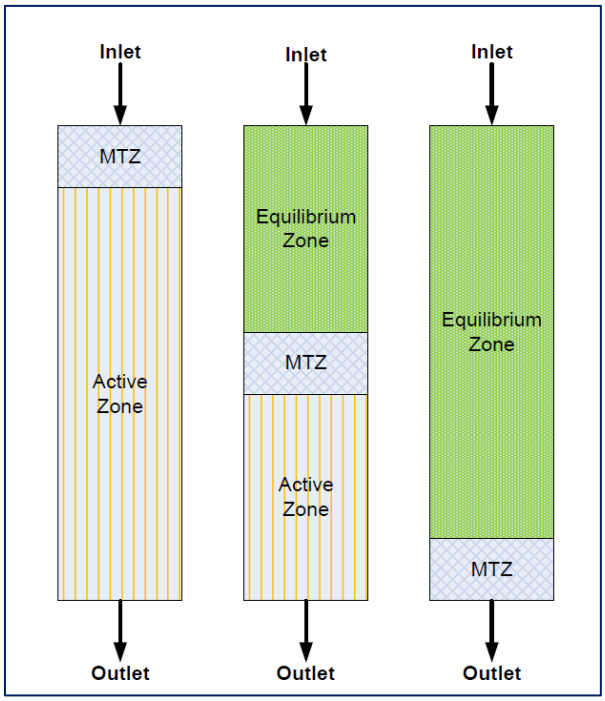

Figure 11: Progress of the MTZ

To evaluate the height of the saturation zone, water-adsorption isotherms can be used; these give a relation among water adsorption capacity, temperature and water partial pressure of the gas to be purified. The amount of molecular sieve required in the saturation zone is calculated using:

$$M_S = \frac{M_{H2O}}{0.65\ C} \tag{3.29}$$

where M_{H2O} is the mass of water to be adsorbed in one cycle and C is the adsorbate loading capacity of the molecular sieve. The coefficient 0.65 is considered to take into account the aging of the adsorbent.

The bed height of the saturation zone is calculated using:

$$H_S = \frac{4M_S}{\pi D^2{}_{selected}\ \rho_b} \tag{3.30}$$

For the ZMS bed sizing, it is assumed that the saturation zone has to contain all the amount of water to be adsorbed.

The height of the MTZ can be estimated using [34]:

$$H_{MTZ} = \left(\frac{u_{adjusted} \cdot 3600}{640}\right)^{0,3} Z = 0.315\ \text{m} \tag{3.31}$$

where Z = 0.26 m for 1.5 mm particle diameter.

The total height of the bed has to be greater than H_{MTZ}.

In commercial vessels, the total height of the bed is greater than the internal diameter. Generally, the ratio L/D is selected on the basis of economic reasons. However, regarding the maximum height, it is important to verify that the adsorbing particles located at the bottom of the bed are not damaged by the weight of the bed above them, including the adsorbed water, and the pressure drop. Long cycles have the advantage to reduce the number of regenerations and, consequently, increasing the adsorbent life. On the other hand, long cycles require bigger and more expensive vessels. It is possible to find commercial vessels having a ratio L/D between 2 and 8. In the present case, a ratio L/D = 8 has been selected to increase the adsorption capacity, in order to have longer adsorption time without creating the risk to damage the adsorbing material.

In the following Table, the characteristics of the ZMS bed are summarized.

Table 18: ZMS bed characteristics

Data	Unit	Value
Total height H_{tot}	m	1.304
Total volume of ZMS	m^3	0.027
Total amount of ZMS	kg	19.44
Total press. drop through the bed	kPa	7.819

c. Evaluation of the removed amount of water and saturation time

To evaluate the total water adsorbed by the bed, the same three cases considered in the previous paragraph are considered. In the following Table, the amount of tritiated water included in the gas to be purified is shown for the three cases.

Table 19: Amount of tritiated water to be removed

	Case#1	Case#2	Case#3
H_2O partial pressure (Pa) from H_2 oxidation (1)	0.012	0.110	1.100
H_2O partial pressure (Pa) from impurities	0	0.110	0.110
Total H_2O partial pressure (kPa)	$1.200 \cdot x\ 10^{-5}$	$2.200 \cdot x\ 10^{-4}$	$1.210 \cdot x\ 10^{-3}$
H_2O mass flow rate (kg/h)	$2.190 \cdot x\ 10^{-6}$	$4.016 \cdot x\ 10^{-5}$	$2.209 \cdot x\ 10^{-4}$

(1) According to [29], for temperature greater than 250 °C, the efficiency of the hydrogen oxidation performed by CuO is close to 100 %.

Only the water adsorbed in the saturation zone will be considered. The height of the saturation zone is:

$$H_S = H_{tot} - H_{MTZ} = 0.989\ m \tag{3.32}$$

The volume of the saturation zone is V_S = 0.021 m^3 and the corresponding ZMS amount is M_s = 15.12 kg.

The maximum amount of water that it is possible to adsorb in V_s can be calculated using (see 3.29):

$$M_{H2O} = M_S\ 0.65\ C \tag{3.33}$$

The adsorbate loading capacity C depends on the water content (partial pressure) in the gas to be purified. In [34], the isotherms for water adsorption of a zeolite type 4A are shown. In the following Table, the loading capacity of a zeolite type 4A, the amount of water adsorbed in the saturation zone and the adsorption time are shown.

Table 20: H_2O adsorbed and saturation time

	Case#1	Case#2	Case#3
Total H_2O partial pressure (kPa)	$1.200 \cdot x\ 10^{-5}$	$2.200 \cdot x\ 10^{-4}$	$1.210 \cdot x\ 10^{-3}$
Water adsorption capacity (kg of H_2O adsorbed / kg of adsorbent) at 25 °C	0.010	0.033	0.055
Amount of adsorbed water (kg)	0.098	0.324	0.541
Time required for the saturation of the bed (d)	1864	336	102

In case#1 the time required to reach the saturation is approx. 5 years; in this case it is convenient to replace the bed instead of proceeding with the regeneration. In case#2, the saturation time is approx. 1 year: in this case, a replacement of the bed could be possible, in case of stop of the reactor operation after 1 year. Otherwise it is possible to proceed with the regeneration. In case#3 it is necessary to regenerate the bed when the saturation is reached.

d. Evaluation of the maximum pressure

The total pressure should not exceed 55 kPa, to avoid the damage of the molecular sieves, but the maximum value of pressure to be considered in phase of design should be approx. 35 kPa [34]. In the following Table the total pressures acting on the particles at the bottom of the beds are shown.

Table 21: Total pressure drops

	Case#1	Case#2	Case#3
Pressure due to ZMS weight (kPa)	9.081	9.081	9.081
Pressure due to H_2O weight (kPa)	0.046	0.151	0.253
Pressure due to pressure drop (kPa)	7.819	7.819	7.819
Total pressure (kPa)	16.946	17.051	17.153

In all cases the total pressure is lower than the value of 35 kPa.

e. Evaluation of the heat required for the regeneration

To evaluate the regeneration flow rate, it is necessary to calculate the heat required for the regeneration of the molecular sieves.

This heat is composed of four contributions: the heat required to desorb the water, the heat required to warm the molecular sieves and the steel bed and the heat loss. The following equations will be used to evaluate the four contributions [34]:

$$Q_W = \left(4200\ \frac{kJ}{kg}\right) M_{H2O} \tag{3.34}$$

$$Q_{ZMS} = M_{ZMS}\left(\frac{1.0\ kJ}{kg\ K}\right)\left(T_{rg} - T_i\right) \tag{3.35}$$

$$Q_{ST} = M_{ST}\left(\frac{0.5\ kJ}{kg\ K}\right)\left(T_{rg} - T_i\right) \tag{3.36}$$

$$Q_L = (Q_W + Q_{ZMS} + Q_{ST}) \cdot 0.1 \tag{3.37}$$

where:

M_{H2O} = Mass of adsorbed water (kg)

M_{ZMS} = Mass of Molecular Sieve inside the bed (kg)

M_{ST} = Mass of Steel of bed (kg)

T_{rg} = 543 K = Temperature of bed and ZMS to be reached for the regeneration

T_i = 298 K = Initial temperature

T_{rg} is usually 30 °C below of the temperature of the regeneration gas.

The material considered for the bed is an austenitic stainless steel type 316L. Considering a steel density of 8000 kg/m^3, the weights of the vessel are shown in the following Table:

Table 22: Weights of the vessel

Data	**Unit**	**Value**
Vessel mass (cylinder)	kg	15.050
Head mass (each)	kg	0.526
Total mass	kg	16.100

Considering the total amount of adsorbed water shown in Table 20 and the total amount of ZMS shown in Table 18, the heat required for the bed regeneration is shown in the following Table:

Table 23: Heat amount required for regeneration

	Case#2	Case#3
Qw [kJ]	1.361 x 10^{+3}	2.272 x 10^{+3}
Q_{ZMS} [kJ]	4.763 x 10^{+3}	4.763 x 10^{+3}
Q_{ST} [kJ]	1.972 x 10^{+3}	1.972 x 10^{+3}
Q_L [kJ]	8.096 x 10^{+2}	9.007 x 10^{+2}
Q_{TOT} [kJ]	8.906 x 10^{+3}	9.908 x 10^{+3}

f. Evaluation of the regeneration flow rate

The flow rate of the regeneration gas will be calculated using the equation [34]:

$$\dot{m}_{rg} = \frac{2.5\ Q_{TOT}}{(C_p)_{Ar}(T_{hot} - T_i)\ t_{heating}}\ [kg/h] \qquad (3.38)$$

where:

T_{hot} = 573 K (Temperature of the inlet gas)

T_i = 298 K (Temperature of the bed at the beginning of the regeneration)

$(C_p)_{Ar}$ = 0.52 kJ/kg K

The coefficient 2.5 assumes that only 40% of the heat is transferred to the bed and heat losses, while the remaining leaves with the hot gas.

The heating time has been selected in order to have a pressure drop, corresponding to a superficial velocity greater than 0.23 kPa/m. In case#2 the heating time is approx. 2% of the adsorption time and in case#3 it is approx. 6% of the adsorption time.

The results of the calculations are shown in the following Table:

Table 24: Argon conditions in regeneration

	Case#2	Case#3
$\dot{m}_{rg}$ (kg/h)	0.965	1.179
q (m^3/h)	1.047	1.279
u (m/h)	50.174	61.292
u (m/s)	0.014	0.017

The volumetric flow rate and the superficial velocity have been calculated considering the gas characteristics corresponding to P = 0.11 MPa and T = 573 K:

- ρ = 0.922 kg/m^3
- μ = 3.764 x 10^{-5} Pa s

Considering the above values of density, dynamic viscosity and superficial velocity, it is possible to calculate the pressure drops, using (3.11); the calculated values are shown in the following Table.

Table 25: Pressure drop values in regeneration

	Case#2	Case#3
ΔP/L (kPa/m)	0.233	0.283

Considering that the value of the purification flow rate is 44.64 kg/h, the percentage values of the regeneration flow rates result:

Table 26: Percentage value of the regeneration flow rate respect to adsorption

	Case#2	Case#3
%	2.16	2.64

In general, the regeneration flow rate has to be as small as possible; a typical value considered for the regeneration is approx. 10 % of the purification flow rate [34].

3.4 PFDs for cover gas purification systems

In the following, two PFDs relevant to cover gas purification systems are shown. The PFDs show only the components dedicated to the purification of the hydrogen isotopes. The first one is the PFD corresponding to the case#1, in which the regeneration of the components is not necessary; the second PFD is referred to the case#3, in which the regeneration of the components is necessary.

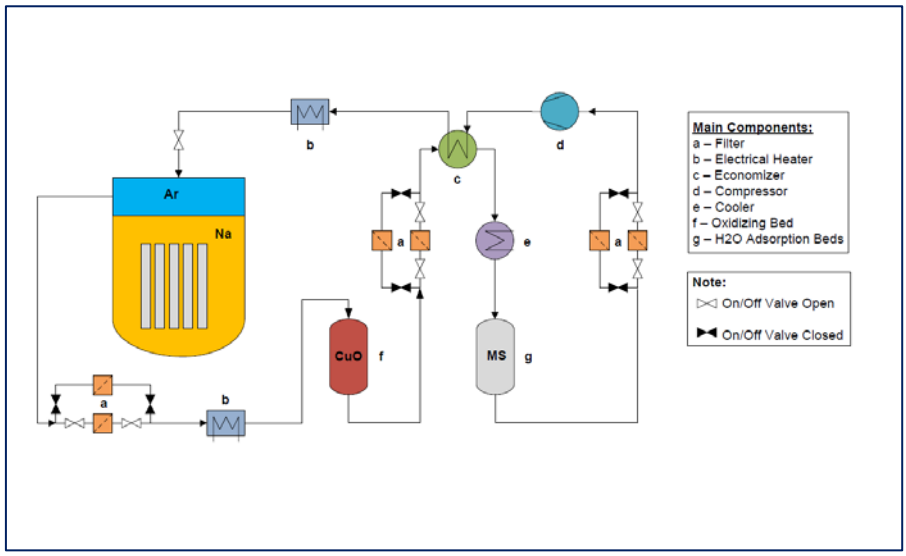

Figure 12: PFD of cover gas purification system – no regeneration

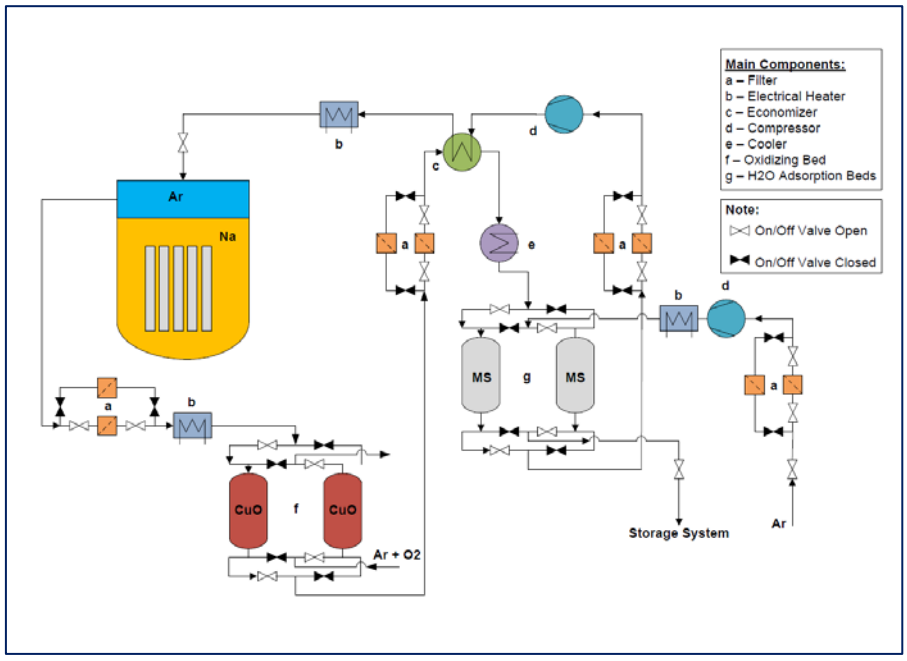

Figure 13: PFD of cover gas purification system – with regeneration

4 Purification systems for gas treatment in fusion

The Coolant Purification System is one of the most important auxiliary circuits of HCLL and HCPB TBMs. In a fusion reactor, the main scopes of CPS are [5]:

- removal of the tritium permeated from the breeding zones into the coolant system;
- transformation of the tritium in a suitable form for the downstream tritium processing systems;
- removal of the impurities from the cooling gas;
- control of the coolant oxidation potential, adding chemical agents (normally H_2/H_2O).

There are two main reasons to remove tritium from the cooling gas: to maintain a low partial pressure in order to limit the tritium release in the environment and to recover the maximum amount of tritium, necessary to feed the fusion reaction.

Not many examples of purification system designs for helium cooled fusion reactors exist. One of the first examples is reported in [38] [39]. Two purification systems are foreseen in this design, one for each of the two coolant systems. Each purification system is able to purify 0.1% of the helium coolant flow. The main scopes of this CPS are:

- extraction of hydrogen isotopes;
- extraction of solid, liquid or gaseous impurities;
- removal of liquid water accidentally entered in the cooling system.

In the following simplified diagram, the purification system is shown [38].

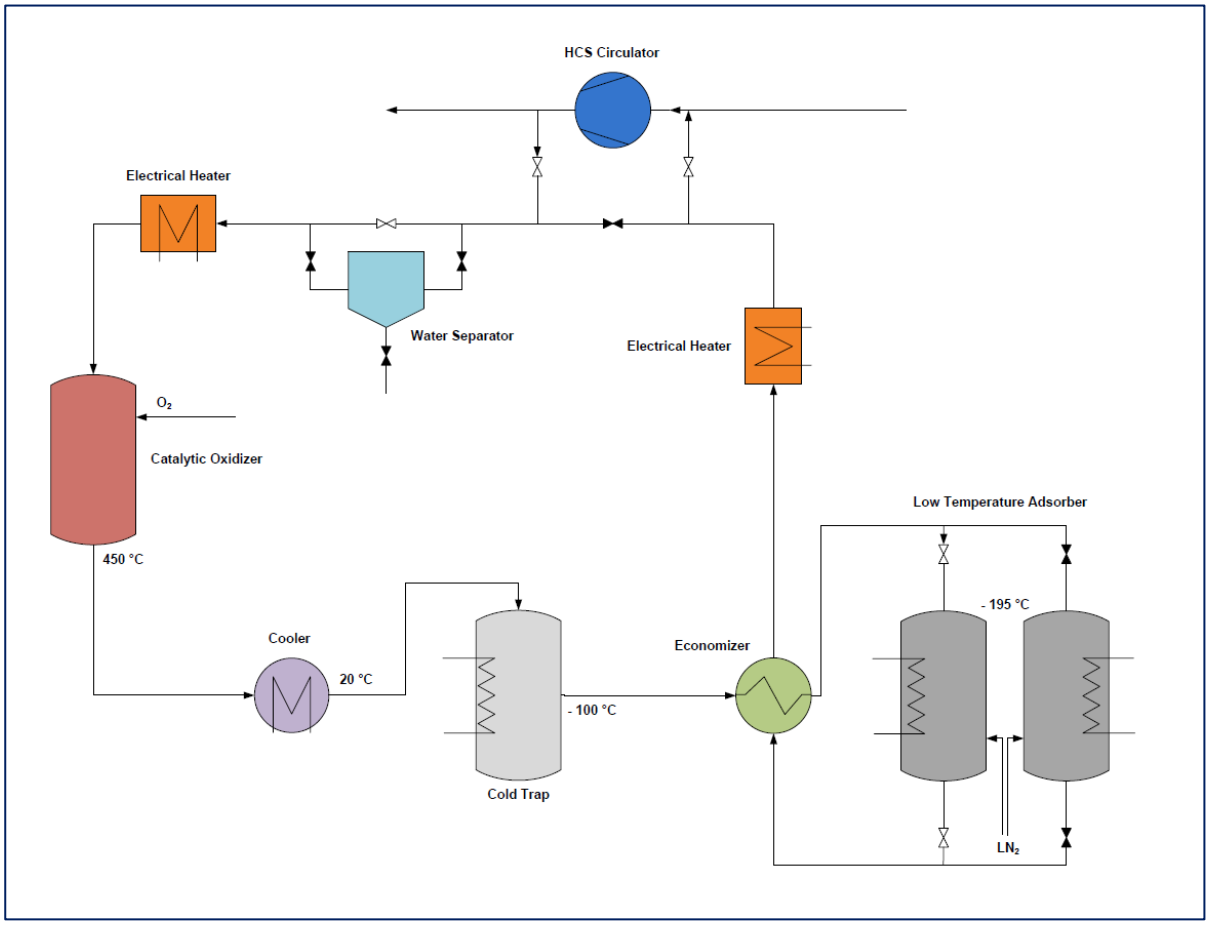

Figure 14: PFD of ITER CPS

The 0.1% of the coolant helium is withdrawn downstream of the main coolant circulator and sent to the CPS. The first component of the system is a water separator. In normal condition, this component is bypassed; it removes the condensed water only in case of presence of droplets due to water leakages. Subsequently, an electrical heater warms up to 723 K the gas before entering in

a catalytic oxidizer, in which the different molecular forms of hydrogen isotopes (Q_2, with Q=H,D,T) are transformed into water (Q_2O). The catalyst consists of precious metals (Pd or Pt) on alumina. An over-stoichiometric flow of oxygen is introduced in the vessel to transform Q_2 into Q_2O. A water cooler reduces the gas temperature at approx. 293 K, before entering into a cold trap, operating at 173 K, in which the water is frozen. The gas outgoing from the cold trap goes through a heat exchanger (economizer) and then enters in a molecular sieve bed, operated at liquid nitrogen temperature; in this component the remaining impurities, such as N_2 and the excess of O_2 from oxidizer, are adsorbed. The bed can also remove hydrogen isotopes not previously oxidized. A second bed can be used when the first one need to be regenerated. Then, the purified helium comes back to the economizer, before going through an electrical heater and reentering in the cooling loop. The CPS has been designed to operate for maximum six days, without intermediate unloading or regeneration of components. At the end of the purification cycle, the cold trap is depressurized, warmed to room temperature and the liquid water drained. For the regeneration, the adsorbing beds are firstly depressurized and warmed to room temperature; then the beds are warmed up to 573 K and purged with pure helium.

In the following Table, the main design data for each CPS are summarized [38].

Table 27: CPS Main Design Data

CPS Design Data	Values
Pressure (MPa)	8.0
Coolant temperature at inlet/outlet of CPS (K)	523/323
CPS flow rate (kg/s)	0.00185
Q_2O partial pressure (Pa)	35
H_2 partial pressure (Pa)	< 10
HT partial pressure (Pa)	< 0.1
DT partial pressure (Pa)	< 0.1
N_2 partial pressure (Pa)	8

According to modified EU-TBM baseline, this type of design seems currently out of date due to the decision to avoid cryogenic temperatures [40].

A different CPS concept for HCPB-TBM is reported in [41]. In this design, the purification system is able to purify 0.35 g/s of the helium coolant flow. The proposed CPS has a configuration similar to that considered in many high temperature gas cooled fission reactors and foresees a process composed of three stages. The three stages have the following scope:

- oxidation of Q_2 and CO into Q_2O and CO_2, using a catalytic oxidizer (CuO-Cu_2O);
- removal of the Q_2O by Pressure Temperature Swing Adsorption (PTSA);
- removal of all remaining impurities by cryogenic PTSA.

A simplified diagram of the purification system is shown in the following Figure.

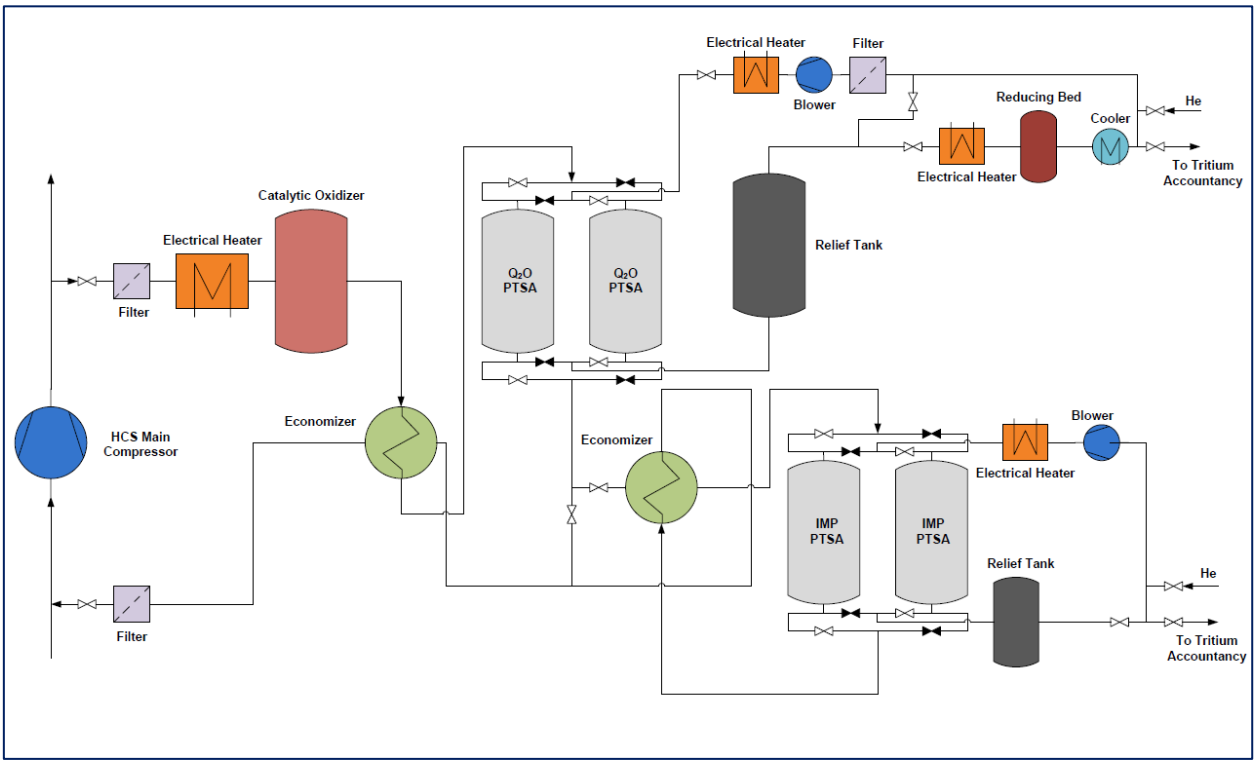

Figure 15: PFD of ITER CPS – ENEA Concept

A stream of approx. 0.35 g/s of the coolant helium is withdrawn downstream of the main coolant circulator and sent to the CPS. After a filter for solid particles, the gas is warmed up to 553 K by an electrical heater before entering in a Cu_2O-CuO catalytic oxidizer, in which Q_2 is transformed into Q_2O and CO into CO_2. The gas leaving the oxidizer passes through an economizer, in which it is cooled at approx. room temperature, and then enters in the PTSA column. Commercial adsorbing beds use two main processes to selectively adsorb some impurities in a gas mixture: TSA (Temperature Swing Adsorption) and PSA (Pressure Swing Adsorption). TSA process is based on principle that the loading capacity of the adsorbent material is lower at high temperature: the adsorbate is trapped at low temperature and desorbed increasing the temperature. In the same way, PSA process is based on the fact that the adsorption capacity is greater at high pressure: switching from high (adsorption) pressure to a lower pressure, the adsorbed material is desorbed. PTSA process uses both principles: adsorption at high pressure and low temperature and desorption at low pressure and high temperature. The adsorbent material included in PTSA (silica gel), removes Q_2O from the stream. From the outlet of the Q_2O-PTSA, a slip stream, corresponding to approx. 25% of the CPS flow rate, is sent to a second economizer and then enters in a PTSA column operating in adsorption phase at cryogenic temperature; in this second PTSA, all remaining impurities (in particular CO_2 and N_2) are removed. The adsorbent material of the cryogenic PTSA is a zeolite molecular sieve type 13X. After going through again the two economizers, with the scope to increase its temperature, the purified gas comes back to the main coolant stream.

The two Q_2O-PTSA columns and the two cryogenic PTSA columns allow a continuous operation of the CPS: when a column is saturated, it is replaced by the second one and placed in regeneration. The regeneration of the Q_2O-PTSA is performed by depressurization of the column, followed by heating at 573 K and purging by hot helium. The desorbed Q_2O is sent to a metallic reducing bed to transform Q_2O into Q_2 and then routed to the tritium accountancy before the final treatment in Tokamak Exhaust Processing (TEP). The cryogenic PTSA is regenerated in similar manner by depressurization, followed by heating at 373 K and purging by helium.

In the following Table, the main data considered for CPS design are summarized [41].

Table 28: CPS Main Design Data - ENEA Concept

CPS Design Data	Values
Pressure (MPa)	8.0
Coolant temperature at CPS inlet (K)	773
CPS flow rate (kg/s)	0.00035
H_2O partial pressure (Pa)	30
H_2 partial pressure (Pa)	1000
HT partial pressure (Pa)	< 0.3
Max. expected impurity concentration (CO, N_2, CQ_4, O_2) (ppmv)	10

H_2 and H_2O are supposed to be included in the coolant gas with the scope to produce natural oxide barriers.

The above CPS design has been afterwards updated with the scope to eliminate the components operating at cryogenic temperature. The first two stages have been maintained, whereas in the third stage the cryogenic PTSA has been replaced by heated getters (see following PFD) [5] [49].

Heated getters using pure zirconium or titanium have had limited applications in the industry due to the high operating temperatures (> 973 K). In the years, new getter materials have been developed; these getters are able to operate at lower temperatures (< 673 K) and with better performances, compared to pure zirconium or titanium [5].

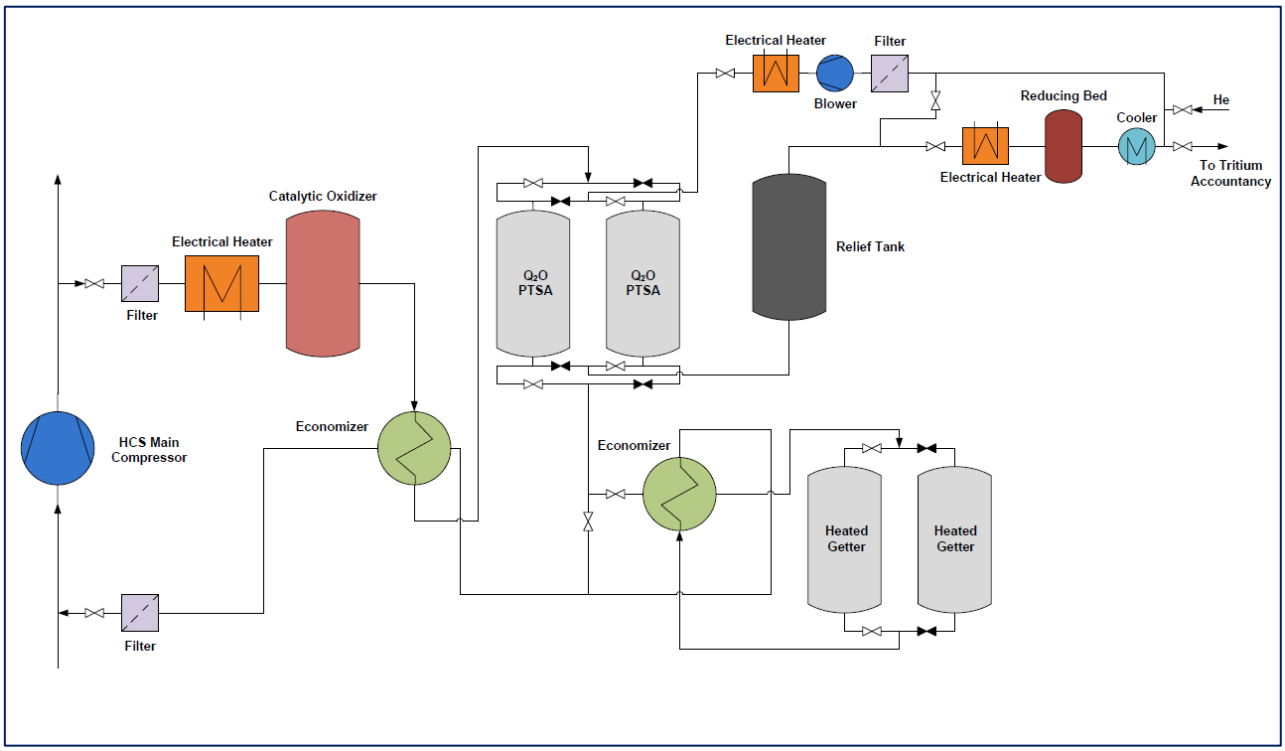

Figure 16: PFD of ITER CPS – ENEA Updated Concept

In the heated getters, the impurities form stable compounds on the surface of the material and then they diffuse in the bulk of the material, if the temperature is sufficiently high, allowing a continuous cleaning of the surface; the getter can operate also at room temperature but, in this case, the diffusion is limited and only the surface of the material is practically available to trap the impurities. The reactions between getter and impurities are irreversible, with the only exception of the hydrogen isotopes that can be removed increasing the temperature [5].

Experiments performed with a getter based on zirconium alloy patented by SAES Getters have demonstrated that impurities, such as O_2, CH_4, H_2, CO, N_2, H_2O and CO_2, can be reduced at a value of 1 ppb or less, even with inlet concentrations higher than expected in the TBM coolant [5].

In the new configuration, it is foreseen to use two heated getters, to be possible to change the working column during the replacement of the saturated one.

As for the previous design, only one column for the oxidizing bed is foreseen; in this case, it has been considered convenient to oversize the dimension instead of considering two beds, the first one operating in oxidation phase and the second one in regeneration phase. Also in this case, two PTSA columns are foreseen for the water adsorption but the adsorbent material considered is a zeolite type 5A, instead of Silica-gel.

The design data at the inlet of CPS are shown in the following Table. Regarding to the impurity concentrations in the feed stream, two different scenarios have been considered: in the first one no addition of hydrogen or water in the Helium Cooling System (HCS) is considered, while in the second one it is foreseen to add hydrogen and water to the coolant to produce natural oxide permeation barriers on helium side [5].

Table 29: CPS Updated Design Data – ENEA Concept

CPS Design Data	**Values**	
Pressure (MPa)	8.0	
Coolant temperature at inlet CPS (K)	343	
CPS flow rate (kg/s)	0.0037	
	Scenario 1	**Scenario 2**
HT partial pressure (Pa)	0.08 ÷ 0.43	0.08 ÷ 0.43
H_2 partial pressure (Pa)	5.5 ÷ 19.3	1000
H_2O + HTO partial pressure (Pa)	8	30
Max. expected impurity concentration (CO, CO_2, N_2, CQ_4, O_2) (ppmv)	10	10

The CPS design has been further updated and made consistent with the ITER requirements foreseen for the conceptual design phase [42]. As shown in the following PFD, the only substantial difference is the employment of two oxidizing beds, allowing the possibility of their regeneration.

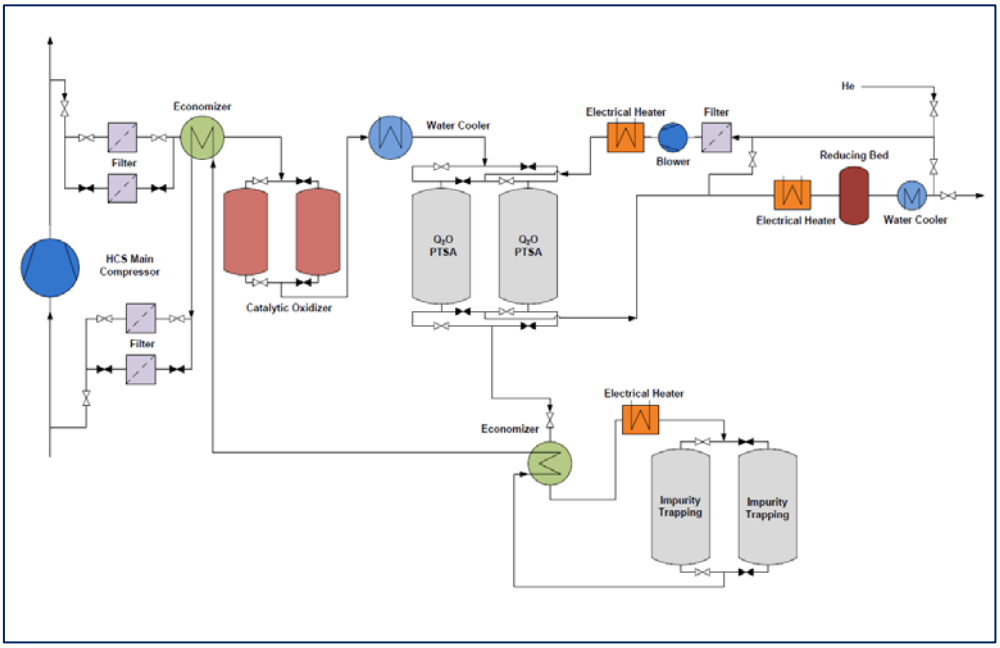

Figure 17: PFD of ITER CPS – ENEA Finalization of Conceptual Design

The design of ITER CPS is currently in progress. At the moment, the purification components seem to be confirmed [43]. Compared to the last CPS version, some design data have been changed; in the following Table some modified data are shown.

Table 30: CPS Modified Design Data

CPS Design Data	Values
CPS flow rate (kg/s)	0.03
H_2O partial pressure (Pa)	10
H_2 partial pressure (Pa)	300

One of the last examples of CPS design is reported in [44]. This system is referred to the Chinese Helium Cooled Ceramic Breeder (HCCB) TBM. This type of TBM is one of the six concepts that will be tested in ITER. In the following Figure, the PFD of the Chinese concept of CPS is shown. The gas is withdrawn downstream of the HCS compressor and passes through a filter, to remove solid particles. A flow controller is used to adjust the gas flow rate. An electrical heater increases the temperature up to 373 – 573 K, and then the gas enters in a catalytic oxidation bed in which Q_2 is transformed in Q_2O. The gas, outgoing from the catalytic bed, is cooled to room temperature by a water cooler and enters in a molecular sieve bed including zeolite type 5A; in this bed, working at less than 323 K, Q_2O is removed. The remaining impurities are removed in the following hot metal getter bed working at 673 – 873 K.

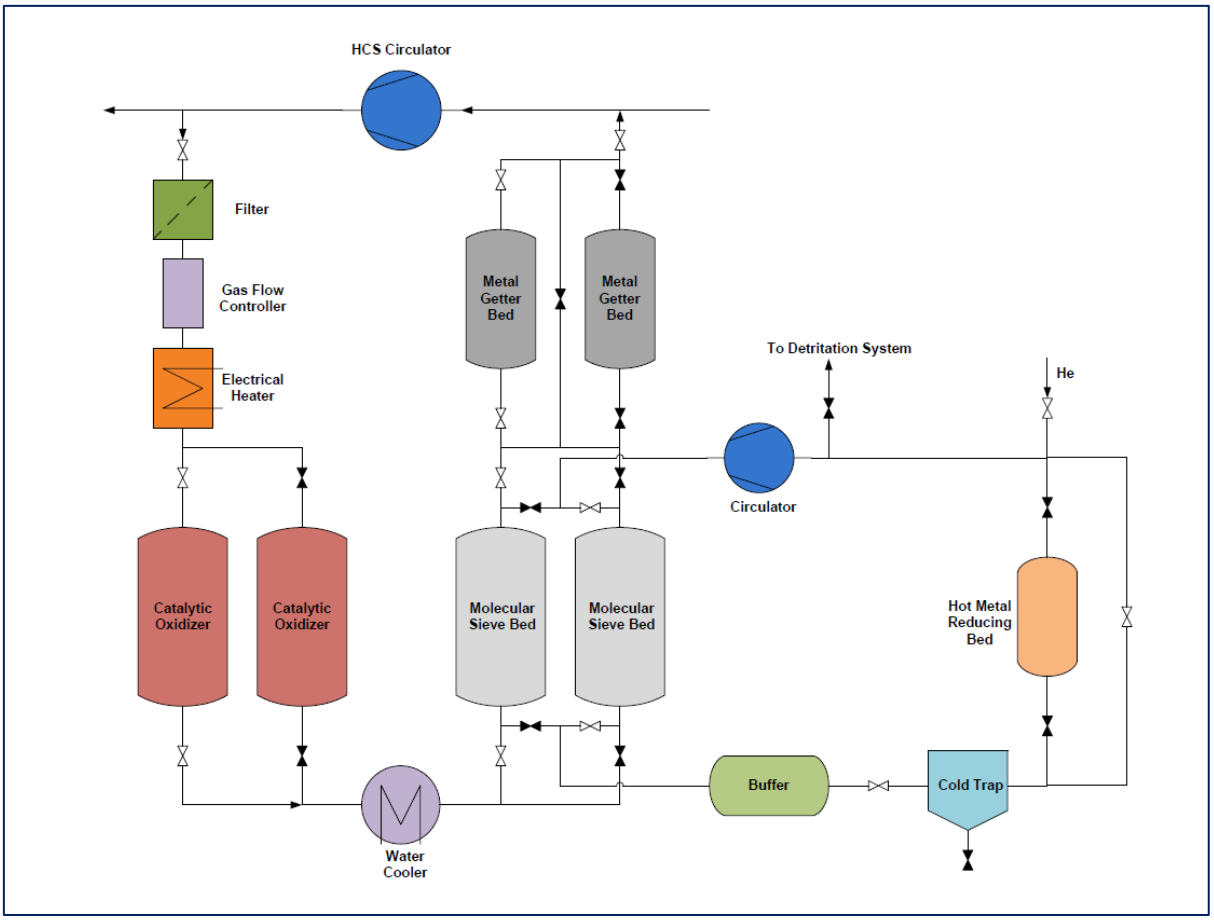

Figure 18: PFD of ITER CPS – Chinese Concept

All the above CPS designs consist of the three stages having the following scopes:

- oxidation of Q_2 and CO into Q_2O and CO_2;
- removal of Q_2O;
- removal of all remaining impurities.

In all the purification systems, the presence of an oxidizing bed to transform Q_2 and CO into Q_2O and CO_2, respectively, is foreseen. Two different types of oxidizing beds are taken into account:

- beds using copper oxide catalytic material type Cu_2O-CuO (or only CuO);
- beds using precious metals (Pd or Pt) on alumina, with the introduction of an over-stoichiometric flow of oxygen in the vessel.

For water removal, the molecular sieve beds are preferred to cold traps because they allow to avoid components working at low temperatures.

For the last stage, hot metal getter beds are considered, in the most recent designs, the reference technology to remove the remaining impurities. The only alternative, based on the use of molecular sieve beds operated at liquid nitrogen temperature, seems to be less attractive due to the low working temperatures.

In conclusion, the most widely used way for tritium removal foresees the transformation of HT into HTO, in high temperature oxidizing beds, and the following adsorption of the generated tritiated water in molecular sieve beds, at room temperature.

5 Tritium purification in DEMO

In the previous chapters, a reference process to remove tritium from the coolant gas of the helium cooled fission reactors and of the ITER fusion reactor has been shown; this process foresees two steps:

- oxidation of H_2/HT into H_2O/HTO
- removal of H_2O/HTO from He using molecular sieves.

In the present chapter, a study of the transferability of the above process to the coolant purification system of DEMO, HCPB concept, will be shown.

For the CPS design, it is necessary to evaluate the following quantities [45]:

- tritium permeation rate ($F_{T,p}$);
- CPS efficiency (η_{CPS});
- fraction of coolant flow rate to be treated (α);
- chemistry of coolant.

As far as tritium permeation rate ($F_{T,p}$) is concerned, the result of a recent simulation performed with EcosimPro simulation tool has been taken into account. This new simulation tool, using the commercial software EcosimPro, is actually under development and it takes into account the updated design of DEMO [46]. In the following Table some parameters used for the simulation are summarized [47].

Table 31: Input data used for the EcosimPro simulation

Data	Unit	Value
Fusion Power	MW	1572
Tritium Breeding Ratio (TBR)	-	1.05
Pulses	N./day	9
Pulse Time	s	7200
Dwell Time	s	2400
Tritium Generation Rate	g/d	189
Coolant Pressure	MPa	8
Coolant Flow Rate (F)	kg/s	2400
Coolant Inlet Temperature	K	573
Coolant Outlet Temperature	K	773

The calculated value of the tritium permeation rate is $F_{T,p}$ = 9 x 10^{-6} g/s, corresponding to approx. 0.4% of the total tritium production [45].

For the CPS efficiency (η_{CPS}) has been considered the value of 90%.

The fraction of coolant flow rate (α) to be treated in the CPS can be evaluated considering the following tritium mass balance equations (see following Figure) [45]:

$$Fc_o = Fc_i + \frac{F_{T,p}}{PRF} \quad (5.1)$$

$$\eta_{CPS} = \frac{c_o - c_u}{c_o} \quad (5.2)$$

$$Fc_i = (F - \alpha F)c_o + \alpha F c_u \quad (5.3)$$

where:

- F = total mass flow rate of the coolant (kg/s);
- c_o = allowable tritium mass fraction at the blanket outlet (kg/kg);
- c_u = tritium mass fraction at the CPS outlet (kg/kg);
- c_i = tritium mass fraction at the blanket inlet (kg/kg);
- $F_{T,p}$ = tritium permeation rate from breeding zone to coolant (kg/s);
- PRF = Permeation Reduction Factor (dimensionless).

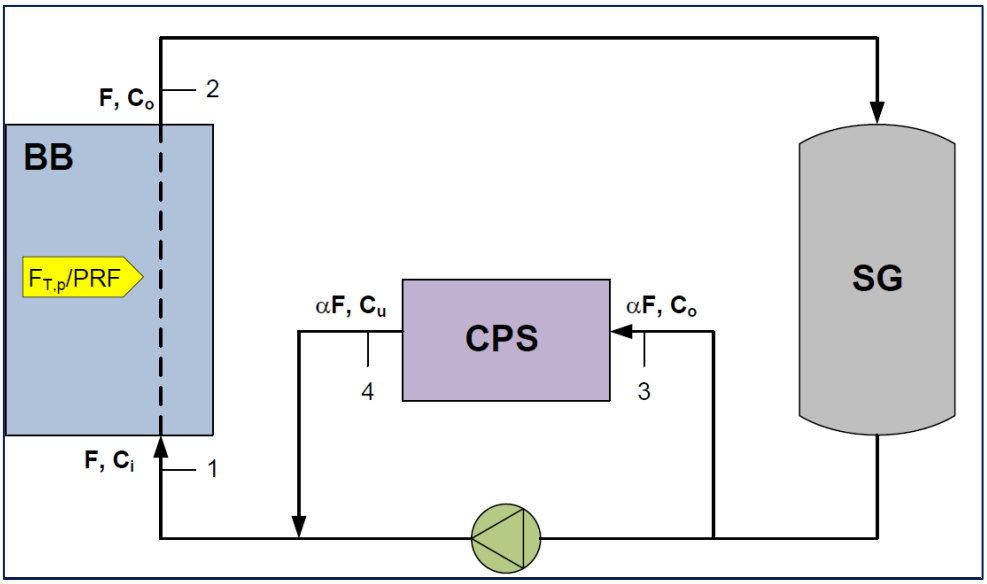

Figure 19: Scheme of the helium cooling loop

In the present study, the Steam Generator contribution will be neglected. By performing a combination of the above equations it is possible to find the expression of the coolant flow rate fraction to be treated by CPS:

$$\alpha = \frac{F_{T,p}/PRF}{Fc_o\eta_{CPS}} \quad (5.4)$$

According to [45], an allowable tritium mass fraction at the blanket outlet (c_o) of 5 ppb (6.667 ppbv) has been considered. Conservatively, a value of PRF = 1 will be considered.

Replacing the above values in (5.4), the calculated coolant fraction is 0.00083333, corresponding to a CPS flow rate of approx. 2 kg/s.

Concerning the chemistry of the coolant, the most important chemical species to be considered for the sizing of the tritium purification system are HT, HTO, H_2 and H_2O. In [5], two different situations have been considered: with and without permeation barriers. Both in HCLL and HCPB cases, helium doped with hydrogen is foreseen as stripping gas of the Tritium Extraction System (TES), with hydrogen concentration included between 0.1 ÷ 1%. Without permeation barriers, the hydrogen present in the HCS is due to the permeation of H_2 from the stripping gas, in addition to

the presence of H_2 as impurity. The presence of water is considered as an impurity and values obtained from fission reactors could be considered for a preliminary evaluation. With permeation barriers, it is necessary to adjust the oxidation potential of helium, adding some chemical agents, normally H_2 and H_2O. The two situations have been compared in [5] for the HCS of ITER HCLL:

Table 32: H_2 and H_2O partial pressures in ITER HCS

Data	Without permeation barriers	With permeation barriers
H_2 partial pressure (Pa)	5.5-19.3	1000
H_2O+HTO partial pressure (Pa)	8	30

In the most recent evaluations performed for ITER, a partial pressure of 300 Pa (x_{H_2} = 37.5 ppmv) for H_2 and a partial pressure of 10 Pa ($x_{H_{H_2O}}$ = 1.25 ppmv) for H_2O have been considered for the cooling gas [43].

In the case of DEMO HCPB 2003, a partial pressure of 1000 Pa (x_{H_2} = 125 ppmv), for the hydrogen, and a partial pressure of 50 Pa ($x_{H_{H_2O}}$ = 6.25 ppmv), for the water, have been considered [48].

In the present analysis, for a conservative evaluation of the CPS flow rate, permeation barriers have not been considered (PRF = 1). However, a conservative sizing of the purification system requires that a certain amount of hydrogen and water is taken into account. For this scope, a parametric calculation will be performed considering different hydrogen concentrations; the maximum hydrogen content considered will be 1000 Pa and the maximum water content will be 50 Pa, according to DEMO specifications.

In the case without chemical control of the cooling gas, an evaluation of the hydrogen amount permeated from TES and of the hydrogen impurity level would be required. In the absence of data relevant to fusion reactors, the results of the experiences relevant to the helium cooled fission reactors will be considered. In these reactors, the level of H_2 in the coolant is included between 0.1 and 10 ppmv. For the present analysis, the minimum hydrogen content considered will be 10 ppmv, corresponding to the maximum level detected in HTGRs.

In the following Table, the levels of the impurities detected in the HTGRs are summarized (see par. 2.3).

Table 33: Impurity levels in HCSs of HTGRs

Reactor Type	Impurity Levels (ppmv)						
	H_2O	H_2	CO	CO_2	CH_4	N_2	O_2
Dragon Reactor	0.1	0.1	0.05	0.02	0.1	0.05	0.1
Peach Bottom	0.5	10	0.5	< 0.05	1	0.5	-
Fort St. Vrain	1	7	3	1	0.1	-	-
HTR-10	≤ 0.2	≤ 3	≤ 3	-	≤ 1	≤ 1	-
HTTR	≤ 0.2	≤ 3	≤ 3	≤ 0.6	≤ 0.5	≤ 0.2	≤ 0.04

To evaluate the minimum water content inside the coolant, the experience from fission reactors will once again be considered. From the above Table, which considers only the reactors actually manufactured, it is possible to see that the water concentration is included between 0.1 and 1 ppmv. For the present analysis, the minimum water content considered will be 1 ppmv, corresponding to the maximum level detected in HTGRs.

Other few chemical impurities can be present in the coolant gas (CO, CO_2, CH_4, N_2, O_2). Analyzing the chemical composition of the cooling gas of the fission reactors, it is possible to see that their concentrations are in general low and, more important, the impurity sources, in case of fusion reactors, should be further reduced due to the absence of a graphite based core (the content of CO, CO_2, CH_4 is mainly connected to the core graphite) and coolant temperatures much lower. For this reason, the presence of these impurities will be neglected in the present analysis (in ITER, the removal of the residual impurities is foreseen to be performed by a heated getter [5], [49], [42]).

The inlet input data considered for the sizing of DEMO CPS are summarized in the following Table.

Table 34: Operating conditions at the inlet of DEMO CPS

Data	Unit	Value
Mass Flow Rate	kg/s	2
Normal Flow Rate (1)	Nm^3/h	4.034×10^4
Pressure	MPa	8
Inlet Temperature	K	573
HT Partial Pressure (2)	Pa	0.05334
H_2 Partial Pressure	Pa	80 ÷ 1000
H_2O Partial Pressure	Pa	8 ÷ 50

(1) The Normal Conditions considered are: T_n = 273.15 K and p_n = 101325 Pa.

(2) All tritium in HCS is considered in HT form.

The following Figure shows a preliminary PFD of the part of the purification system dedicated to the tritium removal.

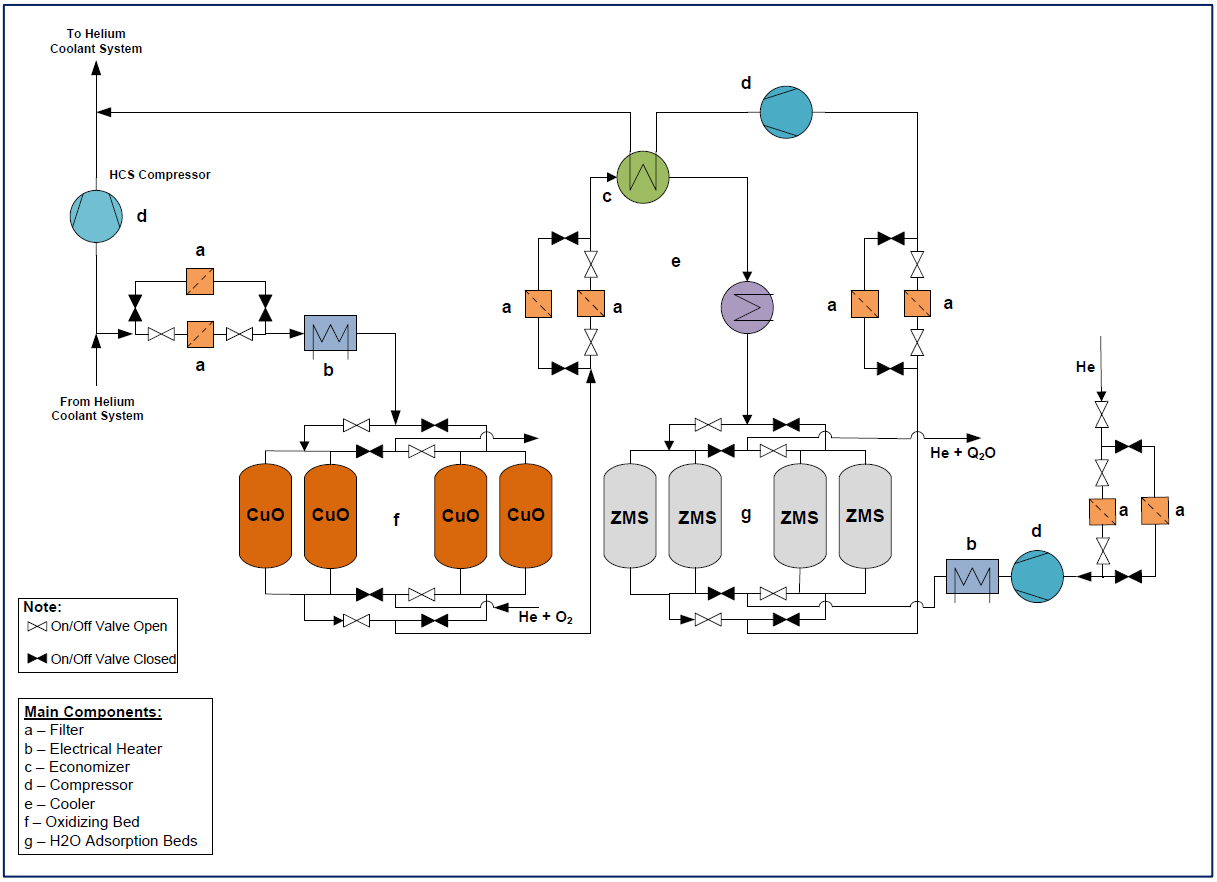

Figure 20: PFD of DEMO Coolant Purification System

5.1 Sizing of the CPS fixed beds

In the following paragraphs a preliminary sizing of the oxidizing beds and of the water adsorption beds to be included in the CPS of DEMO will be described.

5.1.1 Sizing of the oxidizing beds

The oxidizing material is the same considered in chapter 3 (see Table 12).

According to the above PFD, the loop foresees four oxidizing beds; in the first two ones, the Q_2 present in the gas to be purified is oxidized into Q_2O, while in the second two ones the exhausted catalyst is regenerated.

The input data used for each oxidizing bed sizing are shown in the following Table:

Table 35: Operating conditions at the inlet of each Oxidizing Bed

Data	Unit	Value
Mass Flow Rate	kg/s	1
Flow Rate	Nm^3/h	2.017×10^4
Pressure	MPa	8
Inlet Temperature	K	523
HT content	Pa (ppbv)	0.053 (6.667)
H_2 content	Pa (ppmv)	80 ÷ 1000 (10 ÷ 125)

The evaluation of the oxidizing bed dimensions, the amount of catalyst, the required regeneration time and the regeneration flow rate will be performed considering the following steps:

a. evaluation of the internal bed diameter;
b. evaluation of the bed height;
c. evaluation of the catalyst amount;
d. evaluation of the maximum pressure;
e. evaluation of the GHSV;
f. evaluation of the maximum oxidable amount of hydrogen;
g. evaluation of the operating time before regeneration;
h. evaluation of regeneration flow rate.

a. Evaluation of the internal bed diameter

As already done in chapter 3, the internal bed diameter will be evaluated calculating the superficial velocity corresponding to the maximum acceptable value of the pressure drop through the oxidizing bed. For this purpose, Ergun's equation (3.10) will be used.

Assuming a maximum value of $\Delta P/L$ equals to 2.5 kPa/m, up-flow and down-flow operation is allowed. With this value of pressure drop it is possible to solve the equation (3.10) or the equivalent (3.11), to find the corresponding value of the superficial velocity. Also in this case the values $\varepsilon = 0.37$ and $D_p = 4.091$ mm will be used.

For the evaluation of viscosity μ and density ρ, the formulas included in [50] will be used:

- $\rho = 7.221$ kg/m^3;
- $\mu = 2.939 \times 10^{-5}$ Pa s.

Including the above values and solving the equation (3.11) it is possible to find the maximum value of the superficial velocity: $u_{max} = 0.230$ m/s.

The corresponding value of the minimum internal diameter of each bed is:

$$D_{min} = \left(\frac{4\,q}{\pi\,u}\right)^{0.5} = 0.874\,m \qquad (5.5)$$

where q is the actual flow rate of the gas:

$$q = \left(\frac{\dot{m}}{\rho}\right) = 0.138\ m^3/s \tag{5.6}$$

and ṁ = 1 kg/s is the mass flow rate.

The selected internal diameter has to be greater than D_{min}; for the present application the selected diameter will be: $D_{selected}$ = 1.5 m.

The corresponding superficial velocity is:

$$u_{adjusted} = u_{max}\left(\frac{D_{min}}{D_{selected}}\right)^2 = 0.078\ m/s \tag{5.7}$$

The value of ΔP/L, corresponding to the selected internal diameter, can be evaluated replacing the value of $u_{adjusted}$ in equation (3.11); the calculated value results:

$$\left(\frac{\Delta P}{L}\right) = 0.395\ kPa/m \tag{5.8}$$

The minimum pressure drop required to avoid uneven distribution and channeling is: ΔP/L = 0.23 kPa/m [34]; this condition is satisfied.

b. Evaluation of the bed height

In case of gas operation, it is possible to find commercial vessel having a value of L/D in the range 1 ÷ 3. With the scope to maximize the duration of the bed, reducing the number of regeneration, a value of bed height equal to 4.5 m will be considered.

The corresponding total pressure drop is:

$$\Delta P = 1.8\ kPa \tag{5.9}$$

c. Evaluation of the catalyst amount

For the catalyst bulk density, the following value will be considered:

$$\rho_{catalyst} = 830\ kg/m^3 \tag{5.10}$$

The volume of the bed is:

$$V_{bed} = 7.95\ m^3 \tag{5.11}$$

The corresponding amount of catalyst is:

$$M_{catalyst} = 6600\ kg \tag{5.12}$$

d. Evaluation of the maximum pressure

The mass of the catalyst column produces a force of 64746 N, corresponding to a pressure of 36.6 kPa. Adding the above value to (5.9), the resulting pressure is 38.4 kPa. This value is a little higher than the suggested design value of 35 kPa, but still distant from the maximum acceptable pressure of 55 kPa; for this reason the calculated value will be considered acceptable.

e. Evaluation of the GHSV

The calculated value of GHSV results 2537 h^{-1}. For this application, the calculated value of GHSV is acceptable.

f. Evaluation of the maximum oxidable amount of hydrogen

For a preliminary evaluation, a maximum reduction of 70% at the end of operation can be considered. With this assumption, the amount of catalyst available for the hydrogen oxidation is:

$$M_{cat,available} = 0.70 \times M_{catalyst} = 4620 \text{ kg} \quad (5.13)$$

Assuming that the amount of CuO in the catalyst is approx. 45 wt%, the mass of the CuO contained in the bed results M_{CuO} = 2079 kg, corresponding to a number of moles:

$$n_{CuO} = 26136 \text{ mol of CuO}, \quad (5.14)$$

assuming for CuO a molar mass of 79.545 g/mol.

The above value is also the maximum number of Q_2 moles that it is possible to transform into Q_2O:

$$n_{Q2} = 26136 \text{ mol of } Q_2 \quad (5.15)$$

g. Evaluation of the operating time before regeneration

To evaluate the operating time before regeneration, it is necessary to calculate the flow rate of Q_2 = HT + H_2.

Considering the data included in Table 35, the molar fraction of HT is: $x_{HT} = 6.667 \times 10^{-9}$.

The HT flow rate is:

$$\dot{n}_{HT} = x_{HT}\, \dot{n}_{tot} = 1.667 \times 10^{-6} \text{ mol/s} \quad (5.16)$$

where $\dot{n}_{tot} = \frac{p_n \dot{V}_{tot}}{R\, T_n} = 250\ mol/s$

The cases considered are the following:

Table 36: Operating time before regeneration

	Case#1	Case#2	Case#3
H_2 molar fraction (ppmv)	10	37.5	125
H_2 molar flow rate (mol/s)	0.00250	0.00937	0.03125
Q_2 molar flow rate $\dot{n}_{Q2}$ (mol/s)	2.502×10^{-3}	9.372×10^{-3}	3.125×10^{-2}
Time before regeneration (d)	121	32	10

In case#1, the hydrogen level corresponds to the maximum value of impurity measured in helium cooled fission reactors; in this case no permeation barrier is foreseen. In case #2 and case#3 permeation barriers are foreseen; in case#2 the hydrogen content corresponds to the last value estimated for ITER and in case#3 to the value estimated for DEMO HCPB 2003.

In case#1, case#2 and case#3 the regeneration is required after approx. 4 months, 1 month and 1.5 week, respectively. In all cases it would seem possible to use copper oxide catalyst, by performing periodic regenerations and by replacing of the component when the amount of regenerated catalyst will no longer be sufficient (the catalyst suppliers foresee an overall life of approx. one year, considering multiple regenerations). In case#3, a catalyst based on precious metals could be considered as alternative to the copper oxide catalyst. The main drawback of this type of catalyst is the need to introduce inside the oxidizing bed a mixture of oxygen and helium (an additional supply line for oxygen is required); the oxygen is required to carry out the oxidation reaction. The amount of the added O_2 has to be slightly superstoichiometric, according to the equation:

$$2H_2 + O_2 \rightarrow 2H_2O$$

For this reason, a certain amount of O_2 will be present in the gas at the exit of the bed. Another drawback of this material is the higher cost. The main advantage is that regeneration is not necessary any more. However, poisons and masking agents present in the gas could reduce the efficiency and the life of the catalyst.

h. Evaluation of the regeneration flow rate

The regeneration can be carried out considering two pairs of vessels, the first one working in purification phase and the second one in regeneration phase. When the first pair is exhausted, it is placed in regeneration and the second one put in service. For the regeneration of the exhausted catalyst, a flow of helium, with very low concentration of oxygen can be used. The same precautions already described in chapter 3 have to be observed during regeneration. Also in this case, the helium flow rate will be evaluated considering that its function is only to supply oxygen for the regeneration of the catalyst.

For this evaluation, the following data, relevant to the regeneration gas, will be considered:

Table 37: Operating conditions of the regeneration gas He + O_2

Data	Unit	Value
Pressure	MPa	0.2
Temperature	K	473
Density	kg/m^3	0.203
Viscosity	Pa s	2.739×10^{-5}

The regeneration flow rate has to guarantee a pressure drop greater than 0.23 kPa/m, to avoid uneven distribution and channeling. Considering the equation (3.11) and replacing the above values of pressure drop, density and viscosity, it is possible to calculate the minimum value of the superficial velocity. This value is u_{min} = 0.112 m/s, corresponding to the flow rate q_{min} = 0.198 m^3/s.

5.1.2 Sizing of the Molecular Sieve beds

Also in the present analysis, the materials considered for the adsorption of the tritiated water are the Zeolite Molecular Sieves (ZMSs). The main characteristics of a commercial zeolite type 4A are shown in Table 16.

According to the PFD of the purification system, the loop foresees four molecular sieve beds; in the first two ones the tritiated water is adsorbed by ZMSs, while in the second two ones the exhausted material is regenerated.

The gas conditions at the inlet of each molecular sieve bed, operating in adsorption phase, are shown in the following table:

Table 38: Operating conditions at the inlet of each Molecular Sieve Bed, adsorption phase

Data	Unit	Value
Mass Flow Rate	kg/s	1
Flow Rate	Nm^3/h	2.017×10^4
Pressure	MPa	8
Inlet Temperature	K	298
HTO content from HT oxidation	Pa (ppbv)	0.053 (6.667)
H_2O content from H_2 oxidation	Pa (ppmv)	80 ÷ 1000 (10 ÷ 125)
H_2O content from impurities	Pa (ppmv)	8 ÷ 50 (1 ÷ 6.25)

The evaluation of the amount of molecular sieves and the regeneration flow rate will be performed considering the following steps:

a. evaluation of the internal bed diameter;
b. evaluation of the bed height and molecular sieve amount;
c. evaluation of the removed amount of water and saturation time;
d. evaluation of the maximum pressure;
e. evaluation of the heat required for the regeneration;
f. evaluation of the regeneration flow rate.

a. Evaluation of the internal bed diameter

For the evaluation of the internal bed diameter, the same considerations already shown in the Chapter 3 can be applied. In particular, the equations (3.10) and (3.11) can be applied for the pressure drop evaluations.

For the molecular sieve beds, typically the direction of the gas flow is down-flow during adsorption and up-flow during regeneration [34]. According to [34], an allowable pressure drop $\Delta P/L$ = 7.5 kPa/m can be considered. Using this value of pressure drop it is possible to solve the (3.11) to find the corresponding value of the superficial velocity. Also in this case, for the calculation the value ε = 0.37 will be used.

For the evaluation of the dynamic viscosity μ and density ρ the formulas reported in [50] will be used. In this case:

- ρ = 12.442 kg/m^3
- μ = 1.983 x 10^{-5} Pa s

Including the above values in (3.11), the maximum value of the superficial velocity results:

- u_{max} = 0.189 m/s.

The corresponding minimum value of the internal bed diameter is:

$$D_{min} = \left(\frac{4\,q}{\pi\,u_{max}}\right)^{0.5} = 0.734\,m \tag{5.17}$$

where q is the actual flow rate of the gas:

$$q = \left(\frac{\dot{m}}{\rho}\right) = 0.080\,m^3/s \tag{5.18}$$

and $\dot{m}$ = 1 kg/s is the mass flow rate.

For the present analysis, the selected internal diameter is: $D_{selected}$ = 1.0 m.

The corresponding superficial velocity is:

$$u_{adjusted} = u_{max}\left(\frac{D_{min}}{D_{selected}}\right)^2 = 0.102\,m/s \tag{5.19}$$

The $\Delta P/L$ value corresponding to the selected diameter can be evaluate replacing the above value of $u_{adjusted}$ in (3.11), obtaining $\Delta P/L$ = 2.602 kPa/m; this value is greater than the minimum pressure drop $\Delta P/L$ = 0.23 kPa/m required to avoid uneven distribution of the flow and channeling.

b. Evaluation of the bed height and molecular sieve amount

The total height of the bed has to be greater than H_{MTZ}.

The height of the MTZ can be estimated using [34]:

$$H_{MTZ} = \left(\frac{u_{adjusted}\cdot 3600}{640}\right)^{0,3} Z = 0.220\ \text{m} \tag{5.20}$$

where Z = 0.26 m for 1.5 mm particle diameter.

In the present case, a ratio L/D = 3 has been selected to increase the adsorption capacity in order to have longer adsorption time without creating the risk to damage the adsorbing material.

In the following Table, the characteristics of the ZMS beds are summarized.

Table 39: ZMS bed characteristics

Data	Unit	Value
Total height H_{tot}	m	3
Total volume of ZMS	m^3	2.356
Total amount of ZMS	kg	1696
Total press. drop through the bed	kPa	7.806

c. Evaluation of the removed amount of water and saturation time

To evaluate the total water adsorbed by the beds, the same three cases considered in the previous paragraph are considered. In the following Table, the amount of tritiated water included in the gas to be purified is shown for the three cases.

Table 40: Amount of tritiated water to be removed

	Case#1	Case#2	Case#3
H_2O partial pressure (Pa) from H_2 oxidation (1)	80	300	1000
H_2O partial pressure (Pa) from impurities	8	10	50
HTO partial pressure (Pa) from HT oxidation (1)	0.053	0.053	0.053
Total Q_2O partial pressure (Pa)	88.053	310.053	1050.053
Q_2O mass flow rate (kg/h)	0.178	0.628	2.126

(1) The efficiency of the hydrogen oxidation performed by CuO is supposed to be 100 %.

In case#1, hydrogen and water level corresponds to the maximum value of impurity measured in helium cooled fission reactors; in this case no permeation barrier is foreseen. In case #2 and case#3 permeation barriers are foreseen; in case#2 hydrogen and water content corresponds to the last values estimated for ITER [43] and in case#3 to the values estimated for DEMO HCPB 2003 [48].

Only the water adsorbed in the saturation zone will be considered. The height of the saturation zone is:

$$H_S = H_{tot} - H_{MTZ} = 2.780\ m \qquad (5.21)$$

The volume of the saturation zone is V_S = 2.183 m^3 and the corresponding ZMS amount is M_s = 1572 kg.

The maximum amount of water that it is possible to adsorb in V_s can be calculated using (see 3.29):

$$M_{H2O} = M_S\ 0.65\ C \qquad (5.22)$$

The adsorbate loading capacity C depends on the water content in the gas to be purified. In the following Table, the loading capacity of a zeolite type 4A, the amount of water adsorbed in the saturation zone and the adsorption time are shown.

Table 41: Q_2O adsorbed and saturation time

	Case#1	Case#2	Case#3
Total Q_2O partial pressure (kPa)	8.805×10^{-2}	3.100×10^{-1}	1.050×10^{0}
Water adsorption capacity (kg of H_2O adsorbed / kg of adsorbent) at 25 °C	0.190	0.205	0.220
Amount of adsorbed water (kg)	194.1	209.5	224.8
Time required for the saturation of the bed (d)	45	14	4.4

d. Evaluation of the maximum pressure

The total pressure should not exceed 55 kPa, to avoid the damage of the molecular sieves and the value of pressure to be considered in phase of design should be approx. 35 kPa [34]. In the following Table the total pressures acting on the particles at the bottom of the beds are shown.

Table 42: Total pressure drops

	Case#1	Case#2	Case#3
Pressure due to ZMS weight (kPa)	21.195	21.195	21.195
Pressure due to H_2O weight (kPa)	2.426	2.618	2.809
Pressure due to pressure drop (kPa)	7.806	7.806	7.806
Total pressure (kPa)	31.427	31.619	31.810

In all cases the total pressure is lower than the target value of 35 kPa.

e. Evaluation of the heat required for the regeneration

To evaluate the regeneration flow rate, it is necessary to calculate the heat required for the regeneration of the molecular sieves.

This heat is composed of 4 contributions: the heat required to desorb the water, the heat required to warm the molecular sieves and the steel bed and the heat loss. The equations that will be used are (3.34), (3.35), (3.36) and (3.37).

The material considered for the bed is an austenitic stainless steel type 316L. To evaluate the steel mass of the bed, it is necessary to know the thickness of the vessel. To make a preliminary estimation of the thickness, ASME VIII Div. 1 will be considered. The first step to evaluate the minimum thickness is to select the most severe case between adsorption and regeneration. In the following Table, the conditions to be considered for the thickness evaluation are compared.

Table 43: Comparison between adsorption and regeneration conditions

	Adsorption	Regeneration
T_{design} (°C)	40	325
P_{max} (MPa)	8	0.2
P_{design} = 1.1 x P_{max} (MPa)	8.8	0.22
Max. allowable stress (MPa)	113	71

According to ASME VIII Div. 1, the minimum thickness of the vessel results:

$$t = \frac{P_{design} R}{S\,E - 0.6\,P_{design}} \qquad (5.23)$$

where:

R = Internal bed radius

S = Max. allowable stress

E = Welded joint efficiency

The most severe case to be considered is adsorption.

Considering:

R = 500 mm

S = 113 MPa

E = 1

the calculated minimum thickness results t = 40.8 mm; in the present analysis a thickness of 45.0 mm will be considered.

Considering a steel density of 8000 kg/m^3, the results of the weight estimation of each vessel are shown in the following Table:

Table 44: Weight of the vessels

Data	Unit	Value
Vessel mass (cylinder)	kg	3545
Head mass (each)	kg	295
Total mass	kg	4135

Considering the total amount of adsorbed water shown in Table 41 and the total amount of ZMS shown in Table 39, the heat required for the bed regeneration is shown in the following Table:

Table 45: Heat amount required for regeneration

	Case#1	Case#2	Case#3
Qw [kJ]	8.152 x 10^{+5}	8.799 x 10^{+5}	9.442 x 10^{+5}
Q_{ZMS} [kJ]	4.155 x 10^{+5}	4.155 x 10^{+5}	4.155 x 10^{+5}
Q_{ST} [kJ]	5.065 x 10^{+5}	5.065 x 10^{+5}	5.065 x 10^{+5}
Q_L [kJ]	1.737 x 10^{+5}	1.800 x 10^{+5}	1.866 x 10^{+5}
Q_{TOT} [kJ]	1.911 x 10^{+6}	1.982 x 10^{+6}	2.053 x 10^{+6}

f. Evaluation of the regeneration flow rate

The flow rate of the regeneration gas will be calculated using the equation [34]:

$$\dot{m}_{rg} = \frac{2.5\ Q_{TOT}}{(C_p)_{He}(T_{hot} - T_i)\ t_{heating}}\ [kg/h] \qquad (5.24)$$

where:

T_{hot} = 573 K (Temperature of the inlet gas)

T_i = 298 K (Temperature of the bed at the beginning of the regeneration)

$(C_p)_{He}$ = 5.195 kJ/kg K

$t_{heating}$ = 60% of the total adsorption period (h)

The results of the calculations are shown in the following Table.

Table 46: Helium conditions in regeneration

	Case#1	Case#2	Case#3
$\dot{m}_{rg}$ (kg/h)	5.113	17.307	56.488
q (m^3/h)	30.435	103.018	336.238
u (m/h)	38.751	131.167	428.112
u (m/s)	0.011	0.036	0.119

The volumetric flow rate and the superficial velocity have been calculated considering the gas characteristics corresponding to P = 0.2 MPa and T = 573 K:

- ρ = 0.168 kg/m^3
- μ = 3.133 x 10^{-5} Pa s

The pressure drop, corresponding to the calculated superficial velocity, has to be greater than 0.23 kPa/m, according to [34].

Considering the above values of density, dynamic viscosity and superficial velocity, it is possible to calculate the pressure drops, using (3.11); the calculated values are shown in the following Table:

Table 47: Pressure drop values in regeneration

	Case#1	Case#2	Case#3
ΔP/L (kPa/m)	0.151	0.496	1.661

As far as ΔP/L is concerned, for case#1 the regeneration time need to be decreased, in order to increase the flow rate and the pressure drop. Considering 35% of the total adsorption period, the value of the regeneration flow rate is $\dot{m}_{rg}$ = 8.766 kg/h. The corresponding value of the pressure drop is ΔP/L = 0.254 kPa/m.

For the other cases the condition is satisfied and the pressure drop values are suitable for an up-flow operation.

Considering that the value of the purification flow rate is 3600 kg/h, the percentage value of the regeneration flow rate results:

Table 48: Percentage value of the regeneration flow rate respect to adsorption

	Case#1	Case#2	Case#3
%	0.24	0.48	1.57

In general, the regeneration flow rate has to be as small as possible; a typical value considered for the regeneration is approx. 10 % of the purification flow rate [34].

6 Experimental activities

Currently, PTSA (Pressure Temperature Swing Adsorption) is the reference process considered for the removal of tritiated water in the CPSs of HCPB and HCLL TBMs. This process, which considers the use of molecular sieves to adsorb water from the gas to be purified, is widely used in industrial applications requiring the drying of gas. In industrial applications, generally the drying system consists of two beds, one working in purification and the other one in regeneration. The most important difference between fusion and industrial applications is that in fusion the two working conditions are characterized not only by a remarkable difference of temperature, but also by a very different pressure (8 MPa during adsorption and few bar during regeneration).

The candidate materials to be used for water adsorption are the zeolites. It is possible to find various types of zeolites on the market (Type 3A, 4A, 13X. etc.). These zeolites exhibit different performances towards adsorption capacity changing the type of impurity or the conditions of the gas to be purified.

To support the design activity and the material selection an experimental campaign could be performed having the following objectives:

- comparison of the performances of different types of zeolites;
- assessment of the efficiency of the regeneration process, as function of flow rate and temperature;
- evaluation of CO_2 influence on the adsorption process.

The tritiated water contained in the gas used for the regeneration of the adsorbing beds need to be reduced in tritiated gas HT to allow the treatment in the systems dedicated to the final extraction of tritium. Currently, the reference process studied for ITER foresees the use of reducing beds based on metallic alloys. In particular, the material candidate to be used in the reducing beds is the SAES ST909 alloy, a Zr-Mn-Fe alloy using aluminium as binder for pellet formation.

An experimental campaign could be performed having the following objectives:

- determination of the performance of the material;
- determination of breakthrough curves as a function of experimental conditions;
- investigation of the degradation of the bed due to repeated cycles;
- investigation of the effect of increasing H_2 concentration.

Tritium recovery from HTO can be also attained by using Pd-Ag membrane reactor. In such device, the water decontamination is achieved or via isotopic swamping (6.1) or via water gas shift (6.2):

$$HTO + H_2 \leftrightarrow H_2O + HT \quad (6.1)$$

$$HTO + CO \leftrightarrow CO_2 + HT \quad (6.2)$$

The presence of the Pd-Ag membrane allows the continuous recovery of the produced tritiated gas (HT).

An experimental campaign could be performed having the following objectives:

- determination of the Pd-Ag membrane reactor performance for both isotopic swamping and water gas shift reactions;
- selection of suitable catalyst;
- investigation of the operating conditions;
- investigation of the effect of increasing H_2 concentration in the feeding stream.

7 Conclusions

In chapter 2, a review of the coolant purification systems used in HTGRs has been carried out. From this review is emerged that the most widely used process for tritium removal foresees the transformation of HT into HTO, in high temperature copper oxide beds, and the following adsorption of the generated tritiated water in molecular sieve beds, at room temperature.

In chapter 3 an analysis on transferability of the technologies used in ITER and HTGRs for the helium coolant purification to the cover gas of a pool-type SFR, such as ASTRID, has been carried out. The result of this preliminary analysis is that the above described technologies for tritium removal can be applicable to the purification of fission reactor cover gas.

In chapter 4, a review of the coolant purification systems studied for ITER TBMs, using helium as coolant, has been carried out. Also in this case the transformation of HT into HTO, in copper oxide beds, and the following adsorption of the generated tritiated water in molecular sieve beds, at room temperature, is the most considered purification process.

Finally, in chapter 5, a preliminary sizing of a system for tritium removal from the coolant of DEMO reactor, HCPB concept, has been carried out. The scope of this evaluation is to study the transferability of the process considered for ITER and HTGRs, also to DEMO. The result of this preliminary analysis is that the above described process could be applicable also to DEMO.

Annex

Non Evaporable Getter (NEG) for tritium recovery from helium: a new approach for DEMO CPS

As previously described, tritium removal from the coolant gas is based on the oxidation of the Q_2 species onto oxidizing beds and subsequent removal of the Q_2O inside molecular sieve. The technologies used in such process (i.e. oxidizing beds and molecular sieve beds) are reliable and characterized by an high readiness level. However, especially in view of DEMO, also another approach is under investigation. The philosophy of the new approach is to avoid the formation of tritiated water that has to be necessarily treated afterwards. In addition, without the oxidation steps, the follow aspects are eliminated:

- *Regeneration of the metal oxide bed*. 100% regeneration of this component is difficult to achieve and also rather dangerous due to the use of oxygen together with the possible presence of hydrogen.
- *Production of large amount of tritiated waste*. As previously described the copper oxide catalyst can be regenerated several times, but after approximately one year it has to be replaced (see Paragraph 5.1.1). Of course such materials represent a tritiated waste.
- *Tritiated water radiological hazard and processing.* Firstly the radiological hazard of the Q_2O is much higher than Q_2 and, secondly, the process to decontaminate the produced tritiated water is difficult and expensive.

The intent of this Annex is to briefly describe a new approach that has been recently proposed for DEMO CPS. As illustrated in Figure 21, the proposed solution relies on the use of novel getter materials which are characterized by very promising sorption properties. At this moment, the knowledge and the behaviour of such technology under condition relevant for DEMO is very poor and should be implemented with dedicated experiments.

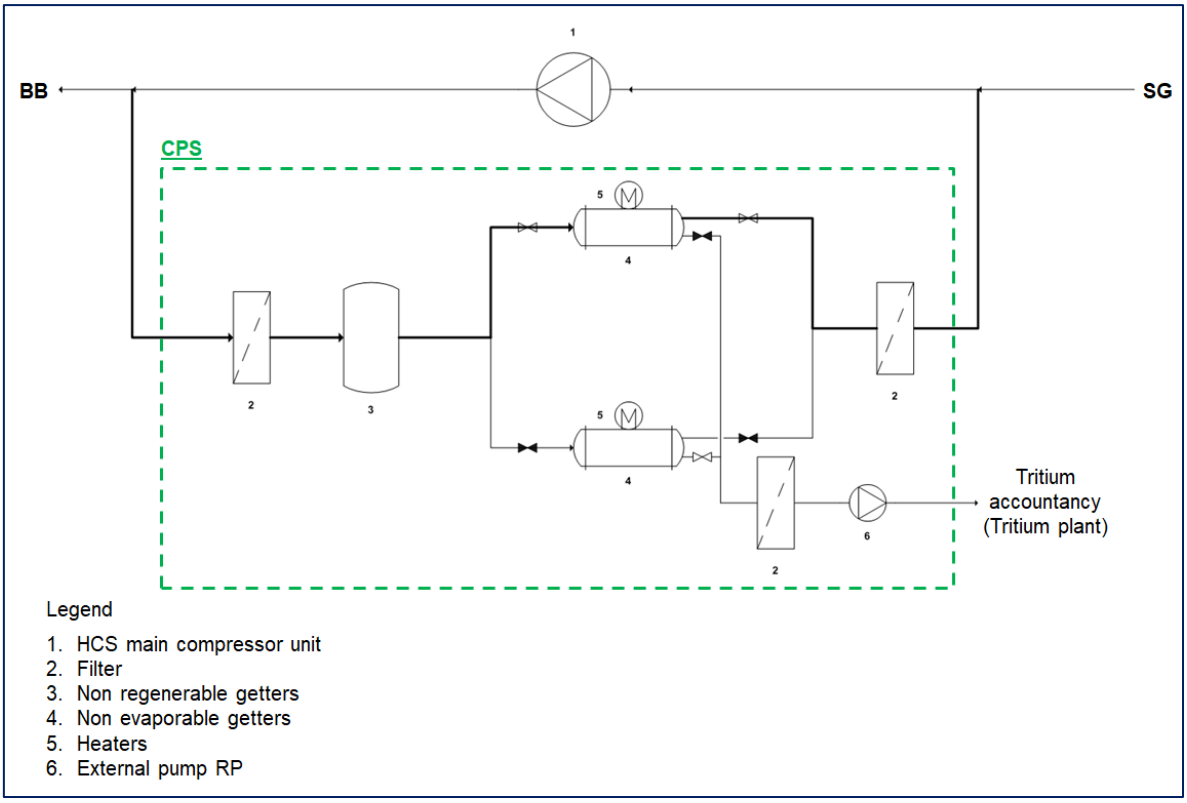

Figure 21: Conceptual design of the CPS for He-cooled blankets based on the use of getter

In practice the CPS is located after the steam generator where the temperature of the coolant is about 300 °C. Only a fraction of the coolant is routed from the HCS to the CPS loop. The following describes the operation of the proposed CPS design.

- The slip stream, at first, encounters the inlet filter for dust and solid particulate removal. The use of high pressure filters made of stainless steel is preferable; an example could be the PORAL INOX filter realized by sinterization at high temperature of granular metallic dust suitable for temperatures up to 450 °C. The main problem with the inlet filter is its maintenance, in this view there are two possibilities: 1) use a double (redundancy) filter configuration or 2) select a cartridge filter with a proper equipment (valves and connections) to ensure its rapid substitution when plugged by impurities. The first solution – double filter configuration – implies a larger space allocation, while the second – single cartridge filter – do not assure protection of the CPS from the access of impurities during substitution of the cartridge.
- The non-regenerable getter has the function of removing impurities. At this stage, it is not possible to define the best location of this impurity removal system. It would be preferable for the NEGs to receive a He-stream with only Q_2 as impurities, in this sense the non-regenerable getter should be placed before the NEGs. On the other hand, the non-regenerable getter may sorb also Q_2 species which are not recovered afterwards. This aspect needs to be clarified in the future the getter performances are experimentally characterized under DEMO relevant conditions.
- Q_2 removal from the helium slip stream by NEGs. To ensure the continuous operation, two identical getters are foreseen: one in operation and one in regeneration by means of an external pump. The exhaust of the external pump will mainly consist of hydrogen isotopes, that should be sent to the tritium plant. Both the NEGs are equipped with their own heating system which usually consists of a common electric heater equipped with an external power supply control unit. The heating system allows warm up of the alloy and control of temperature during activation, regeneration, and (if necessary) also during sorption.
- Outlet filters. The presence of these outer filters (before the HCS and the tritium plant) is foreseen to recover dust or particles released by the getter. Only dedicated experimental tests can verify if the NEGs release particles during their operation.

For what concern the NEG, three different getter alloys produced by SAES getter are considered:

- ST101 (Zr 84wt.%, Al 16 wt.%);
- ST 707 (Zr 70wt.%, V 24.6wt.%, Fe 5.6wt.%);
- ZAO (Zr-V-Ti-Al).

According with the Sieverts' parameters provided by SAES getter, and assuming a maximum tritium concentration in the coolant loop of 5 ppb, the values of the Sieverts' constant and the hydrogen concentration at the getter surface for the three alloys (calculated according with Eqs. A.1 and A.2) are listed in Table 49.

$$P_0 = C_0 P_{He} = (5 \times 10^{-9}) \times (8 \times 10^{6}) = 4 \times 10^{-2} Pa = 3 \times 10^{-4} torr \quad \text{(A.1)}$$

$$q_0(T) = [P/K(T)]^{1/2} = \left[P/10^{(A-B/T)}\right]^{1/2} \quad \text{(A.2)}$$

Table 49: Sieverts' constants K(T) and surface equilibrium concentrations $q_0(T)$ at pressure P_0 and at temperatures of 300 and 500 °C, for some getter alloy

$P_0=3\times10^{-4}$ torr	Sieverts' parameters		Embrittlement limit q_e (torr l/g)	Temperature T (K)			
				573		773	
Getter alloy	A	B		K(T) Torr/(torr l/g)^2	q_0(T) (torr l/g)	K(T) Torr/(torr l/g)^2	q_0(T) (torr l/g)
ST707	4.8	6116	20	1.338E-06	14.98	7.726E-04	0.62
ST101	4.82	7280	20	1.303E-08	151.74	2.524E-05	3.45
ZAO	5.76	7290	~100	1.090E-07	52.46	2.134E-04	1.19

By considering that a suitable alloy for the CPS should provide a tritium concentration at the getter surface, q_0 (T), as high as possible (in order to reduce the quantity of the getter material to be used), but lower than the half of the embrittlement limit (q_e). It is evident that at 573 K the ZAO alloy exhibits the best performance. For this type of alloy, the follow provides a feasibility study to evaluate its applicability inside the CPS.

In order to assess the mass of the getter and its area at first it is necessary to establish the sorption regime (i.e. surface vs. diffusion limited) and then use the appropriate equations. For this application, the sorption flux of the getter is limited by surface kinetics, therefore the equations to be used are the follows:

$$M = \frac{F_{T_{BB}}\tau_S}{q_0\left[1 - exp\left(-\frac{k_i P_0}{Lc_0}\tau_S\right)\right]} \quad (A.3)$$

$$A_G = \frac{M}{\rho L} \quad (A.4)$$

where τ_S is the time of the sorption cycle defined as:

$$\int_0^{\tau_S} A_G \Gamma_S(T,t)dt = F_{T_{BB}}\tau_S \quad (A.5)$$

$F_{T,BB}$ is the tritium permeation rate from the blanket into coolant (g s^{-1}) and Γ_S is the hydrogen sorption flux (g $s^{-1}m^{-1}$) on the getter which is function of the hydrogen partial pressure in the coolant P(t) and the equilibrium pressure P_{eq}(t) at the getter surface:

$$\Gamma_S(T,t) = k_i(T)\{P_{test} - P_{eq}(T,t)\} \quad (A.6)$$

Therefore, by using the input data in Table 50 and by assuming several sorption times, it is possible to calculate the mass and the area of the ZAO alloy required to sorb the tritium permeated in the coolant. By considering a sorption time from 6 to 10 days, Table 51 illustrates the mass and the area of the required ZAO alloy and the tritium inventory, $Q(\tau_S)$, at the end of each sorption cycle.

Table 50: Main data used in the simulation of the NEGs feasibility study

T generation rate	Coolant pressure	Coolant flowrate	T permeation rate from blanket, $F_{T,BB}$		% of T generation rate
189 g/d	8 MPa	2400 kg/s	8.0×10^{-6} g/s	0.023 torr l/s(STP)	0.37 %

Table 51: Mass M and area AG of the ZAO alloy at 300 °C

τ_S (days)	6	7	8	9	10
M (kg)	0.507	0.589	0.673	0.756	0.840
A_G (m^2)	0.874	1.016	1.160	1.304	1.449
$Q(\tau_S)$ (torr l)	2.64E+0.4	3.08E+0.4	3.52E+04	3.96E+0.4	4.40E+04

In order to guarantee the continuous operation of the CPS, a minimum of two getters have to be foreseen: one in operation and one in regeneration. In order to assess the regeneration time (τ_{reg}), it is necessary to consider the sum of different contribution: the warm-up time (τ_w), the duration of the regeneration plateau (τ_R) and the cool down time (τ_C), see Figure 22. Then it is essential to verify that the regeneration time is shorter than the sorption time ($\tau_{reg} < \tau_S$).

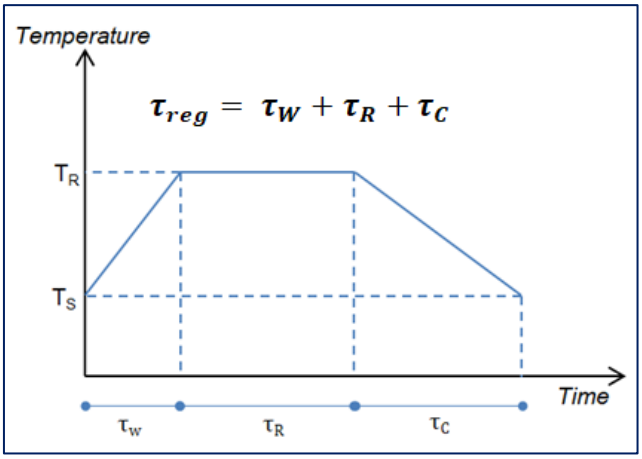

Figure 22: Sum of the different contribution of the regeneration time of the getter

In order to assess the regeneration time of the ZAO alloy different regeneration temperatures (from 550 °C up to 700 °C) and different speeds for the external pumping system (from 1000 to 3000 l/s) have been considered. In general by increasing the regeneration temperature, the hydrogen diffusivity increases thus the regeneration plateau (τ_R) is shorter; however this means a longer warm-up and cool-down time. Table 52 clearly illustrates that by operating the regeneration at 600 °C with, a regeneration plateau of about 153 hours and by assuming an external pumping speed of 1000 l/s, it is possible to obtain low hydrogen concentration inside the getter (q_i) at the end of the regeneration time and there are still about 83 hours left for the cool down phase. For this calculation a ramp up of 2 °C/min has been assumed.

Table 52: Regeneration time (τ_0 in h) and time available for cool-down (τ0 in h) for the ZAO getter using an external pump with a speed of S=1000 l/s and a sorption time of 10 days. The negative (red) values indicate that under such conditions there is no time for the cool-down phase

T_R (°C)	550		600		650		700	
q_i (torr l/g)	τ_R	τ_0	τ_R	τ_0	τ_R	τ_0	τ_R	τ_0
0.1	4.93	232.98	1.53	235.97	0.54	236.54	0.21	236.45
0.01	49.41	188.51	15.36	222.14	5.42	231.66	2.13	234.54
0.001	494.15	-256.23	153.65	83.85	54.22	182.86	21.30	215.37
0.0001	4941.58	-4703.67	1536.54	-1299.04	542.23	-305.15	212.97	23.70

The described feasibility study is enough to conclude that, from a theoretical point of view, the ZAO alloy can be used to sorb the Q2 species from the helium coolant. However a large experimental campaign is required to verify several aspects, such as: i) possibility to operate the getter at 8 MPa, ii) actual getter surface, iii) tritium compatibility, iv) effect of the impurities, etc.

References

[1] A. Ciampichetti et al. – Analisi del trasporto del trizio nei sistemi SFR – ENEA Report NNFISS-LP3-020 (2011)

[2] S. Tosti et al. – Tritium in fusion. Production, uses and environmental impact – Chapter 1 – R.D. Penzhorn – Natural and man-made sources of tritium: applications of tritium – Nova Science Publishers (2013)

[3] S. Tosti et al. – Tritium in fusion. Production, uses and environmental impact – Chapter 2 – F. Moro et al. – The deuterium-tritium fuel cycle in tokamak devices – Nova Science Publishers (2013)

[4] Kaye & Laby Online – Tables of physical & chemical constants (16th edition 1995) – 4.7 Nuclear fission and fusion, and neutron interactions – www.kayelaby.npl.co.uk

[5] A. Ciampichetti et al. – The coolant purification system of the European test blanket modules: preliminary design – Fus. Eng. Des. 85 (2010) 2033-2039

[6] H.L. Brey – The evolution and future development of the High Temperature Gas Cooled Reactor – GENES4/ANP2003 – Kyoto – Paper 1194 (2003)

[7] N. Sakaba et al. – Helium chemistry for Very High Temperature Reactors – Jou. Nuc. Sci. Tec. 47 (2010) 269-277

[8] R.D. Burnette et al. – Chemical impurities in the helium coolant at the Peach Bottom HTGR – Gulf General Atomic Report – GULF-GA-A10809 (1971)

[9] R. Simon – The primary circuit of the DRAGON High Temperature Reactor Experiment – International Conference SMiRT 18 – Beijing – (2005)

[10] R.D. Burnette et al. – Primary coolant chemistry of the Peach Bottom and Fort St. Vrain high temperature gas-cooled reactors – IAEA Specialists Meeting on Coolant Chemistry, Plate-out and Decontamination in Gas-cooled Reactors – Juelich (FRG) – 2-4 December 1980

[11] B. Castle – NGNP Reactor Coolant Chemistry Control Study – INL/EXT-10-19533 – Rev. 1 (2010)

[12] R.P. Wichner et al. – Distribution and transport of Tritium in the Peach Bottom HTGR – ORNL-5497 – (1979)

[13] W.R. Corwin et al. – Generation IV Reactors Integrated Materials Technology Program Plan: Focus on Very High Temperature Reactor Materials – Oak Ridge National Laboratory – ORNL/TM-2008/129 – August 2008

[14] A.L. Habush et al. – Fort St. Vrain Nuclear Generating Station Construction and Testing Experience – Nuc. Eng. Des. 26 (1974) 16-26

[15] H.G. Olson et al. – The Fort St. Vrain High Temperature Gas-Cooled Reactor – Evaluation and Removal of Primary Coolant Contaminants – Nuc. Eng. Des. 61 (1980) 315-322

[16] Z. Wu et al. – The design features of the HTR-10 — Nuc. Eng. Des. 218 (2002) 25-32

[17] M.S. Yao et al. – The helium purification system of the HTR-10 — Nuc. Eng. Des. 218 (2002) 163-167

[18] S. Saito et al. – Present status of the High Temperature Engineering Test Reactor (HTTR) — Nuc. Eng. Des. 132 (1991) 85-93

[19] N. Sakaba et al. – Short descriptions of other systems of the HTTR — Nuc. Eng. Des. 233 (2004) 147-154

[20] General Atomics – Gas Turbine Modular Helium Reactor (GT-MHR) Conceptual Design Description Report – 910720 – Rev. 1 – (1996)

[21] Horizon 2020 – Proposal number N. 754586 - 2016

[22] G. Locatelli et al. – Generation IV nuclear reactors: Current status and future prospects – Energy Policy 61 (2013) 1503-1520

[23] IAEA – International Working Group on Fast Reactors – Specialists' Meeting on Fast Reactor Cover Gas Purification – IWGFR/61 – (1986)

[24] P. Michaille et al. – The French experience concerning the contamination by inactive and radioactive impurities and the purification of the cover gas of LMFBRs – IAEA/IWGFR – Specialists' Meeting on Fast Reactor Cover Gas Purification – IWGFR/61 – (1986)

[25] M. Schneider – Fast Breeder Reactor in France – Science and Global Security – 17 (2009) 36-53

[26] T.A. Renner et al. – Tritium and Hydrogen Transport in LMFBR Systems: EBR-II, CRBR, and FFTF – ANL-78-64 (1978)

[27] International Atomic Energy Agency (IAEA) – Fission and corrosion product behaviour in liquid metal fast breeder reactors (LMFBRs) – IAEA-TECDOC-687 (1993)

[28] BASF – Puristar R3-11G T5x3 – Data Sheet

[29] M. Haruta et al. – Catalytic combustion of hydrogen I – Its role in hydrogen utilization system and screening of catalyst materials – International Journal of Hydrogen Energy – 6 (1981) 601-608

[30] POROCEL – Application Bulletin #1C: Fixed Bed Adsorber Design Guidelines – August 2010

[31] S. Ergun - Fluid flow through packed columns - Journal of Chemical Engineering Progress – 48 (1952) 89-94

[32] POROCEL – Application Bulletin #3: Fixed Bed Pressure Drop Calculation– August 2010

[33] NIST Chemistry WebBook, SRD 69 – webbook.nist.gov

[34] GPSA – Engineering Data Book – 14th Edition

[35] UOP – An Introduction to Zeolite Molecular Sieves – Data Sheet

[36] UOP – Purification of olefin and polymer process streams – Data Sheet

[37] Grace Davison – SYLOBEAD MS 514 – Data Sheet

[38] L.V. Boccaccini et al. – European Helium Cooled Pebble Bed (HCPB) Test Blanket – ITER Design Description Document Status 1.12.1998 – FZKA 6127 (1999)

[39] M. Dalle Donne et al. – European helium cooled pebble bed blanket: Design of blanket: module to be tested in ITER – Fus. Eng. Des. 39-40 (1998) 825-833

[40] D. Demange et al. – Overview of R&D at TLK for process and analytical issues on tritium management in breeder blankets of ITER and DEMO – Fus. Eng. Des. 87 (2012) 1206-1213

[41] I. Ricapito et al. – Tritium processing systems for the helium cooled pebble bed test blanket module – Fus. Eng. Des. 83 (2008) 1461-1465

[42] A. Aiello et al. – Finalization of the conceptual design of the auxiliary circuits for the European test blanket systems – Fus. Eng. Des. 96-97 (2015) 56-63

[43] A. Aiello – Conceptual design of ITER European TBMs Ancillary Systems – ENEA presentation. September 2017

[44] L. Deli et al. – Recent progress of China HCCB TBM tritium system – Fus. Eng. Des. 109-111 (2016) 416-421

[45] A. Santucci et al. – The coolant purification system in DEMO: interfaces and requirements – Fus. Eng. Des. 124 (2017) 744-747

[46] E. Carella et al. – Tritium behaviour in HCPB breeder blanket unit: modelling and experiments – Fus. Sci. Tech. 71 (2017) 357-362

[47] E. Carella et al. – Tritium modelling in HCPB breeder blanket at a system level – Fus. Eng. Des. 124 (2017) 687-691

[48] L. A. Sedano – Tritium Cycle Design for He-cooled Blankets for DEMO – Ciemat Technical Report N. 1110 – June 2007

[49] A. Aiello et al. – European testing blanket modules auxiliaries design – Fus. Eng. Des. 86 (2011) 602-606

[50] H. Petersen – The properties of Helium: Density, Specific Heats, Viscosity and Thermal Conductivity at pressure from 1 to 100 bar and from Room Temperature to about 1800 K – Risö Report N. 224 – September 1970